NORTHEAST UTILITIES

THE CONNECTICUT LIGHT AND POWER COMPANY
WESTERN MASSACHUSETTS ELECTRIC COMPANY
HOLYOKE WATER POWER COMPANY
NORTHEAST UTILITIES SERVICE COMPANY
NORTHEAST NUCLEAR ENERGY COMPANY

General Offices • Selden Street, Berlin, Connecticut

P.O. BOX 270
HARTFORD, CONNECTICUT 06141-0270
(203) 665-5000

September 19, 1984

Docket No. 50-423
A04078

Director of Nuclear Reactor Regulation
Mr. B. J. Youngblood, Chief
Licensing Branch No. 1
Division of Licensing
U.S. Nuclear Regulatory Commission
Washington, D.C. 20555

Reference: (1) B. J. Youngblood letter to W. G. Counsil, Request for Additional Information for Millstone Nuclear Power Station, Unit 3, dated May 25, 1984.

Dear Mr. Youngblood:

Millstone Nuclear Power Station, Unit No. 3
Response to Requests for Additional Information

Attached are Northeast Nuclear Energy Company's (NNECO) responses to the requests for additional information forwarded in Reference (1).

If there are any questions related to this information, please contact our licensing representative directly.

Very truly yours,

NORTHEAST NUCLEAR ENERGY COMPANY
et. al.

BY NORTHEAST NUCLEAR ENERGY COMPANY
Their Agent

W. G. Counsil

W. G. Counsil
Senior Vice President

Aperture Card Dist

B001
1/40 oversize Drawings

STATE OF CONNECTICUT)
) ss. Berlin
COUNTY OF HARTFORD)

Then personally appeared before me W. G. Counsil, who being duly sworn, did state that he is Senior Vice President of Northeast Nuclear Energy Company, an Applicant herein, that he is authorized to execute and file the foregoing information in the name and on behalf of the Applicants herein and that the statements contained in said information are true and correct to the best of his knowledge and belief.

Lorraine J. D'Amico
Notary Public

My Commission Expires March 31, 1988

NRC Letter May 25, 1984

Question 210.47

during the review of the classification of the Feedwater System, Figure 10.4-6 Sheet 2 of 2, it was found that the following 3 lines have been incorrectly classified Safety Class 3. These lines should be classified Safety Class 2. The line numbers are:

3 FWA-004-139-3 (A-)

3 FWA-004-140-3 (B-)

3 FWA-004-141-3 (C-)

It is requested that the applicant revise Figure 10.4-6, Sheet 2 of 2 in a future FSAR amendment.

Response:

Refer to revised FSAR Figure 10.4-6, Sheet 2 of 2.

DOCUMENT/ PAGE PULLED

ANO. 8410120212

NO. OF PAGES 1

REASON

- ☐ PAGE ILLEGIBLE
  - ☐ HARD COPY FILED AT: PDR CF
    OTHER ____________
  - ☐ BETTER COPY REQUESTED ON ___/___/___
- ☒ PAGE TOO LARGE TO FILM
  - ☒ HARD COPY FILED AT: PDR (CF)
    OTHER ____________
  - ☐ FILMED ON APERTURE CARD NO 8410120212-01

Question 810.1

1.) Provide further information as to how individuals without automobiles will be evacuated during an emergency.

Response

The nature of the environment within the 10 mile emergency planning zone of the Millstone Nuclear Station is primarily rural to suburban. Even cities such as New London are primarily suburban in nature. For this reason, public transportation is not a key method of transportation utilized by residents or transients. The private automobile is by far the primary mode of transportation. For this reason the number of individuals without automobiles requiring transportation in an emergency is not an issue. The evacuability study performed by Storch Engineers and submitted by Northeast Utilities dealt primarily with a conservative method of assigning passenger loading to private automobiles. The utilization of buses for school children was included in the report. Individuals with ambulatory problems are required to register with their local civil preparedness offices. In the event of an evacuation, special transportation will be arranged by the civil preparedness office for these individuals.

2.) Provide an estimate of the confirmation time(s) to verify that an evacuation has been completed.

Response

The estimation of confirmation times to verify that an evacuation has been completed are as follows.

8 minutes for two miles
33 minutes for five miles
163 minutes for ten miles

This information was taken from FEMA-REP3-Dynamic Evacuation Analyses; Independent Assessments of Evacuation Time from the Plume Exposure Pathway EPZs of 12 Nuclear Power Stations.

NRC Letter May 25, 1984

Question 492.7

Q.492.4 mentioned Seabrook rather than Millstone 3 (page 4 of response to Q.492.4). We therefore do not have confidence that you performed the required review of the Westinghouse standard response on flow measurement to assure that it applies to your plant. In order to provide this assurance, please answer the following questions.

(1) The instrumentation uncertainties cited are the generic bounding values for Westinghouse instrumentation. Plant-specific instrumentation uncertainties exceeding the bounding values cited in the Westinghouse response should be identified and used for the plant-specific analysis. Identify any instrumentation which deviates from the Westinghouse instrumentation and provide the uncertainty value pertinent to this instrumentation and measurement arrangement with comparison to the Westinghouse generic value. The bases or sources for the uncertainty value should also be provided. The sources can be from purchase specifications, manufacturing specifications, calibration data provided by instrumentation vendor or obtained on site, published industry standard or other justifiable bases.

(2) For the RCS flow measurement, the Westinghouse generic response states: "It is assumed for this error analysis, that this flow measurement is performed within seven days of calibrating the measurement instrumentation, therefore, drift effects are not included (except where necessary due to sensor location)." Does you plant operating procedure have provisions that require the RCS flow measurement be performed within seven days of calibrating the measurement instrumentation? If not, what are the drift uncertainty values associated with each component such a P Cell, local meter, RTD, thermocouple, process rack and sensors? What is the effect on the overall flow measurement uncertainty?

(3) The Westinghouse report states: "It is also assumed that the calorimetric flow measurement is performed at the beginning of a cycle, so no allowance has been made for feedwater venturi crud buildup;" and "If venturi fouling is detected by the plant, the venturi should be cleaned, prior to performance of the measurement. If the venturi is not cleaned, the effect of the fouling on the determination of the feedwater flow, and thus, the steam generator power and RCS flow, should be measured and treated as a bias, i.e., the error due to venturi fouling should be added to the statistical summation of the rest of the measurement errors."

(a) How do you assure that the venturi is clean at the beginning of a cycle? Is the venturi cleaned at the beginning of every cycle?

(b) How do you detect the venturi fouling and to what extent of uncertainty can you detect fouling?

(c) Describe the design provisions and procedures to clean the venturi if fouling is detected.

(d) How do you determine the error on feedwater flow measurement due to the fouling effect if the venturi is not cleaned or if the venturi fouling is not detected?

(e) If the venturi is not cleaned prior to the calorimetric flow measurement because no fouling is detected, an error component should be added. The magnitude of the error component should depend on the minimum detectable value of fouling.

Response:

1. NNECO is currently in the process of evaluating the uncertainties associated with the instrumentation used in the Reactor Coolant System Flow Measurement. The results of this evaluation will be forwarded when complete.

2. As part of the instrument uncertainty analysis the effects of drift will be studied. If an instrument is not calibrated within seven (7) days of performing the flow measurement the effects of drift will be added to the overall flow measurement uncertainty.

3. A. Prior to initial plant startup, main feedflow venturis were installed clean. In addition, the section of feedwater piping with the venturis will be flushed prior to initial plant startup. At the beginning of subsequent fuel cycles venturis will be inspected. If venturi fouling is discovered during inspection the venturis will be cleaned.

   B. Venturi fouling is detected using the performance monitoring program. Plant performance data is collected automatically daily and trended on a monthly basis. The plant parameters specifically reviewed for determination of venturi fouling are - electrical output, feedwater flow, main stream flow, and first stage turbine pressure. The base relationship of these parameters will be established during start-up testing and the first month of operation by review of the collected performance monitoring data. During this period the venturi will be presumed to be clean. During the monthly performance review the trended daily data for the mean electrical output mean stream flow and mean turbine first stage bowl pressure will be compared to the mean feedwater flow. If the trend of the monthly review indicates that the relationship has deviated, corrective action will be taken before performing the next precision heat balance RCS flow measurement. The corrective action will involve inspecting and cleaning the venturi.

   C. During the first refueling outage, inspection ports will be added upstream and downstream of the venturis. Cleaning will be done by hydrolasing when required.

   D. The effect of fouling as a result of crud buildup is not taken into account in the feedwater flow measurement. The venturi fouling term is a bias that will result in a higher measured feedwater flow, and, in turn a higher RCS flow than actual measured value. Therefore, if the feedwater venturi is not cleaned, the effect of the fouling on the determination of the feedwater flow and thus the steam generator power and RCS flow is such that all values will be treated in a conservative manner. A visual inspection of the feedwater flow venturi will be done during each refueling outage to detect any buildup of fouling. The feedwater flow venturis will be cleaned as deemed necessary after the inspections. This will correct any deviations caused by feedwater flow venturi fouling.

E. Prior to the start of each cycle the venturis will be inspected and cleaned if necessary. Because venturis will be verified clean at the beginning of each cycle it will be unnecessary to add an error component due to fouling on the RCS Flow Measurement.

NRC Letter: May 25, 1984

Question No. 210.46

The staff review of the FSAR Section 3.9.3 finds that asymmetric LOCA load effects resulting from postulated ruptures in the primary coolant loop have not been addressed. An acceptable basis for evaluating the asymmetric LOCA loadings is provided in NUREG-0609, "Asymmetric Blowdown Loads on PWR Primary Systems," which addressed the resolution of Generic Task Action Plan A-2. We require that you provide in the FSAR a discussion to specifically address the consideration of asymmetric LOCA loads with respect to satisfying the guidelines in NUREG-0609.

Response:

Please refer to FSAR Section 3.9.N.1.4.3. Additional information regarding evaluation of asymmetric loading effects due to postulated ruptures in the primary coolant loop is contained in the response to NRC Question 480.37.

NRC Letter: May 25, 1984

Question No. Q480.37

In the unlikely event of a pipe rupture inside a major component subcompartment, the initial blowdown transient would lead to nonuniform pressure loadings on both the structure and the enclosed component(s). To ensure the integrity of these design features, we request that you provide the following information for each subcompartment analyzed:

a. Provide the peak and transient loadings on the major components used to establish the adequacy of the supports design. This should include the load forcing functions [e.g., f (t), f_x (t), f_y (t)] and transient moments [e.g., M (t), M_x(t), M_y(t)], as resolved about a specific, identified coordinate system.

b. Provide the projected area used to calculate these loads and identify the location of the area projections on plan and section drawings in the selected coordinate system. This information should be presented in such a manner that confirmatory evaluations of the loads and moments can be made.

c. For each compartment, provide a table of blowdown mass flow rate and energy release rate as a function of time for the break which was used for the component supports evaluation.

d. Describe and justify the nodalization sensitivity study performed for the major component supports evaluation, where transient forces and moments acting on the components are of concern.

e. Discuss the manner in which movable obstructions to vent flow (such as insulation, ducting, plugs, and seals) were treated. Provide analytical and experimental justification that vent areas will not be partially or completely plugged by displaced objects. Discuss how insulation for piping and components was considered in determining volumes and vent areas.

f. Provide justification for the initial atmospheric conditions assumed in the analysis. An acceptable approach would be to assume air at maximum allowable temperature, minimum absolute pressure, and minimum relative humidity.

Response:

The following subcompartments were analyzed for postulated pipe rupture events:

- Reactor Pressure Vessel (RPV) Cavity
- Steam Generator (SG) Cubicle

The pressurizer cubicle also was analyzed, but will be submitted after 1.47
completion of a reanalysis due to as-built modifications to this 1.48
cubicle.

The peak and transient loadings (Item a) and the projected area (Item b) 1.49
used to calculate these loads are provided in the following discussion, 1.51
followed by specific responses to Items c through f of Q480.37.

Items a and b: 1.53

- [Reactor Nozzle Guillotine 1.55

Configuration 2.1

Figures Q480.37-1 and Q480.37-2 show the reactor cavity geometry for the 2.2
postulated break at the inlet nozzle from Reactor Coolant Loop 2 2.3
(Cubicle B). The global coordinate system is defined as follows: 2.4

Origin - on containment centerline and 17 feet-6 inches below 2.8
reactor nozzle centerlines 2.9
X - horizontal, south 80.4° west 2.10
Y - horizontal, south 9.6° east 2.11
Z - vertical upward 2.12

The local coordinate system is chosen, as shown in these figures, so 2.16
that local x points from the RPV centerline away from the broken nozzle. 2.17
Therefore, vertical forces will be aligned with local z (= global Z), 2.18
horizontal forces will be aligned with local x, and overturning moments 2.20
will be about the local y axis. Other loading components due to the 2.21
slight asymmetry of the RPV nozzle layout are ignored.

The nodal volumes for the asymmetric pressurization analysis, shown on 2.22
Figures Q480.37-1 and Q480.37-2, also are assumed to be symmetric about 2.23
the x-z plane. (See FSAR Figure 6.2-23 for overall nodal arrangement.) 2.24

Projected Areas 2.26

Figures Q480.37-3 through Q480.37-5 show the projected areas over which 2.27
the asymmetric pressures act on the RPV, the neutron shield tank (NST), 2.28
and the primary shield wall (PSW). The projected areas (square inches) 2.31
are shown as arrows, each of which represents the force (pounds) due to
a unit (psi) pressure rise in the particular nodal volume. Because of 2.34
the radiation shielding just below the RPV nozzles, ambient pressure is
assumed below elevation 14 feet-2 inches (NST top). 2.36

Figure Q480.37-3 is divided into two parts to show the elevation ranges 2.37
(A) above and (B) below the RPV nozzle centerlines. Due to symmetry, it 2.39
is understood that each projected area shown includes its mirror image
across the x-z plane and there is no net y-force or net moment about the 2.40
z axis; therefore, each force can be applied as if in the x-z plane.
Consequently, moment arms about the z axis are not shown. 2.41

The projected areas on the x-y (horizontal) plane are shown in plan view 2.42
on Figure Q480.37-4. Most of these vertical forces are directed 2.43
downward on the NST, RPV dome, and control rod drive mechanism (CRDM)
shroud. The exception is the upward force on the flange where the RPV 2.45
and dome are bolted together. The symmetry assumption cited above for 2.46
horizontal forces also is made for the vertical forces. In 2.48
Figure Q480.37-4, projected areas of Nodes 1 through 6 are shown for
each side and must be added before being applied in the x-z plane. 2.50

Figure Q480.37-5 shows both horizontal and vertical forces in an 2.51
elevation view (x-z plane section). The effective elevations of the 2.52
horizontal forces in Nodes 1, 3, and 6 also apply to Nodes 2, 4, and 5,
respectively. 2.53

Figure Q480.37-6 shows plan and elevation views of the refueling cavity 2.54
and lower internals storage area. Although the pressure increases and 2.55
pressure differences in these regions are small relative to those in the
reactor cavity, the projected areas and moment arms are large, so their 2.56
contributions to loads on the concrete walls and PSW (and through the 2.57
grout to the NST) cannot be ignored. It is noted that all horizontal 2.58
forces below elevation 24 feet-6 inches mutually cancel, therefore, they
were not considered. 3.1

Jet Impingement Effects 3.3

A disk-type jet is postulated to issue from the guillotine break and 3.4
impinge on exposed areas of the PSW and NST. Jet effects are confined 3.6
to nodal volumes 1 and 3 (Figure Q480.37-4) in which the calculated
pressures are already high. Conservatively, the higher of the 3.8
calculated jet-impingement pressure or the calculated asymmetric
pressure rise, was applied on any area. 3.9

Over the target area of the PSW inner wall, the calculated average jet 3.10
pressure was relatively low, due to both the distances and the shallow 3.11
impingement angles, so the calculated asymmetric pressure rise was
applied. Conversely, over the NST top target area, which is very close 3.12
to the nozzle and is nearly normal to the jet, impingement pressures 3.13
prevailed. Therefore, a calculated target area of 2,540 square inches 3.14
(Figure Q480.37-4) was deducted from the combined projected areas of 3.15
Volume 1. The pressurization force (over the target area only) was 3.16
replaced by the calculated downward component of jet impingement force 3.17
(207,400 pounds) with a rise time equal to the assumed break-opening
time (1 millisec). The centroid of the target area was 117.42 inches 3.18
from the RPV centerline. Transient pressure forces were applied as 3.19
usual over the remaining areas.

Force and Moment Histories 3.21

The net loads due to combined pressurization and jet impingement were 3.22
calculated as functions of time. The projected areas and moment arms 3.24
(Figures Q480.37-3 through Q480.37-6) and the pressure histories
(Figures Q480.37-7 through Q480.37-10) were input to Stone & Webster 3.25
Program No. ME-171 (ASYMPR) (see FSAR Appendix 3A.2.13). The results 3.27

are shown in Figures Q480.37-11 through Q480.37-13 for the RPV and
Figures Q480.37-14 through Q480.37-16 for the PSW. The loads on the NST 3.30
top are distributed among these curves on the basis of the anticipated
load path. Specifically, NST vertical force is lumped with the RPV 3.31
because the nozzle supports are very stiff vertically, while the grout 3.32
has no vertical stiffness. Conversely, NST overturning moment is lumped 3.33
with the PSW because the PSW and grout are much stiffer than the NST and
nozzle supports to horizontal and bending loads. 3.34

- Steam Generator Cubicle 3.36

Configuration 3.37

FSAR Figures 6.2-19 through 6.2-22 show the SG Cubicle A (Loop 1) 3.38
geometry and subcompartment nodalization for asymmetric pressurization 3.40
(refer to FSAR Section 6.2.1.2). The global coordinate system, defined 3.42
under Reactor Nozzle Guillotine for the reactor cavity, is used
throughout this discussion. In this system, Cubicle A lies in the -X, 3.44
+Y quadrant. Cubicle B, modeled for certain postulated breaks, is 3.45
obtained by reflection of Cubicle A across the Y-Z plane plus minor 3.46
changes.

Projected Areas 3.48

Figures Q480.37-17 through Q480.37-19 show the projected surface areas 3.49
of the SG and reactor coolant pump (RCP) within the elevation ranges 3.51
shown on Figure Q480.37-20. Each projection on the global system is 3.52
indicated by an arrow with the associated force for a unit pressure
rise. Since each force element is normal to the local surface, moments 3.53
about the vertical centerlines vanish. Overturning moments are 3.54
generated by both horizontal and vertical force components.

Postulated Breaks and Resultant Loads 3.56

Asymmetric pressure calculations were made for several break locations 3.57
(Figure Q480.37-21 and FSAR Table 3.9B-15) within the SG cubicle. The 4.2
analyzed breaks are listed in Table Q480.37-1, along with a summary of
the peak loads resulting on the SG and RCP. Break 7 (SG Intrados 4.3
Split), having the largest postulated opening area, clearly dominates
most (9 of 10) listed load components. The sole exception is vertical 4.5
force on the RCP, which is largest during Break 8. Breaks 4 and 8 also 4.6
lift the SG nearly as forcefully as does Break 7.

Pressurization for a feedwater line guillotine was also calculated (FSAR 4.7
Figure 3.6-10, Cubicle B, Break Location 4 or 5). Full lateral 4.11
separation of pipe ends was assumed. Moments on the SG for the FW line 4.12
guillotine were resolved about the upper support elevation, since the
generated forces are basically confined to this region. For all other 4.14
breaks, moments were resolved about the intersection of the inlet and
outlet nozzle centerlines (see Table Q480.37-1 for elevations). 4.15

Based on these comparisons, time history loads (Figures Q480.37-22 4.16
through Q480.37-43) are shown only for Breaks 7, 4, and FWL. The signs 4.19
of each load component are for Cubicle B.

Item c: 4.21

Refer to revised FSAR Section 6.2.1.2 for the mass and energy release 4.22
tables used for the component supports evaluation. 4.23

Item d: 4.26

Subcompartment nodalization is described and justified in the response 4.27
to NRC Question 480.9. The justification given in this response applies 4.29
to all subcompartment analyses performed for the major component
supports evaluation. The pressurizer subcompartment is presently being 4.31
reanalyzed for consistency with the guidelines of the Subcompartment
Analysis Procedures (NUREG/CR-1199). Results will be submitted in a 4.33
future FSAR amendment.

Item e: 4.35

Refer to revised FSAR Section 6.2.1.2 for a discussion of the manner in 4.36
which movable obstructions to vent flow are treated. 4.37

Item f: 4.40

The initial containment temperature was selected at the maximum 4.41
allowable 120°F, and the initial air partial pressure was selected at 4.43
the minimum allowable, 9.0 psia. The initial relative humidity was 4.45
taken at 50 percent. This is the expected minimum during normal 4.46
operation. However, in extreme conditions, the humidity may go as low 4.47
as 10 percent. The sensitivity of the calculated subcompartment 4.48
pressure differential to the initial relative humidity was determined
for the spray line break in the pressurizer cubicle. The pressure 4.50
differential increased by less than 0.2 psi (approximately 3 percent)
when the humidity was decreased from 50 percent to 10 percent. This 4.53
difference in cubicle pressure differential is not significant;
therefore, the assumption of 50 percent relative humidity is acceptable. 4.54

In addition, the Subcompartment Analysis Procedures (NNREG/CR-1199) are 4.55
in general support of the above conclusion regarding sensitivity to 4.56
relative humidity.

TABLE Q480.37-1

PEAK ASYMMETRIC LOADS

Steam Generator (at elevation 24 ft-5.1 in.)

Break	Flow Area (in.^{2})	Forces (kip) F_x	F_y	F_z	Moments (in.-kip) M_x	M_y	M_z
11	196.6	137	51	79	6,742	17,207	0
9	196.6	63	30	62	6,806	9,537	0
7	707	301	174	292	16,457	34,798	0
3	196.6	116	71	69	8,262	17,136	0
FW	478	191	79	59	7,354[2]	17,808[2]	0
4	500	98	99	273	12,001	29,557	0
8[1]	500	67	63	272	11,884	28,692	0

Coolant Pump (at elevation 17 ft-6 in.)

Break	Flow Area (in.^{2})	Forces (kip) F_x	F_y	F_z	Moments (in.-kip) M_x	M_y	M_z
11	196.6	55	50	5	3,617	4,661	0
9	196.6[3]	48	29	13	1,125	3,004	0
7	707	91	79	14	6,056	8,198	0
3	196.6[3]	35	36	5	2,775	3,028	0
FW	478	4	2	2	258	570	0
4	500	23	35	13	2,359	1,639	0
8	500[3]	19	36	24	1,385	1,113	0

NOTES:

1. Loop closure weld, formerly Break 12.
2. Resolved at elevation 49 feet-8.5 inches.
3. Conservative (high) value based on another nearby break.

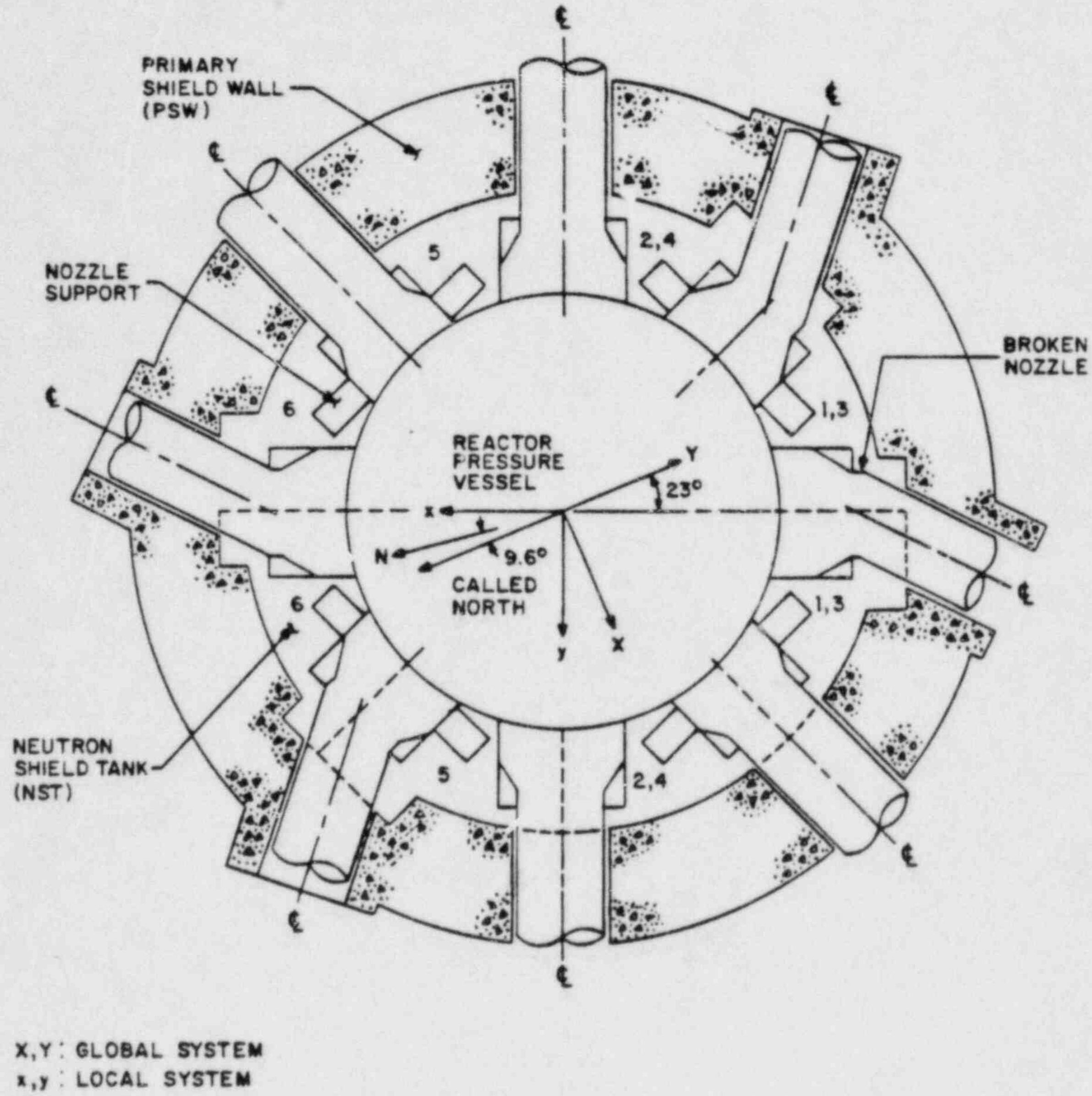

FIGURE Q480.37-1
UPPER REACTOR CAVITY
NODAL ARRANGEMENT
MILLSTONE NUCLEAR POWER STATION
UNIT 3
FINAL SAFETY ANALYSIS REPORT

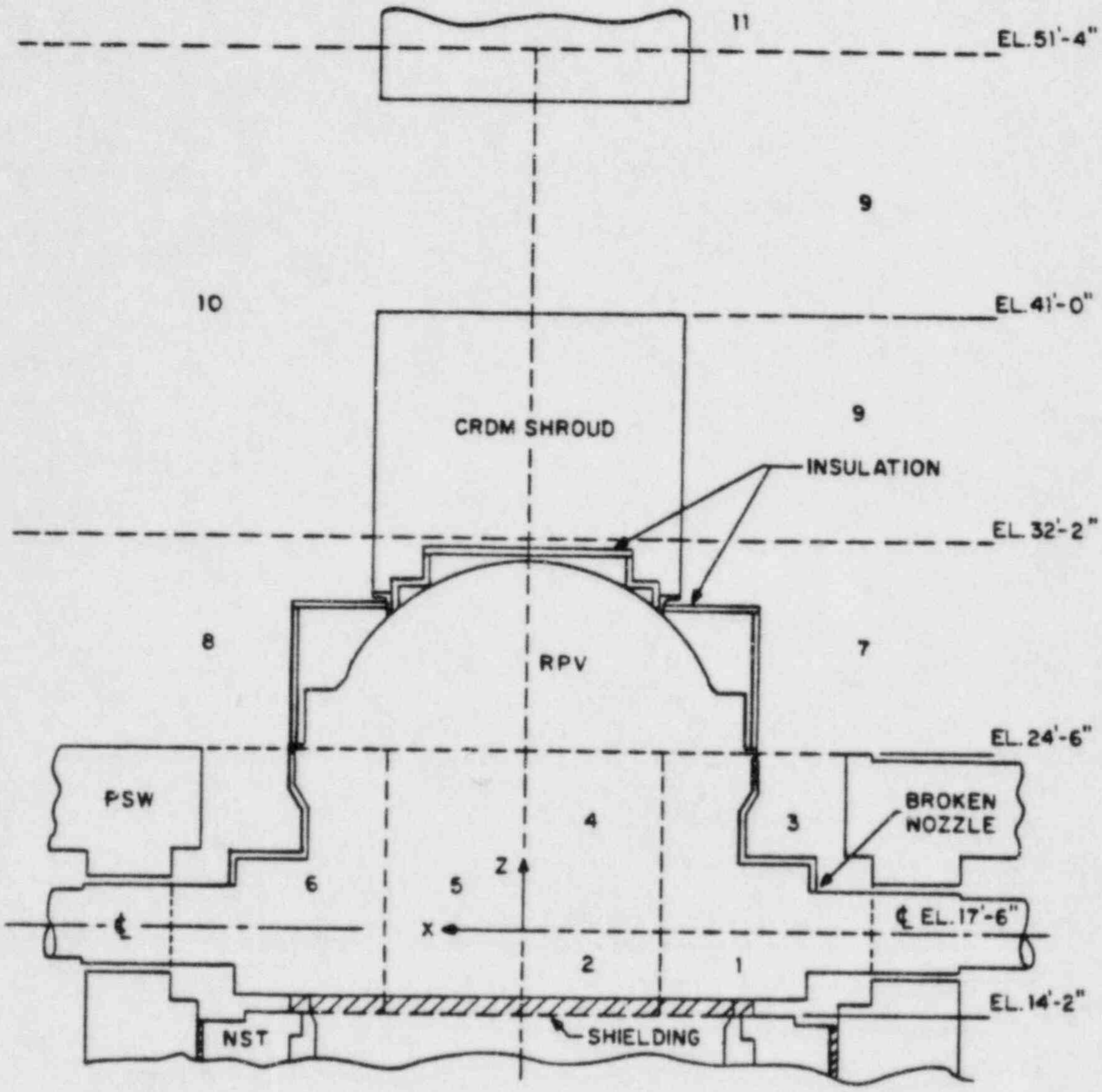

FIGURE Q480.37-2

ELEVATION VIEW OF NODAL ARRANGEMENT IN UPPER REACTOR CAVITY AND CRDM HOUSING

MILLSTONE NUCLEAR POWER STATION
UNIT 3
FINAL SAFETY ANALYSIS REPORT

(A) BETWEEN ELEVATIONS 17'-6" AND 24'-6"

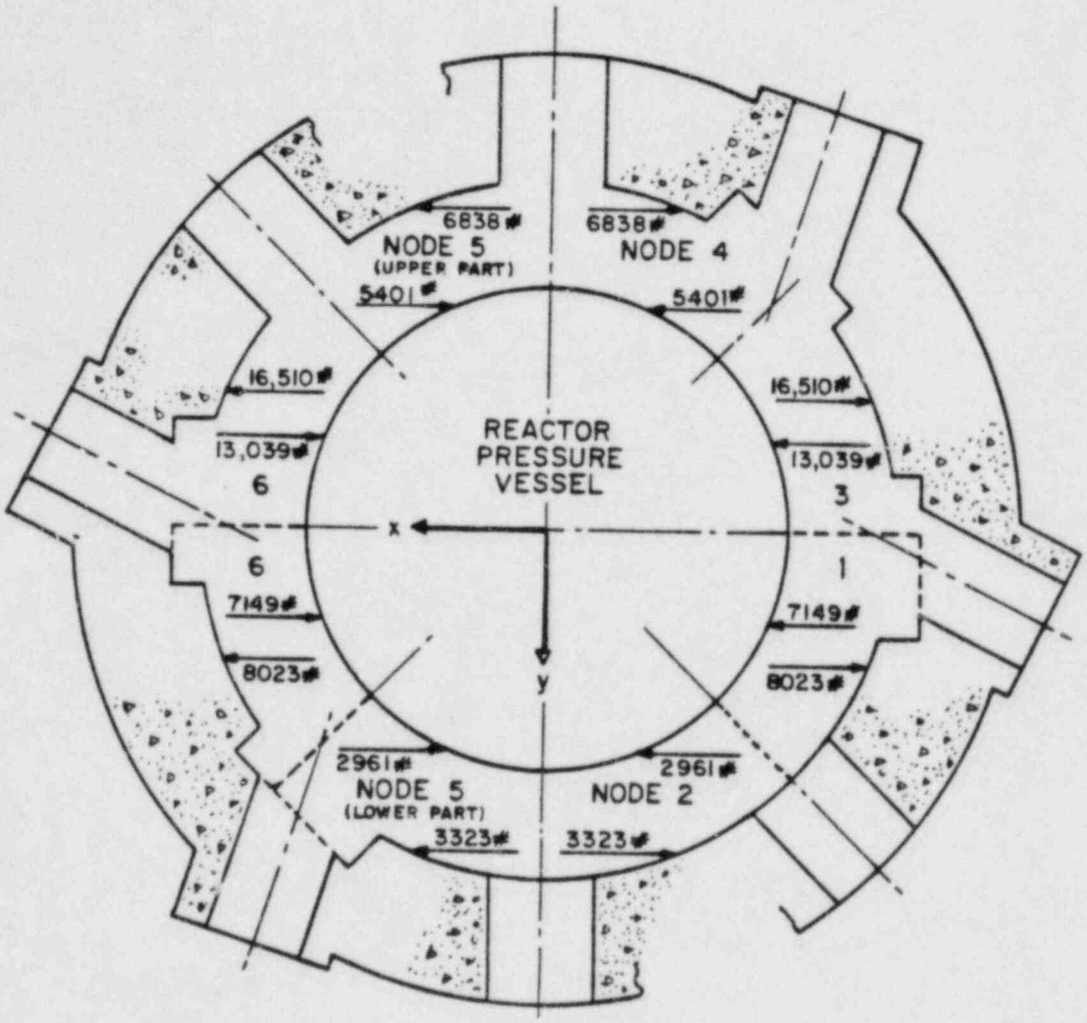

(B) BETWEEN ELEVATIONS 14'-2" AND 17'-6"

NOTE

INCLUDES PIPING INSIDE PSW BUT
EXCLUDES PSW PENETRATIONS

FIGURE Q480.37-3
HORIZONTAL FORCES ON RPV AND
PSW DUE TO UNIT PRESSURES
MILLSTONE NUCLEAR POWER STATION
UNIT 3
FINAL SAFETY ANALYSIS REPORT

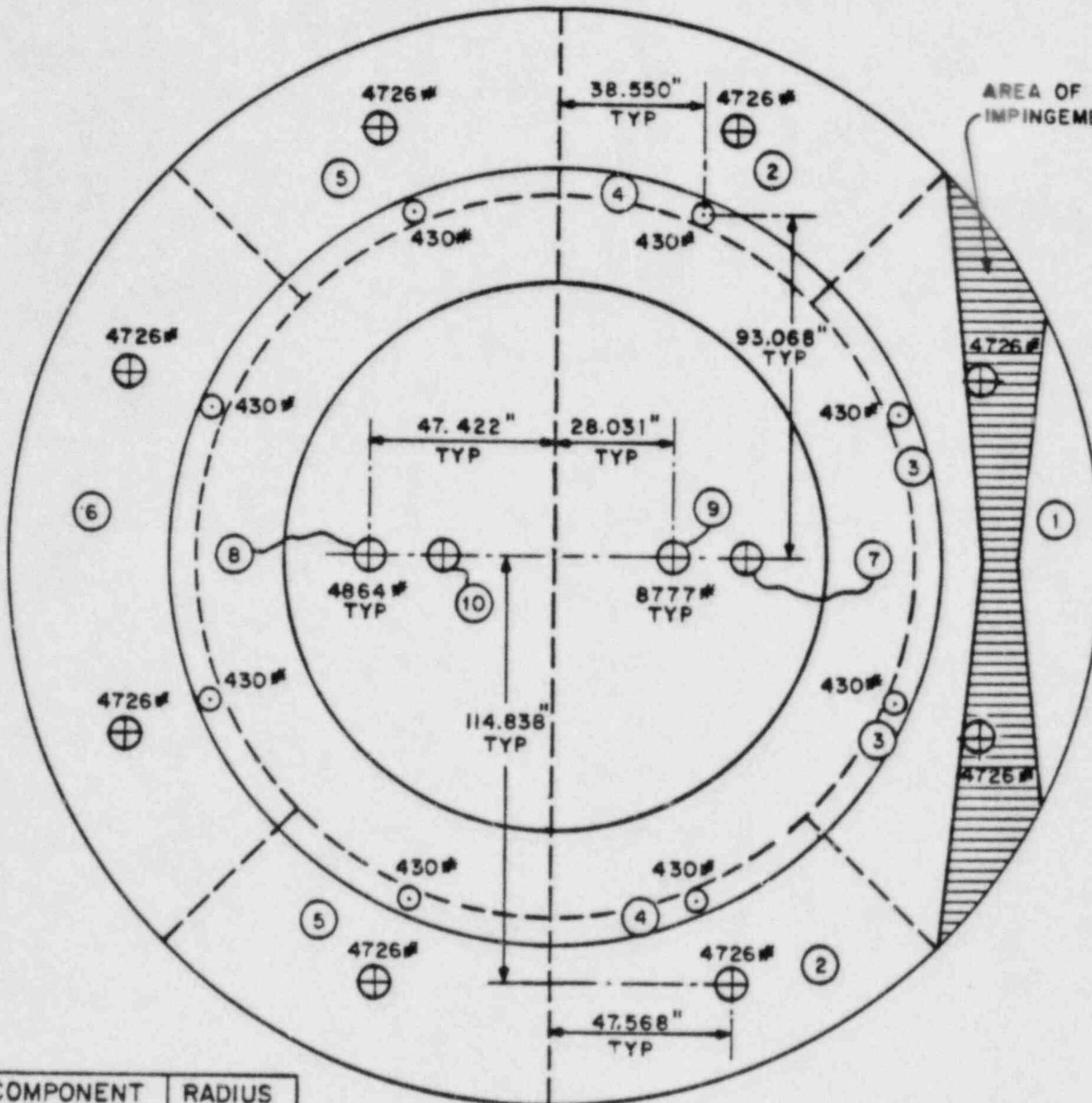

COMPONENT	RADIUS
CRDM	74.75"
RPV FLANGE	106.00"*
RPV SHELL	100.70"*
NST + GROUT	150.00"

* INCLUDES INSULATION

LEGEND

○ = NODE NUMBER

⊙ = UPWARD FORCE

⊕ = DOWNWARD FORCE

FIGURE Q480.37-4
VERTICAL FORCES ON CRDM, RPV, AND NST DUE TO UNIT PRESSURES IN ADJACENT NODES
MILLSTONE NUCLEAR POWER STATION
UNIT 3
FINAL SAFETY ANALYSIS REPORT

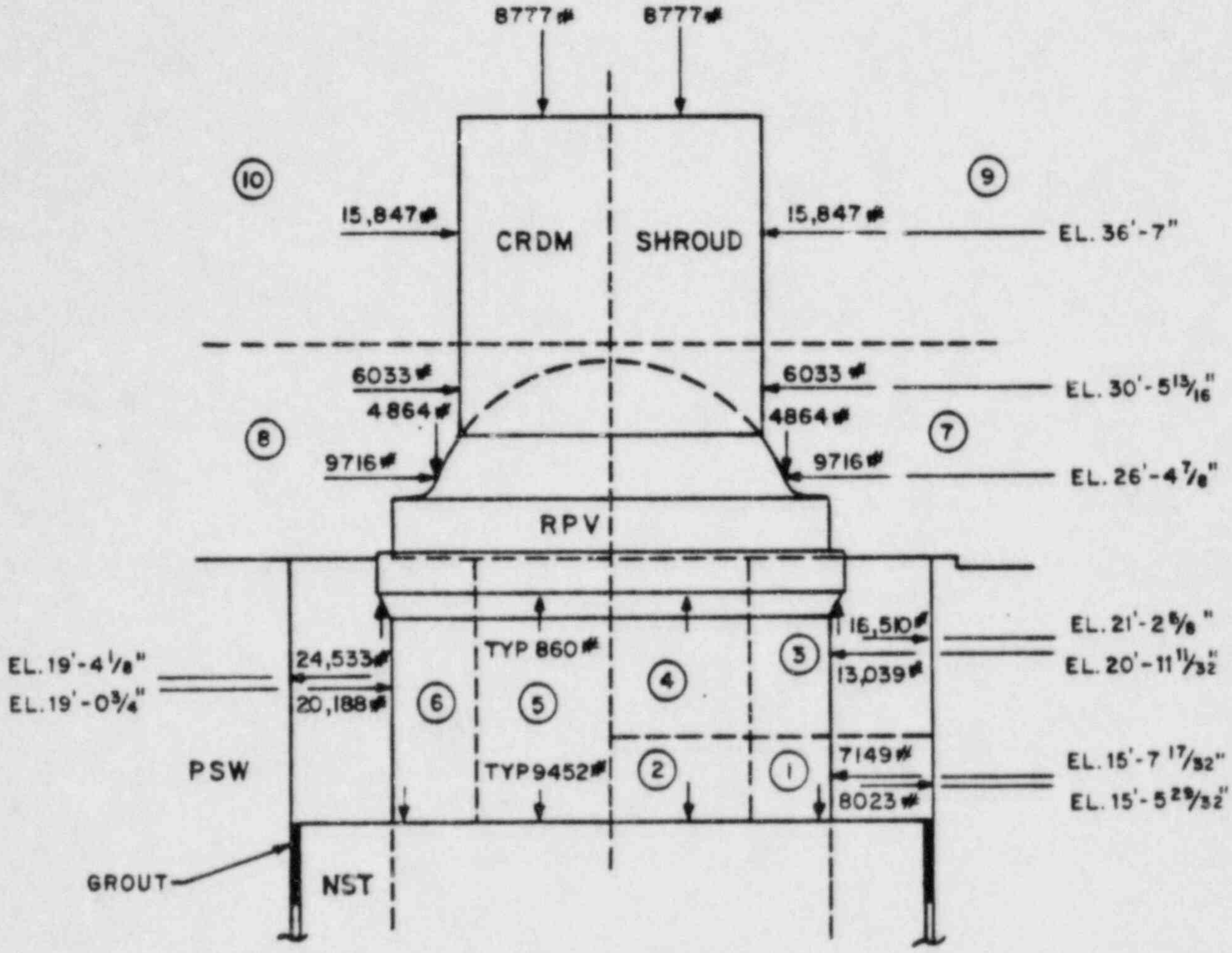

FIGURE Q480.37-5
ELEVATION VIEW OF RPV AND VICINITY SHOWING FORCES DUE TO UNIT PRESSURES
MILLSTONE NUCLEAR POWER STATION
UNIT 3
FINAL SAFETY ANALYSIS REPORT

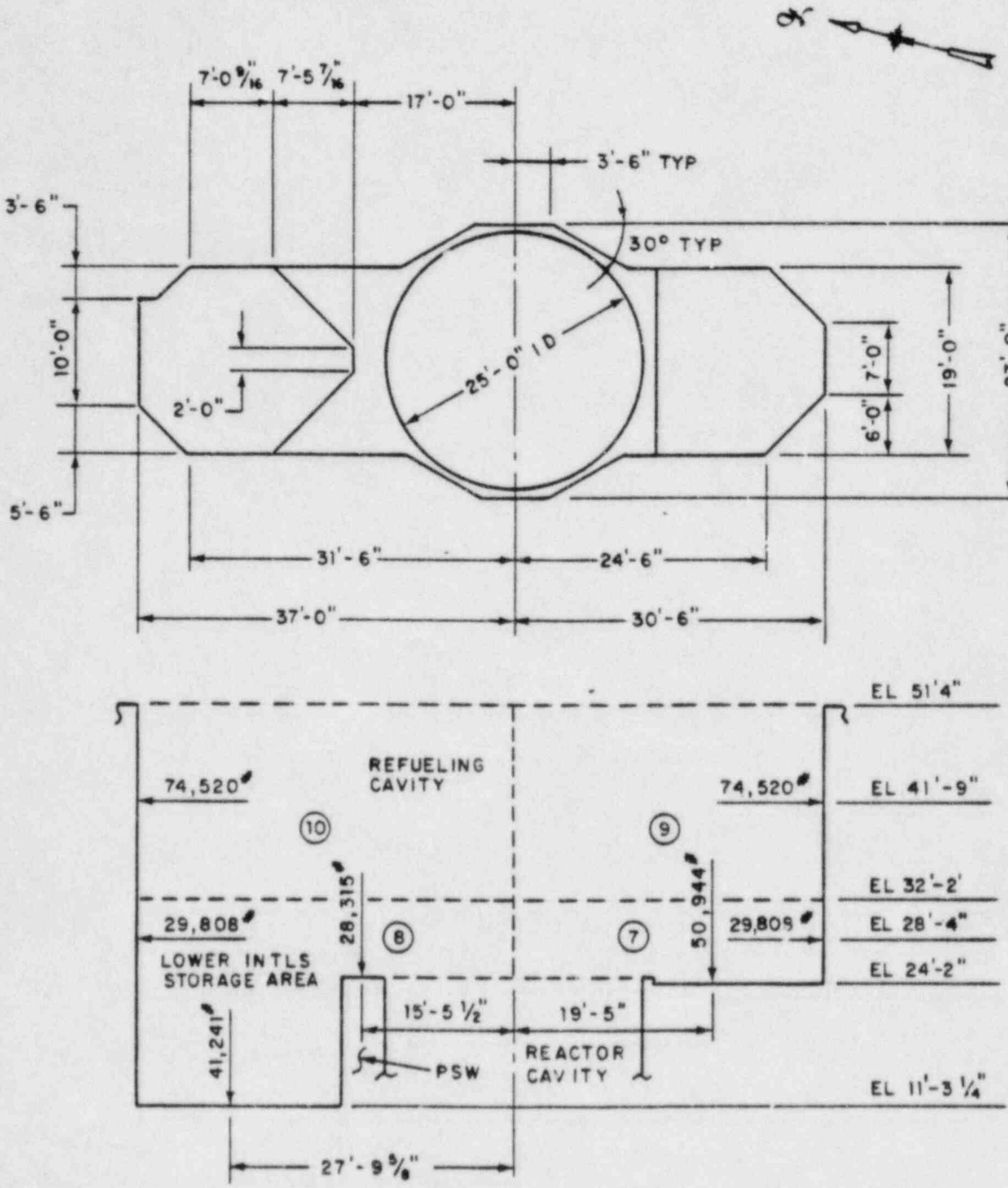

FIGURE Q480.37-6
NODAL ARRANGEMENT IN REFUELING CAVITY WITH FORCES DUE TO UNIT PRESSURES
MILLSTONE NUCLEAR POWER STATION
UNIT 3
FINAL SAFETY ANALYSIS REPORT

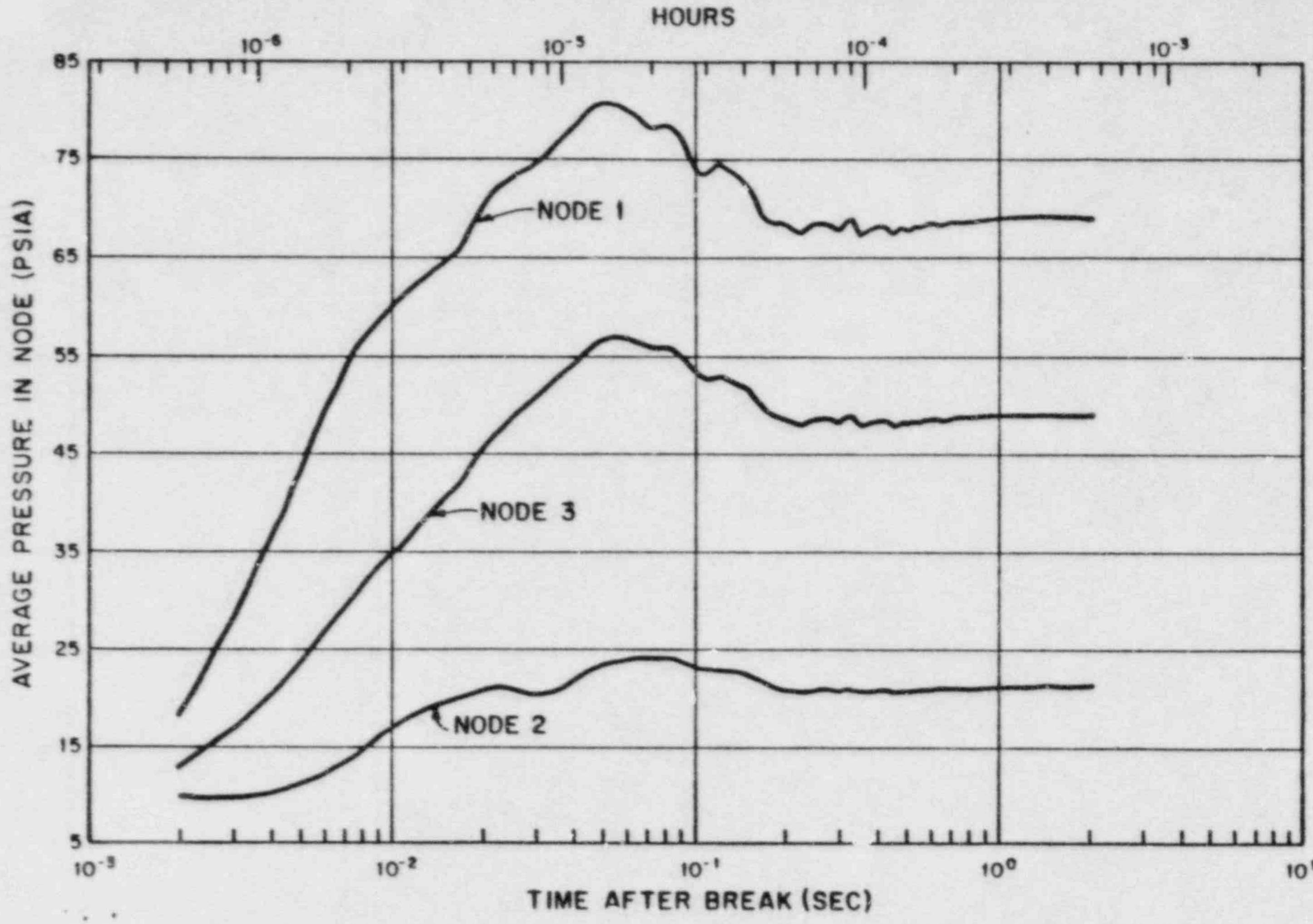

FIGURE Q480.37-7
REACTOR CAVITY PRESSURE TRANSIENTS
NODE NUMBERS 1,2,3
COLD LEG 100 SQ. IN. BREAK
MILLSTONE NUCLEAR POWER STATION
UNIT 3
FINAL SAFETY ANALYSIS REPORT

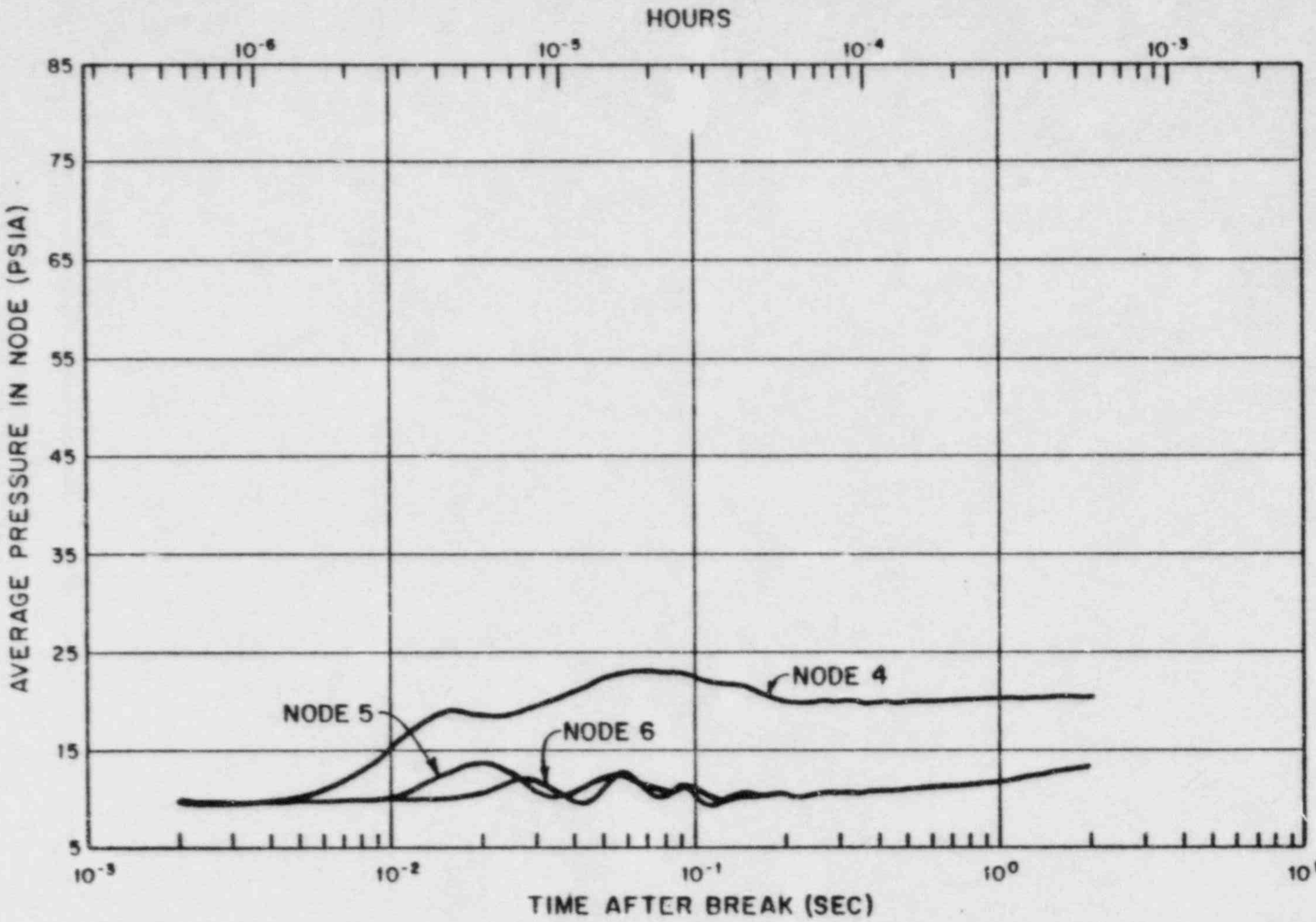

FIGURE Q480.37-8
REACTOR CAVITY PRESSURE TRANSIENTS
NODE NUMBERS 4,5,6
COLD LEG 100 SQ. IN. BREAK
MILLSTONE NUCLEAR POWER STATION
UNIT 3
FINAL SAFETY ANALYSIS REPORT

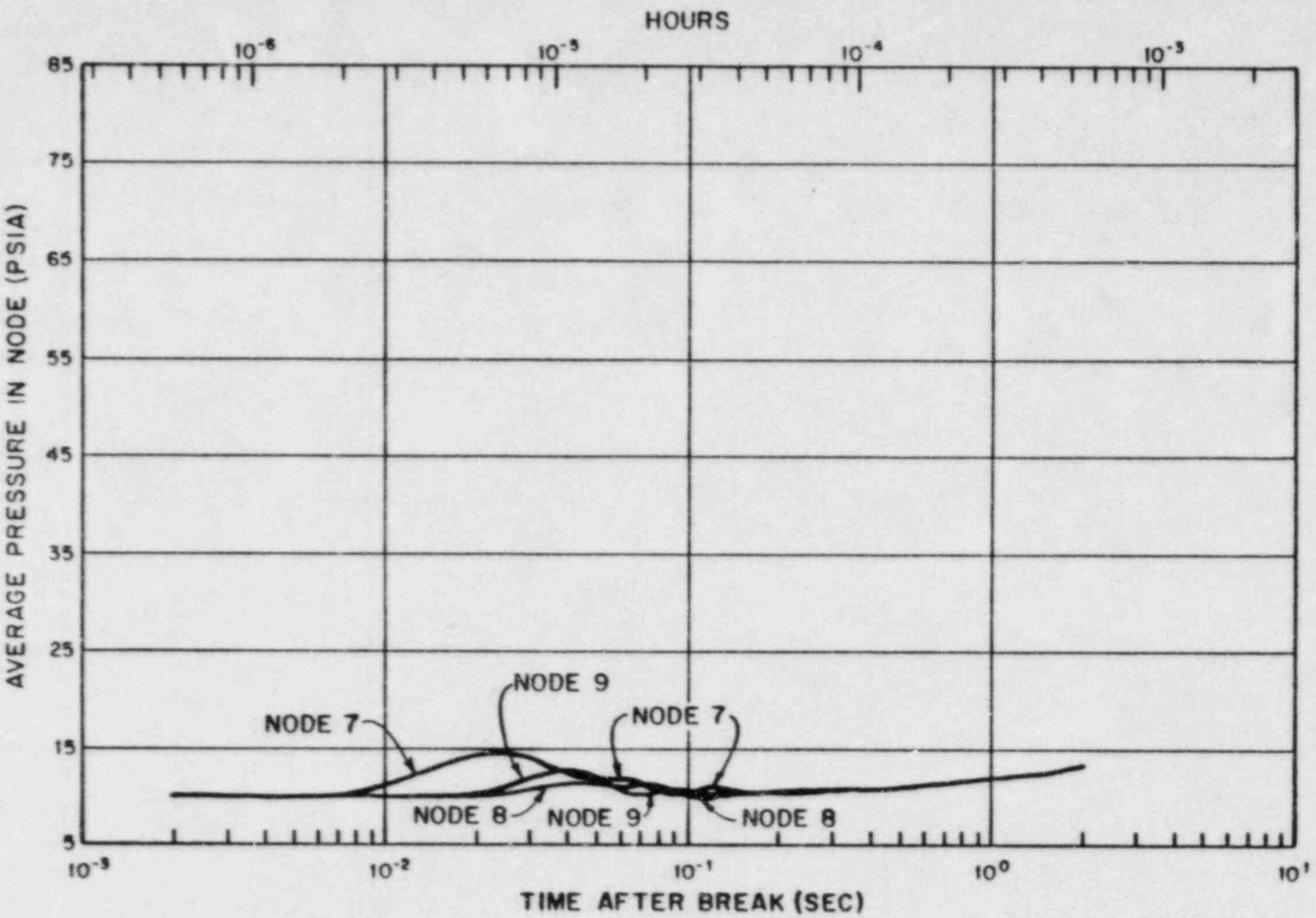

FIGURE Q480.37-9
REACTOR CAVITY PRESSURE TRANSIENTS
NODE NUMBERS 7,8,9
COLD LEG 100 SQ. IN. BREAK
MILLSTONE NUCLEAR POWER STATION
UNIT 3
FINAL SAFETY ANALYSIS REPORT

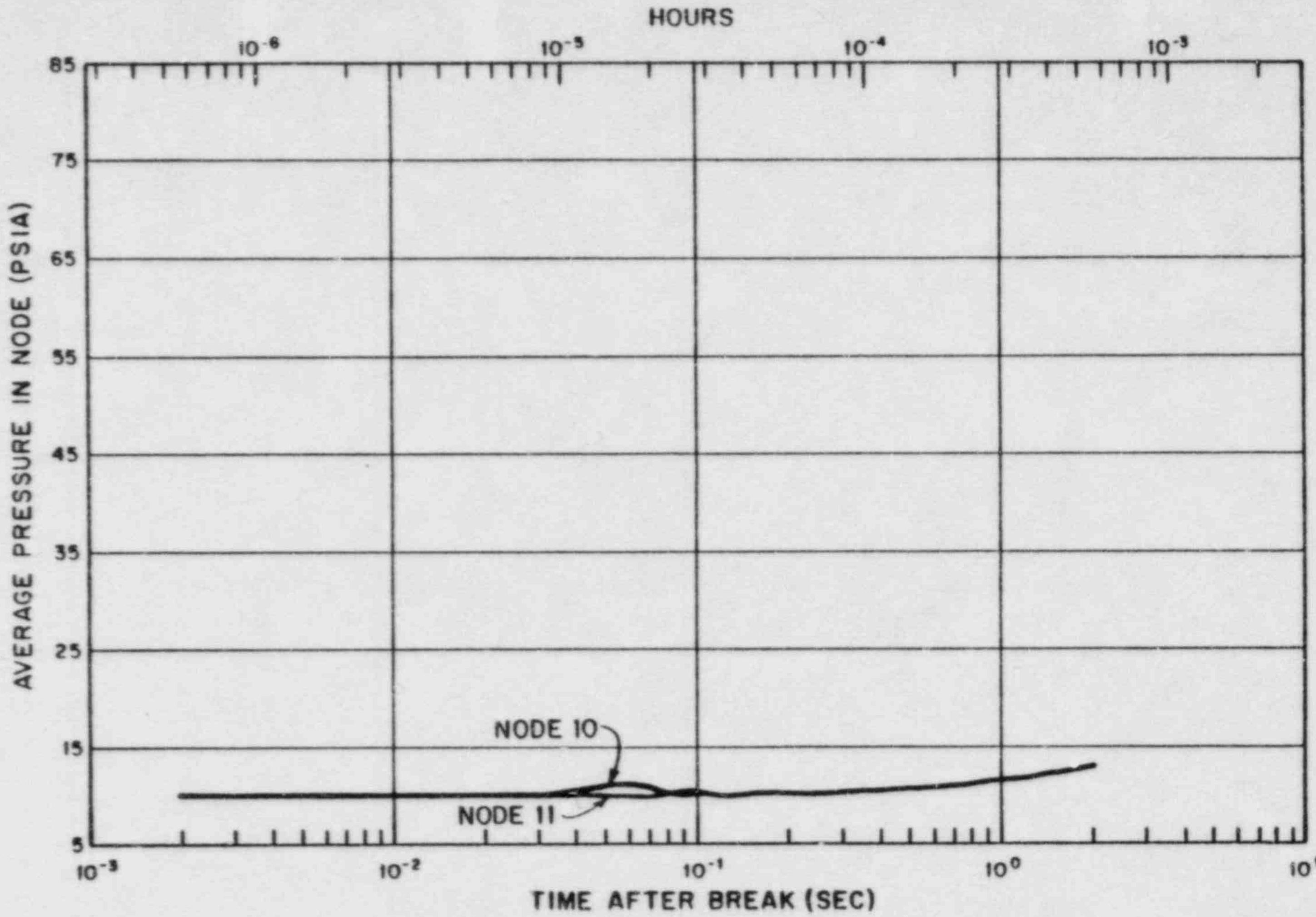

FIGURE Q480.37-10
REACTOR CAVITY PRESSURE TRANSIENTS
NODE NUMBERS 10,11
COLD LEG 100 SQ. IN. BREAK
MILLSTONE NUCLEAR POWER STATION
UNIT 3
FINAL SAFETY ANALYSIS REPORT

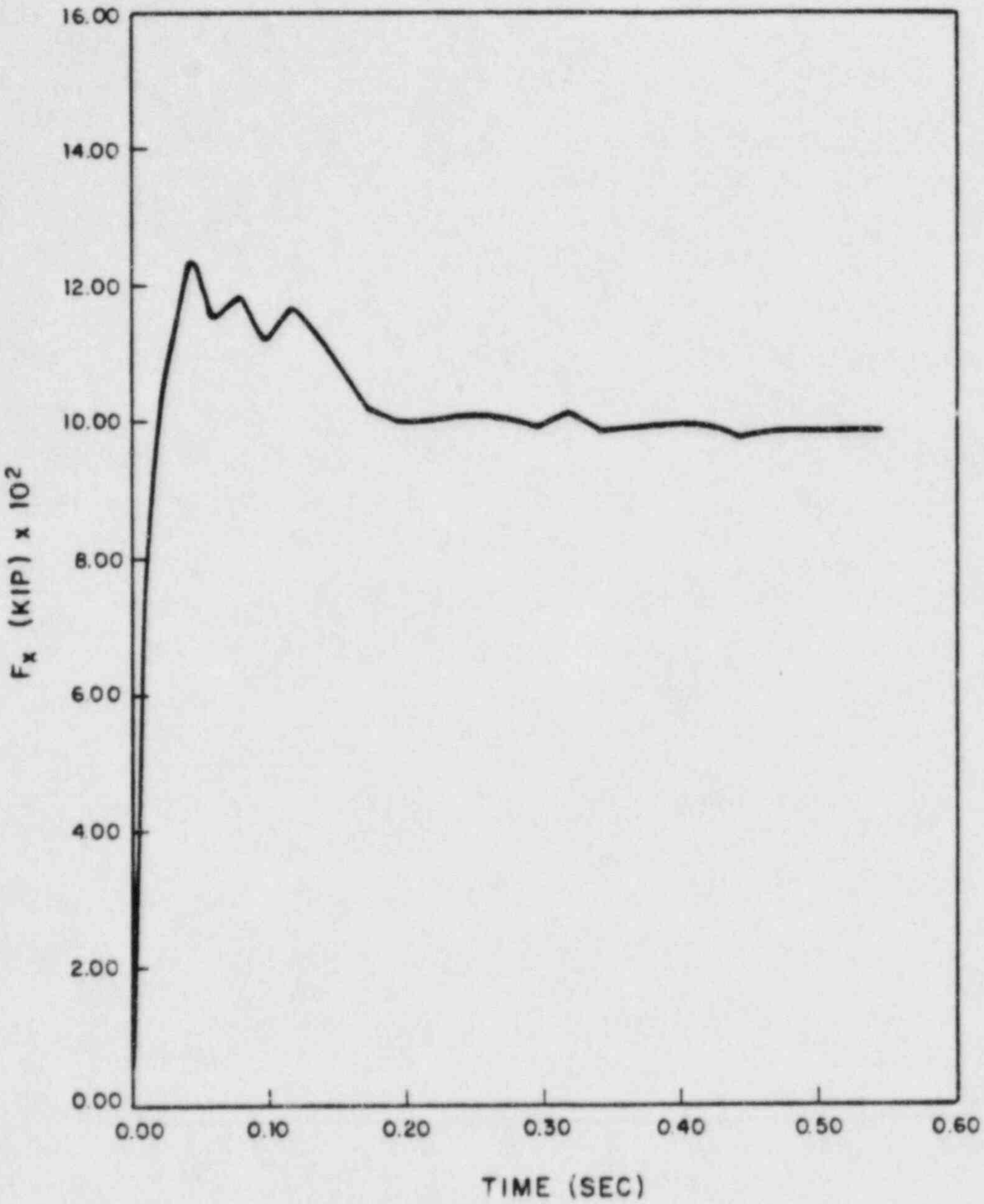

FIGURE Q480.37-11
HORIZONTAL FORCE ON RPV
AWAY FROM BREAK
MILLSTONE NUCLEAR POWER STATION
UNIT 3
FINAL SAFETY ANALYSIS REPORT

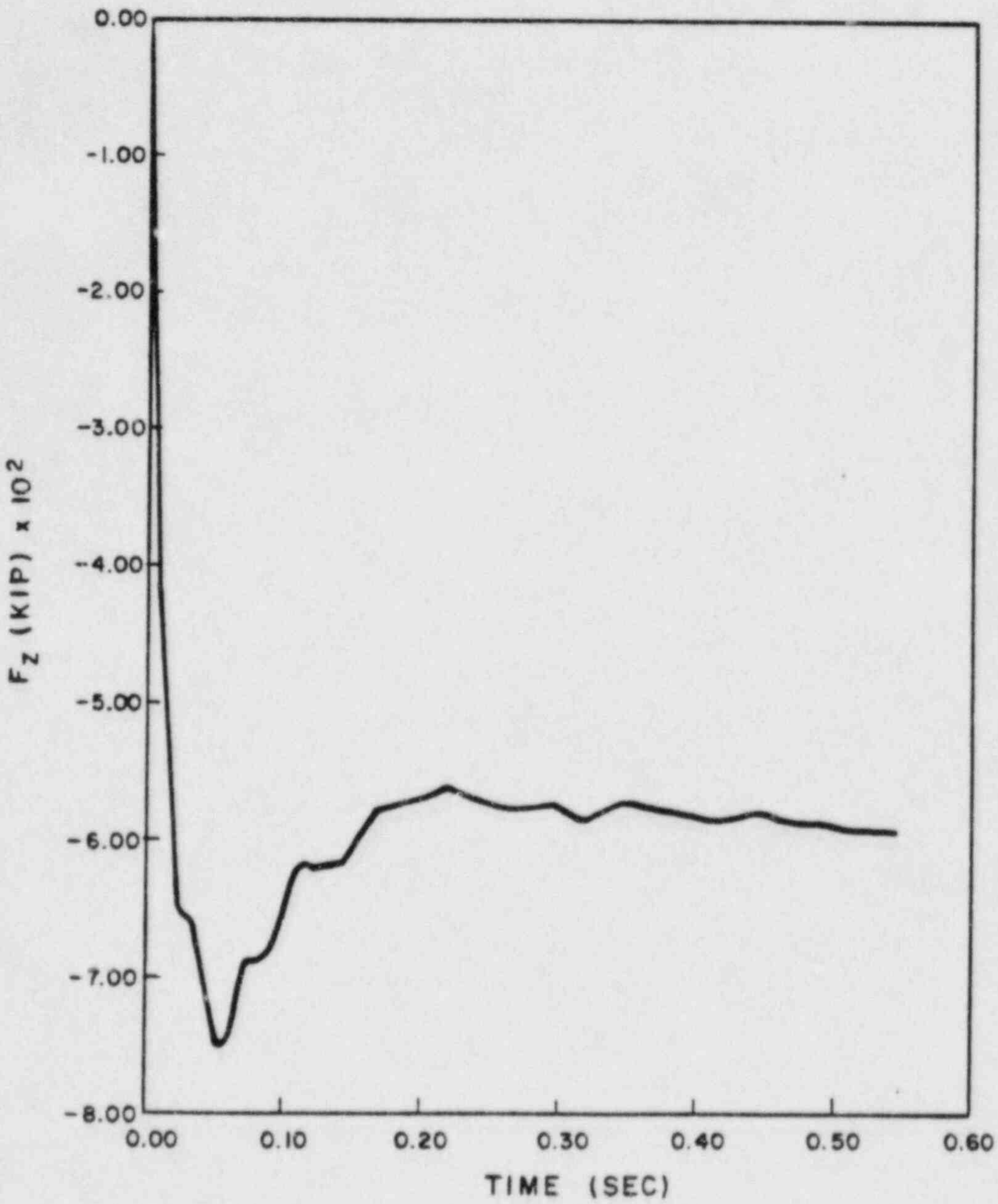

FIGURE Q480.37-12
VERTICAL UPWARD FORCE ON RPV AND TOP OF NST
MILLSTONE NUCLEAR POWER STATION
UNIT 3
FINAL SAFETY ANALYSIS REPORT

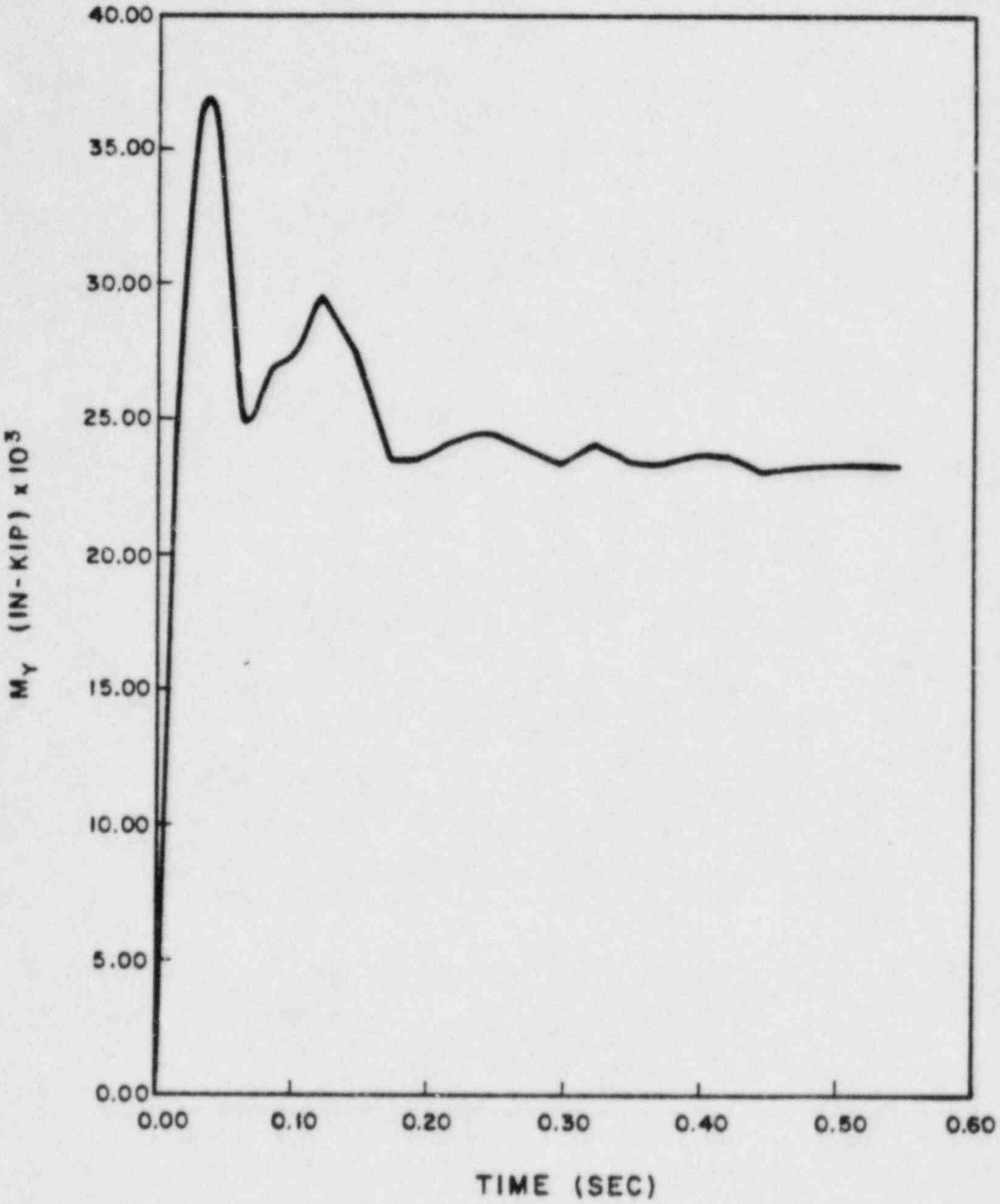

FIGURE Q480.37-13
OVERTURNING MOMENT ON
RPV AT ELEVATION 17'-6"
MILLSTONE NUCLEAR POWER STATION
UNIT 3
FINAL SAFETY ANALYSIS REPORT

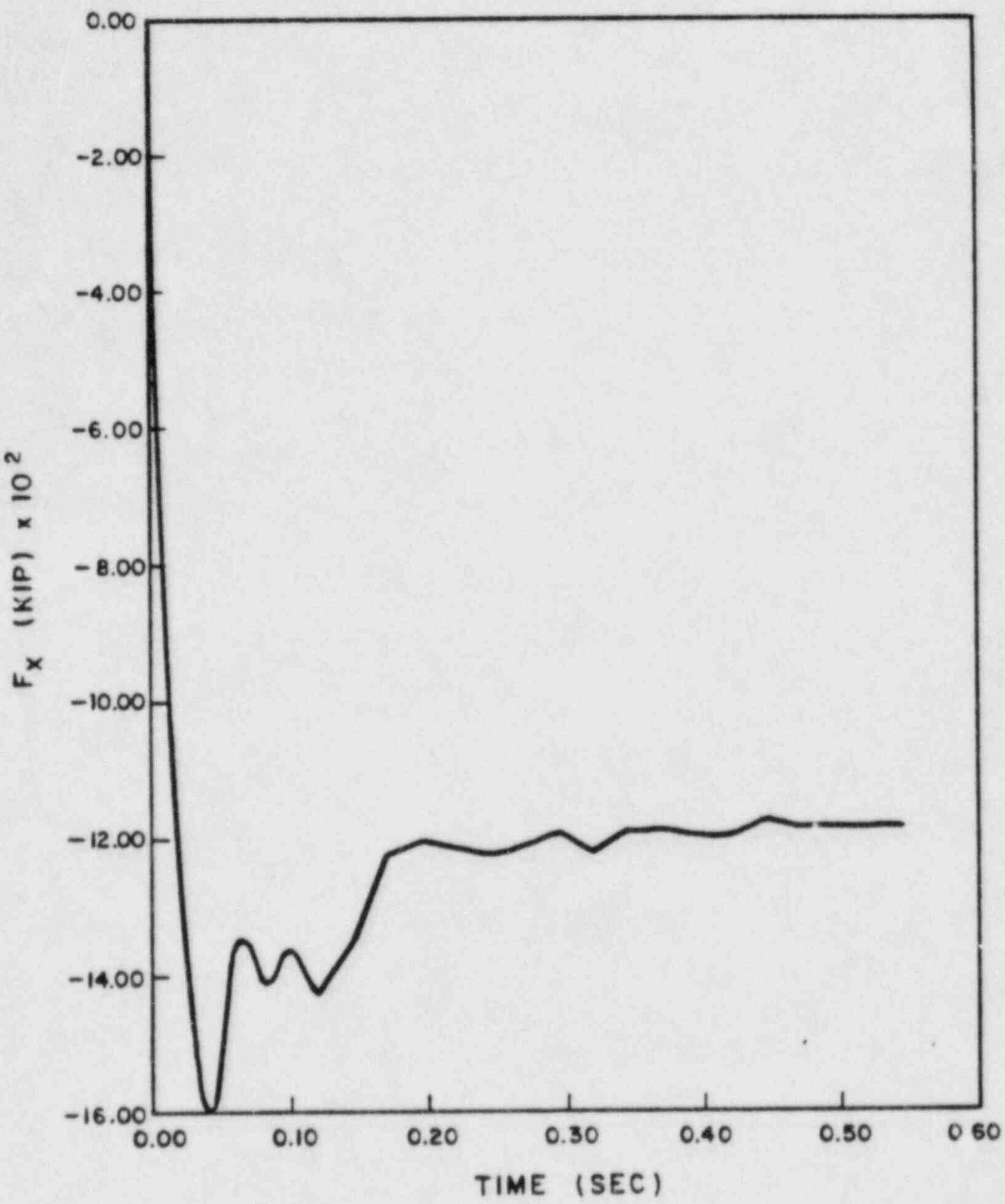

FIGURE Q480.37-14
HORIZONTAL FORCE ON PSW/
NST AWAY FROM BREAK
MILLSTONE NUCLEAR POWER STATION
UNIT 3
FINAL SAFETY ANALYSIS REPORT

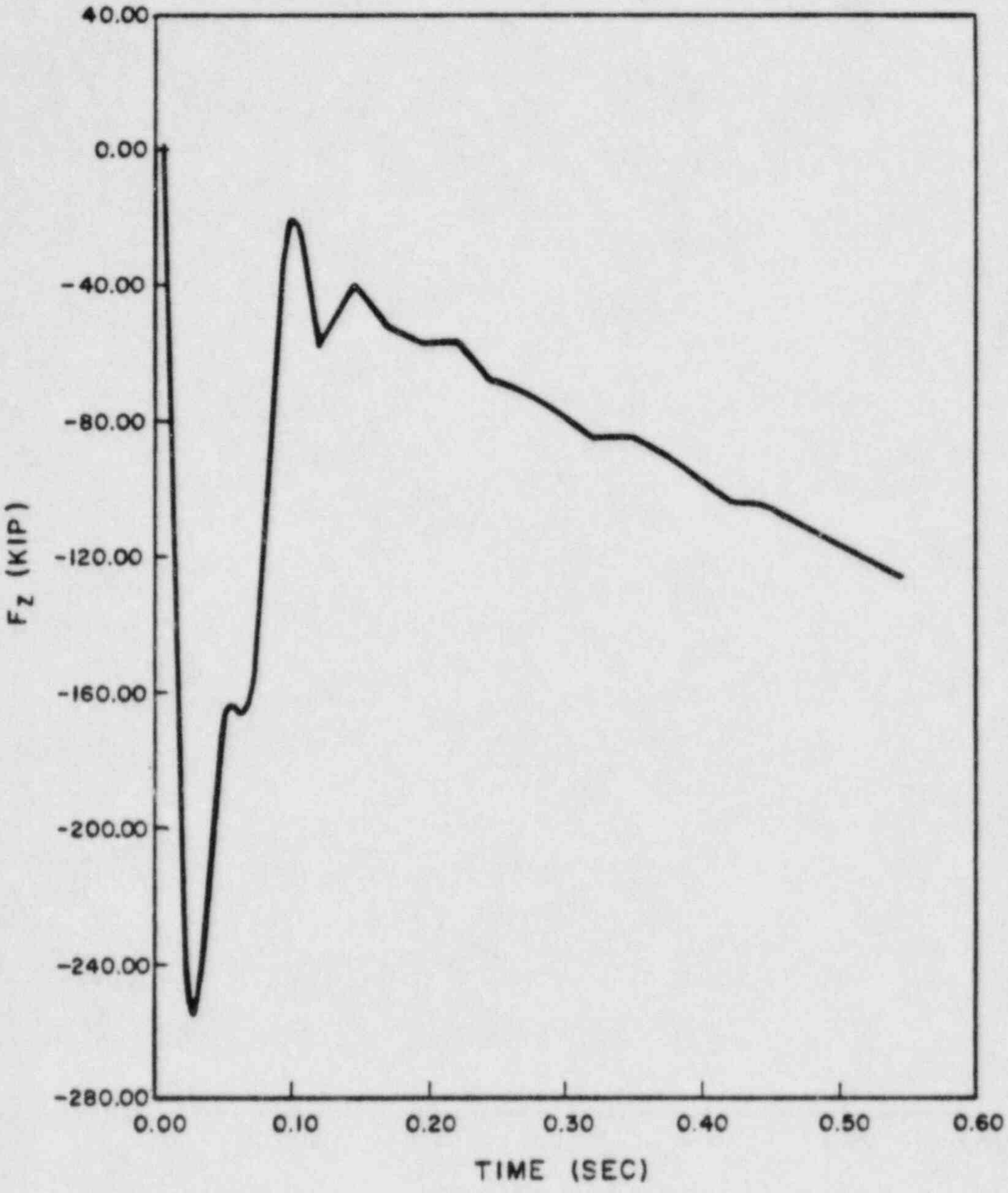

FIGURE Q480.37-15
VERTICAL UPWARD FORCE ON PSW
MILLSTONE NUCLEAR POWER STATION
UNIT 3
FINAL SAFETY ANALYSIS REPORT

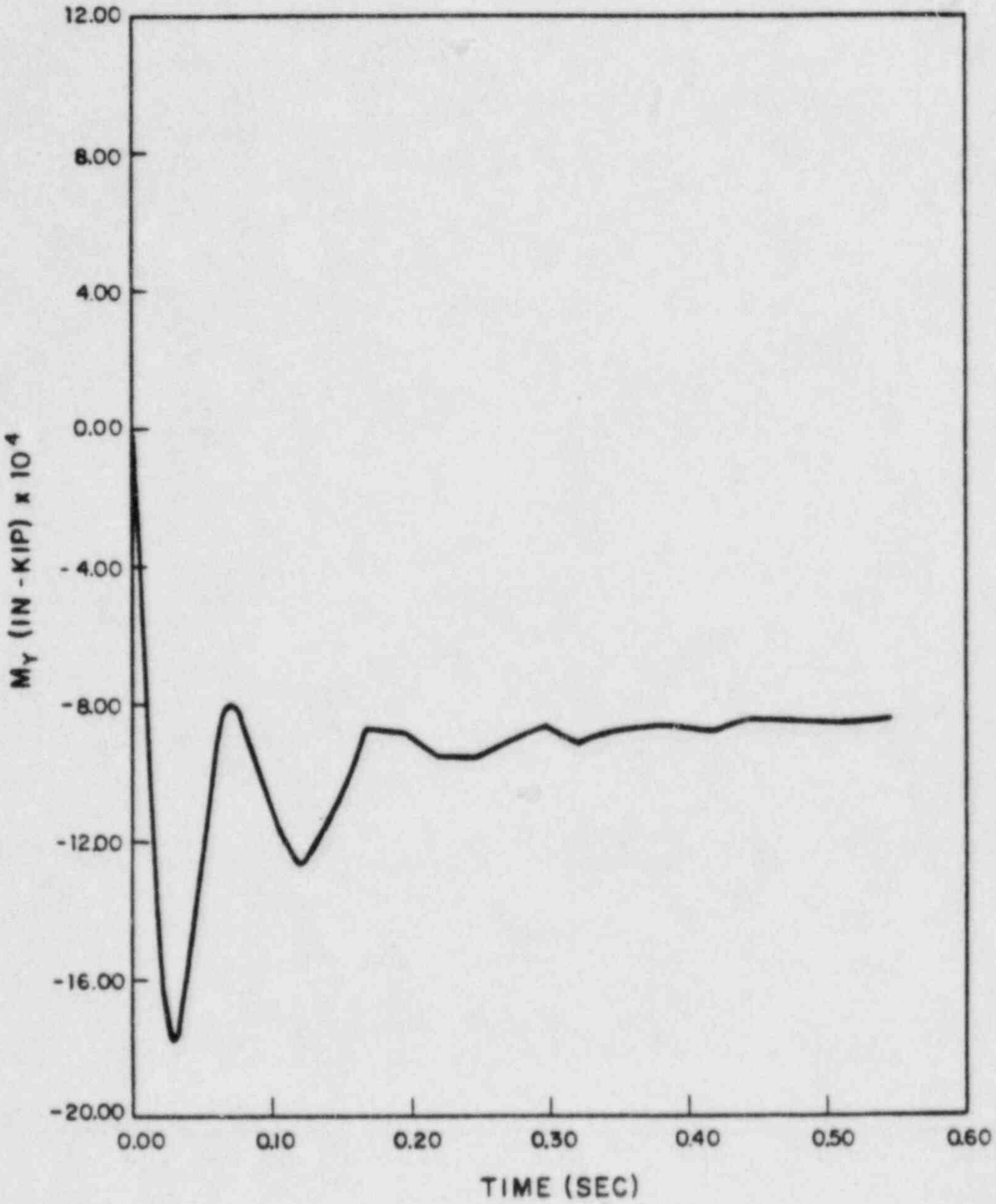

FIGURE Q 480.37-16
OVERTURNING MOMENT ON
PSW/NST AT ELEVATION 17'-6"
MILLSTONE NUCLEAR POWER STATION
UNIT 3
FINAL SAFETY ANALYSIS REPORT

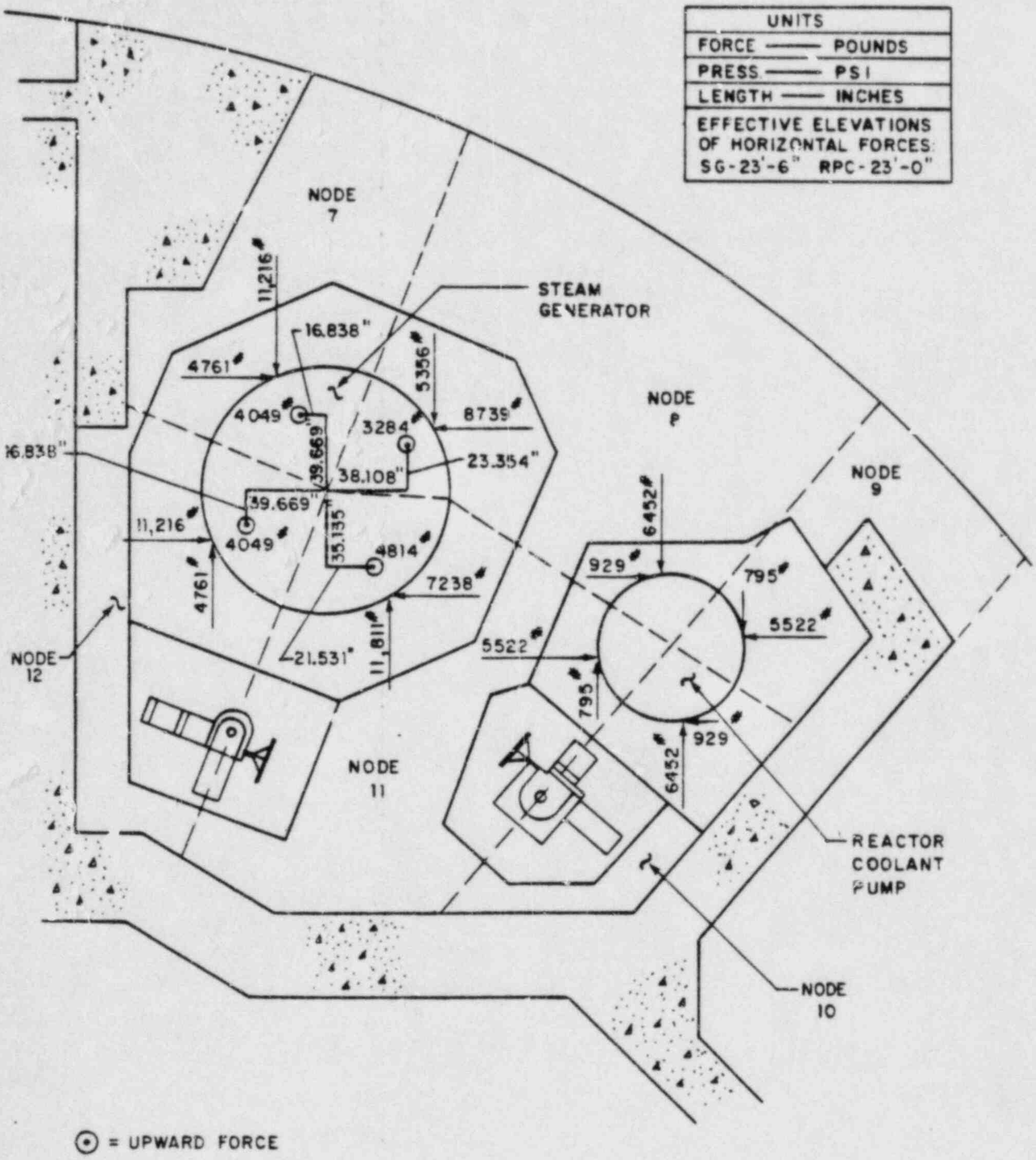

FIGURE Q480.37-17
FORCES ON STEAM GENERATOR AND PUMP DUE TO UNIT PRESSURE IN EACH NODE BETWEEN ELEVATIONS 17'-6" AND 28'-6"
MILLSTONE NUCLEAR POWER STATION
UNIT 3
FINAL SAFETY ANALYSIS REPORT

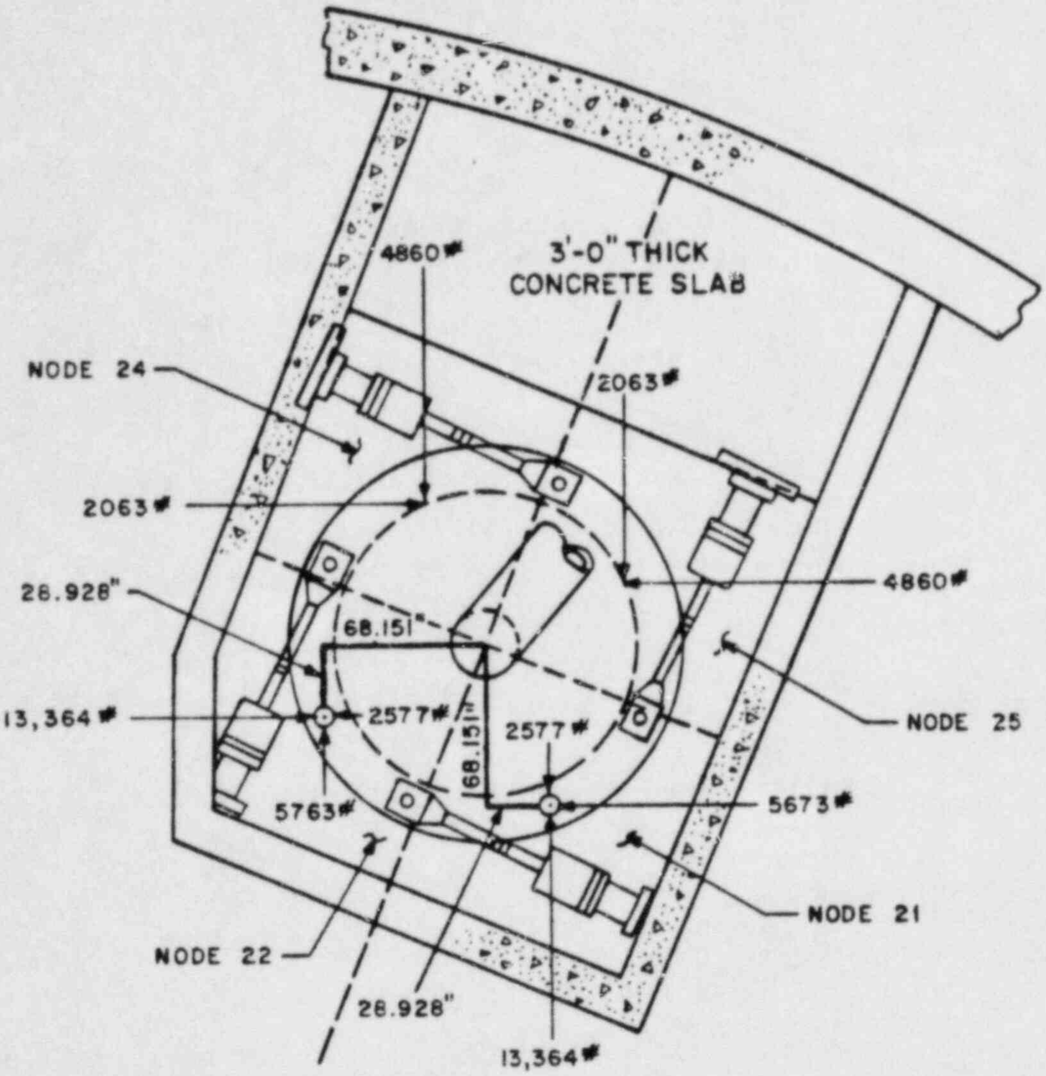

NOT SHOWN NODE	OPPOSITE
19	21
20	22
26	24
27	25

EFFECTIVE ELEVATIONS OF HORIZONTAL FORCES	
NODES	ELEV
19 - 22	57'-1 13/16"
24 - 27	49' - 10"

⊙ = UPWARD FORCE

FIGURE Q480.37-18
FORCES ON STEAM GENERATOR
DUE TO UNIT PRESSURES
BETWEEN ELEVATIONS 51'-4"
& 61'-4" (NODES 19-22) OR
48'-4" & 51'-4" (NODES 24-27)
MILLSTONE NUCLEAR POWER STATION
UNIT 3
FINAL SAFETY ANALYSIS REPORT

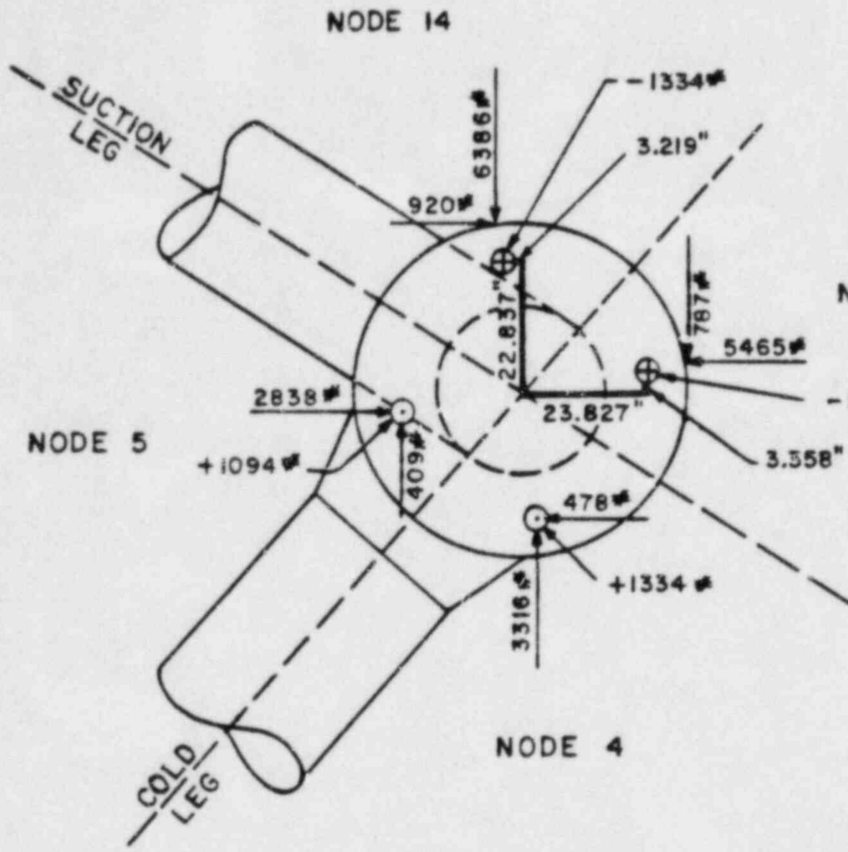

NOT SHOWN	
NODE	OPPOSITE
2	4
3	5
16	14
17	15

EFFECTIVE ELEVATIONS OF HORIZONTAL FORCES	
NODES	ELEV
2 - 5	14'-7"
14 - 17	33'-9 3/8"

⊙ = UPWARD FORCE

⊕ = DOWNWARD FORCE

FIGURE Q480.37-19
FORCES ON REACTOR COOLANT PUMP DUE TO UNIT PRESSURES BETWEEN ELEVATIONS 3'-8" & 17'-6" (NODES 2-5) OR 28'-6" & 48'-4" (NODES 14-17)
MILLSTONE NUCLEAR POWER STATION UNIT 3
FINAL SAFETY ANALYSIS REPORT

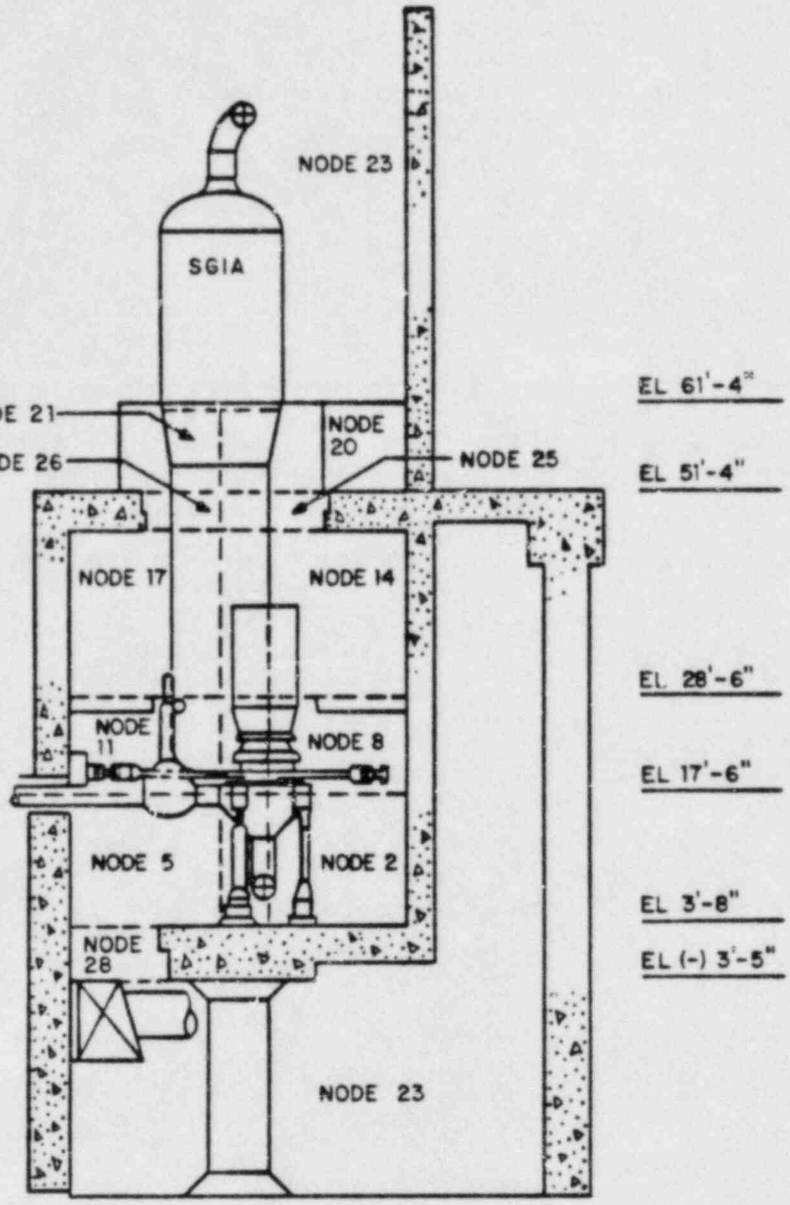

SECTION 1-1

NODE 23 IS THE CONTAINMENT

FIGURE Q480.37-20

ELEVATION VIEW (SECTION 1-1) OF THE STEAM GENERATOR CUBICLE 1A

MILLSTONE NUCLEAR POWER STATION UNIT 3

FINAL SAFETY ANALYSIS REPORT

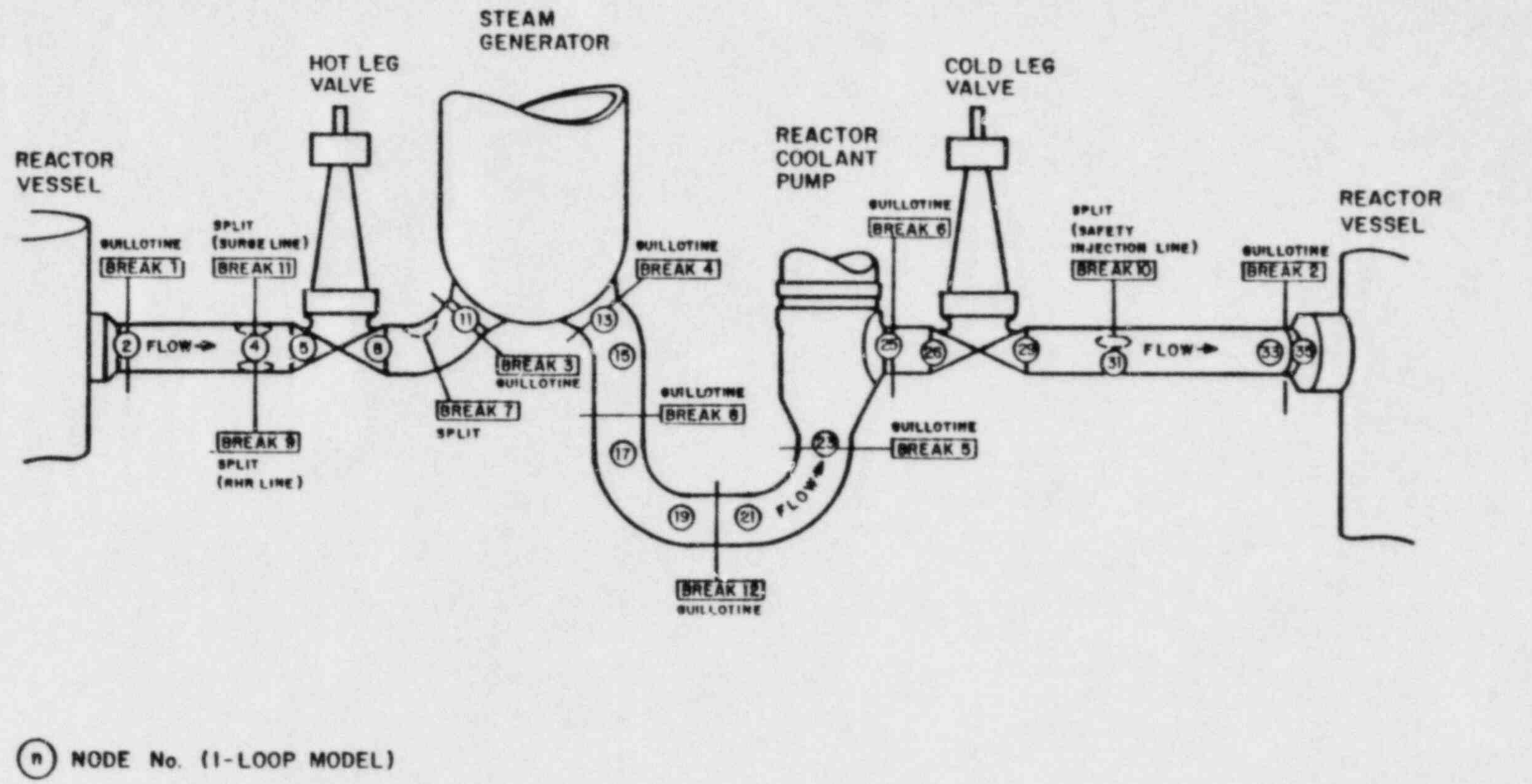

FIGURE Q480.37-21
POSTULATED BREAK LOCATIONS IN SG CUBICLE (WCAP-8082)
MILLSTONE NUCLEAR POWER STATION
UNIT 3
FINAL SAFETY ANALYSIS REPORT

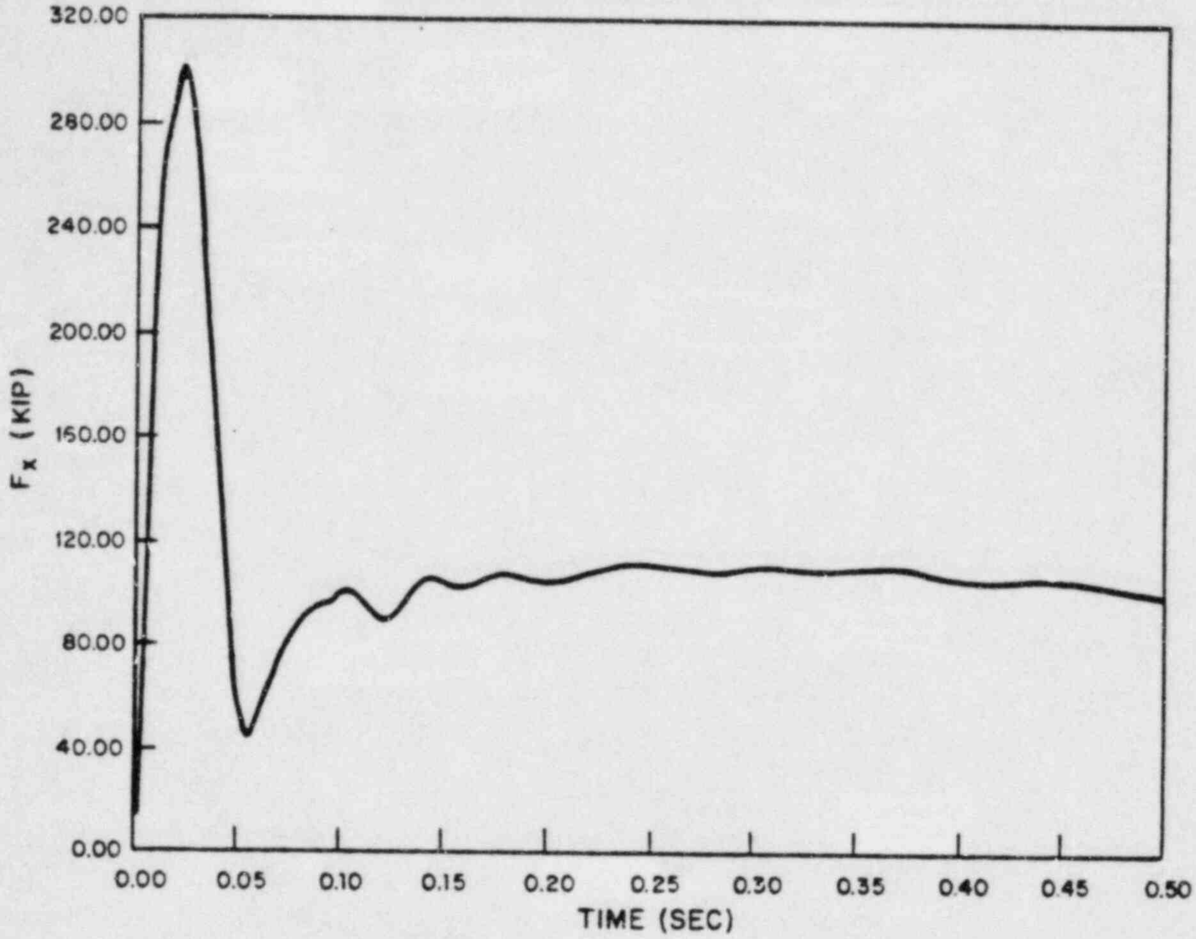

FIGURE Q480.37-22

NET FORCE IN GLOBAL X DIRECTION ON SG - BREAK 7

MILLSTONE NUCLEAR POWER STATION
UNIT 3
FINAL SAFETY ANALYSIS REPORT

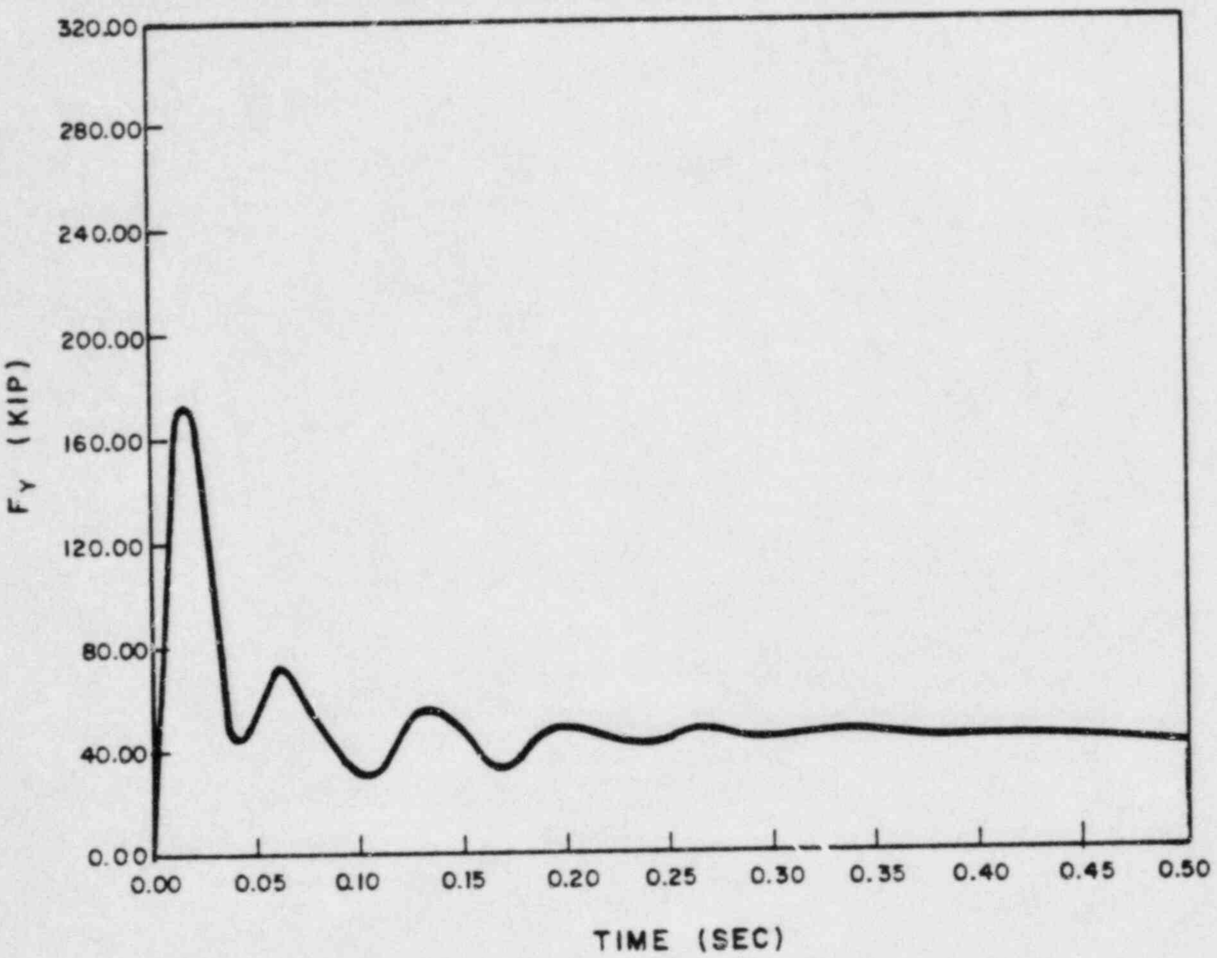

FIGURE Q480.37-23
NET FORCE IN GLOBAL Y
DIRECTION ON SG-BREAK 7
MILLSTONE NUCLEAR POWER STATION
UNIT 3
FINAL SAFETY ANALYSIS REPORT

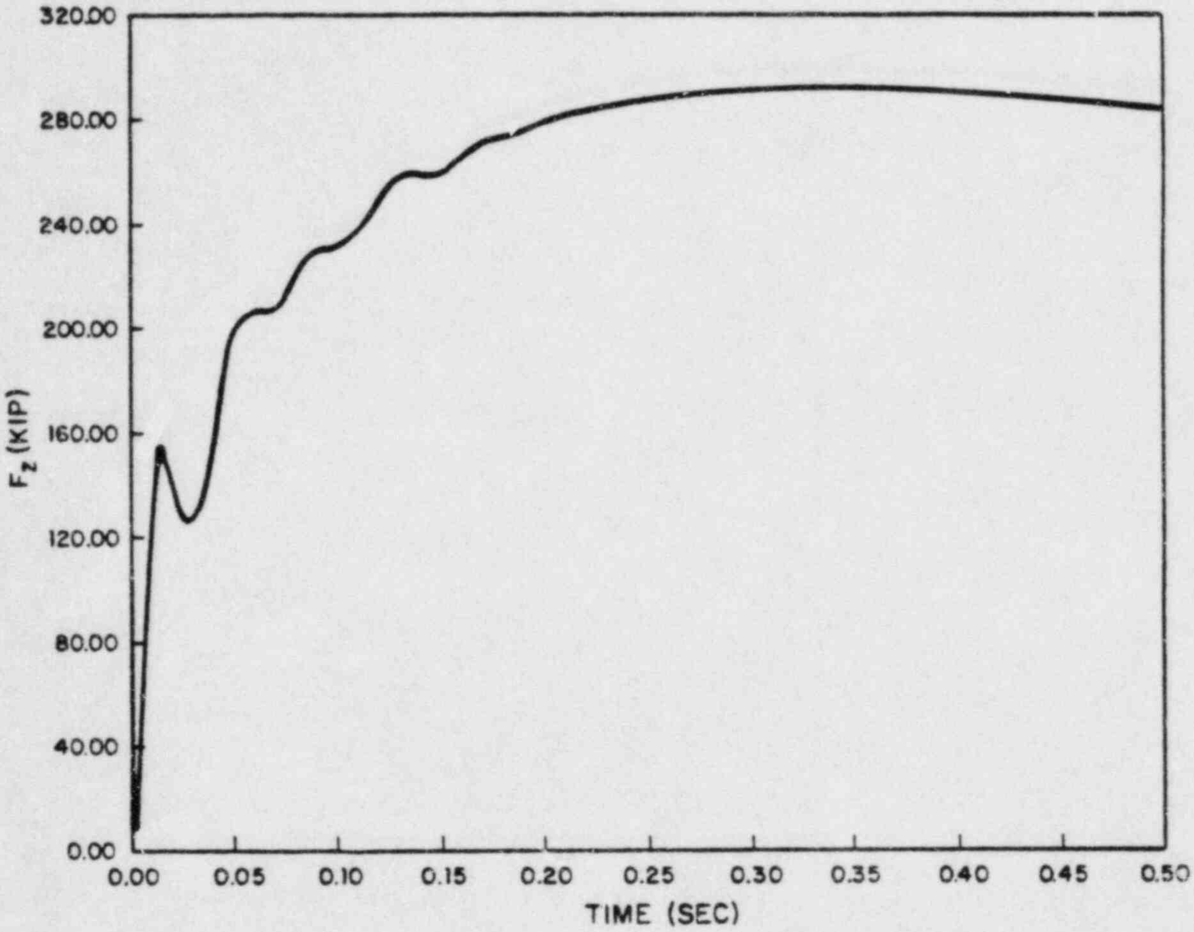

FIGURE Q480.37-24
NET FORCE IN GLOBAL Z DIRECTION ON SG-BREAK 7
MILLSTONE NUCLEAR POWER STATION
UNIT 3
FINAL SAFETY ANALYSIS REPORT

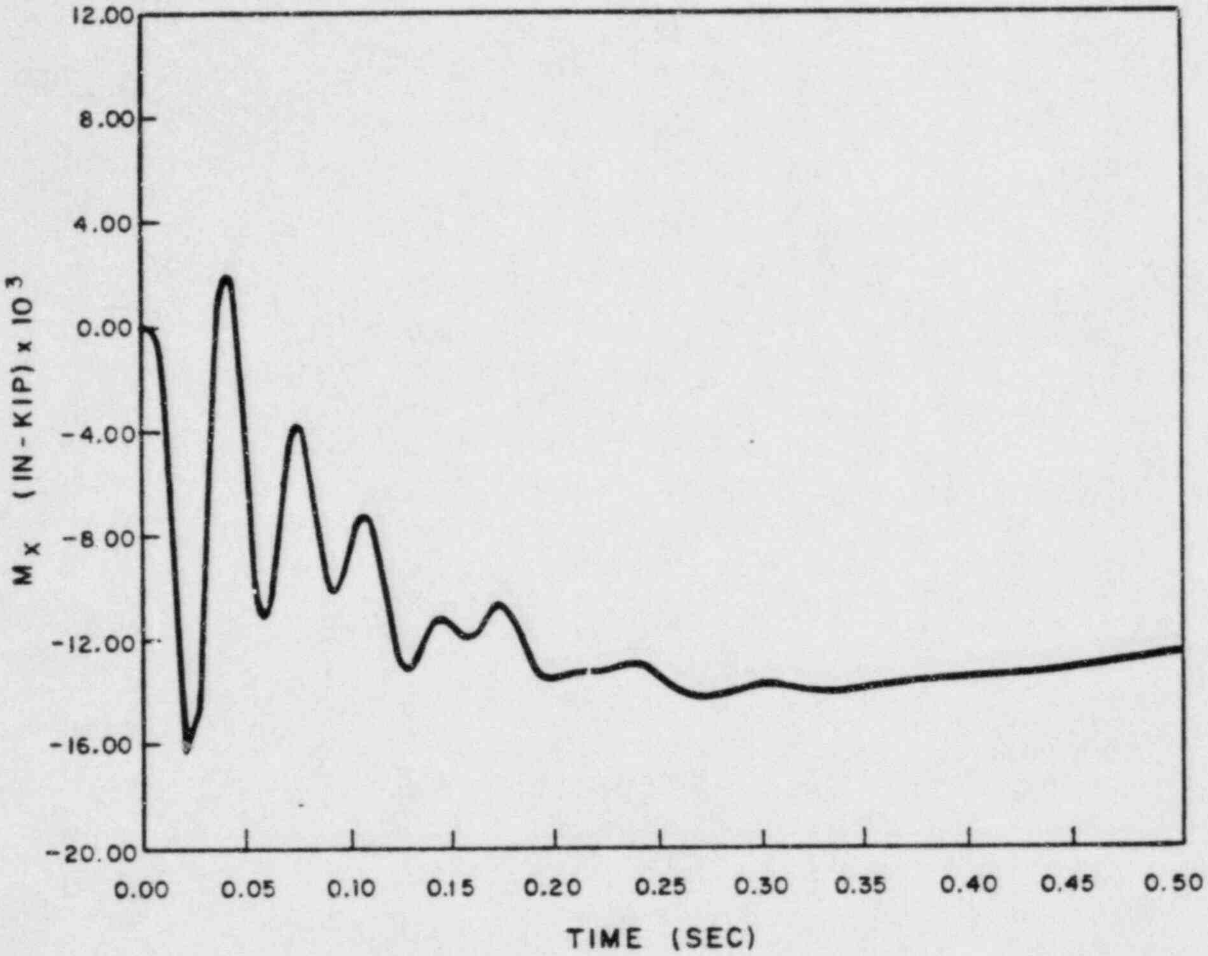

FIGJRE Q480.37-25

NET MOMENT ABOUT GLOBAL X AXIS AT SG NODE 12 - BREAK 7

MILLSTONE NUCLEAR POWER STATION

UNIT 3

FINAL SAFETY ANALYSIS REPORT

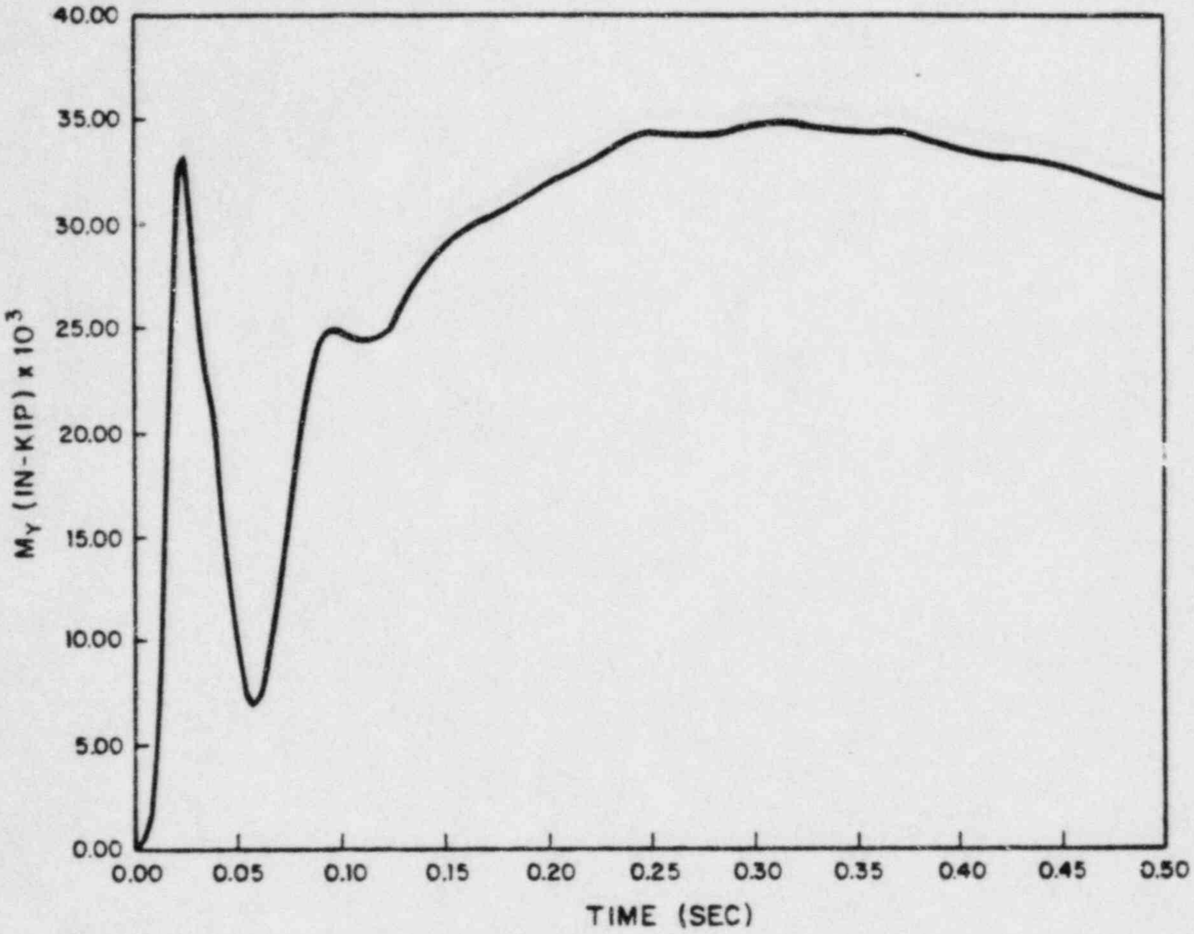

FIGURE Q480.37-26

NET MOMENT ABOUT GLOBAL Y AXIS AT SG NODE 12-BREAK 7

MILLSTONE NUCLEAR POWER STATION
UNIT 3
FINAL SAFETY ANALYSIS REPORT

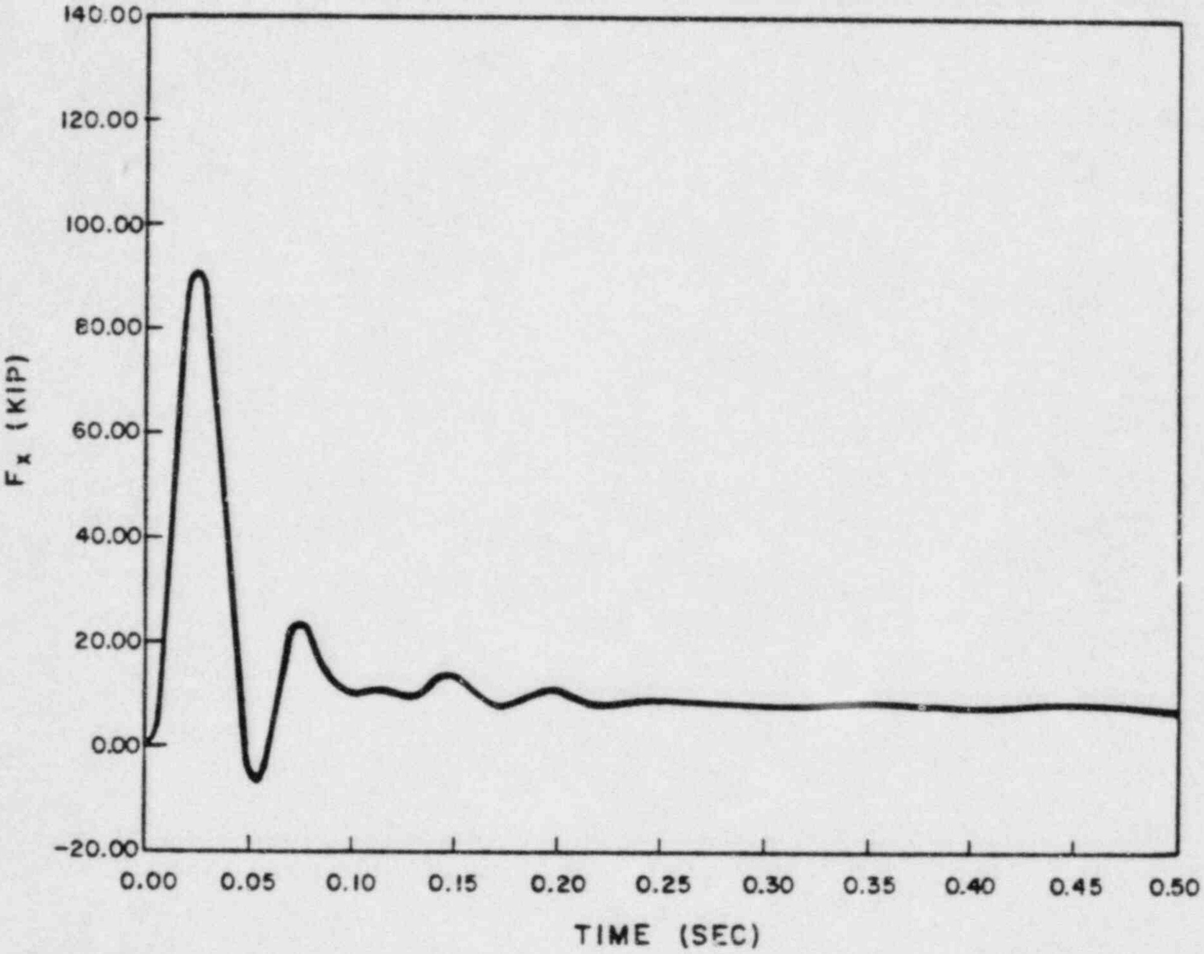

FIGURE Q480.37-27
NET FORCE IN GLOBAL X
DIRECTION ON RCP - BREAK 7
MILLSTONE NUCLEAR POWER STATION
UNIT 3
FINAL SAFETY ANALYSIS REPORT

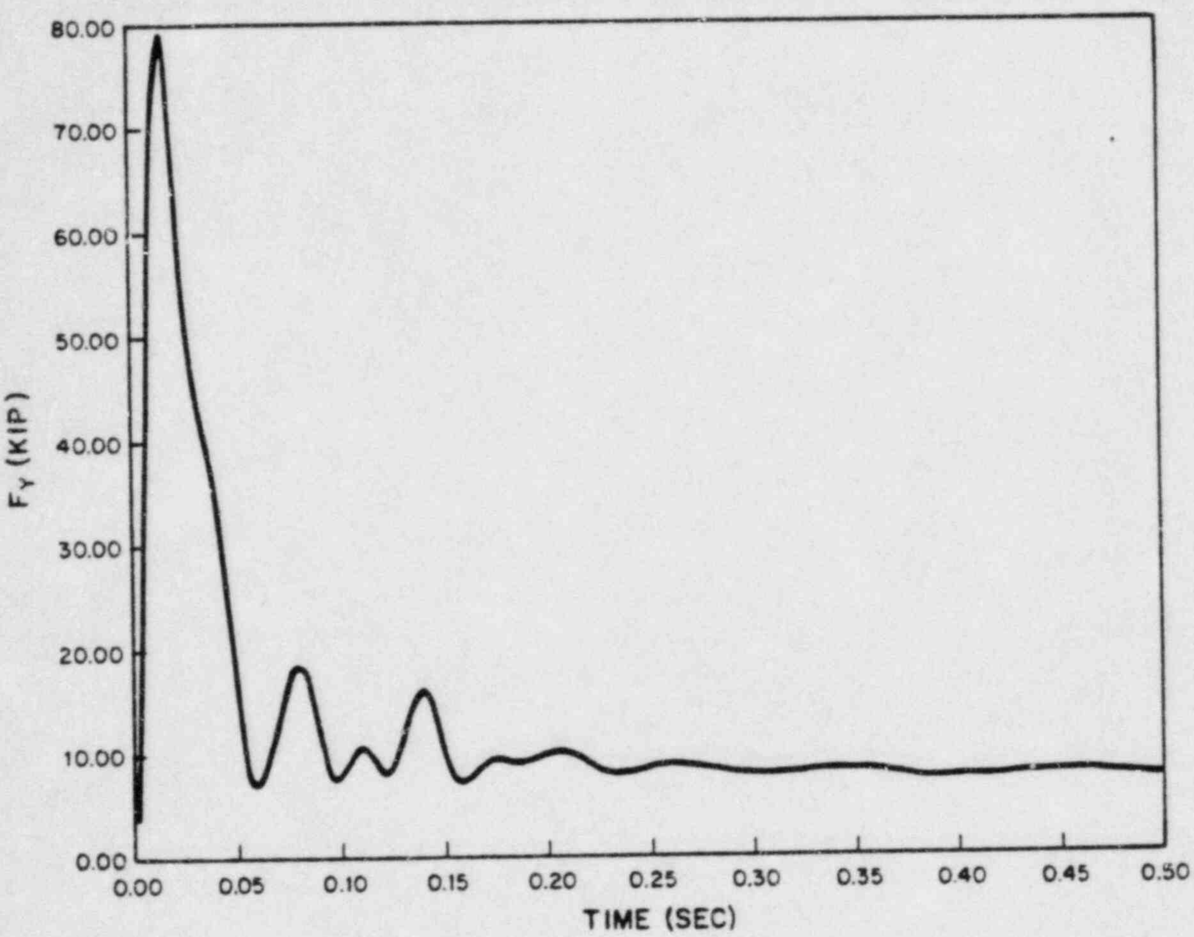

FIGURE Q480.37-28
NET FORCE IN GLOBAL Y
DIRECTION ON RCP-BREAK 7
MILLSTONE NUCLEAR POWER STATION
UNIT 3
FINAL SAFETY ANALYSIS REPORT

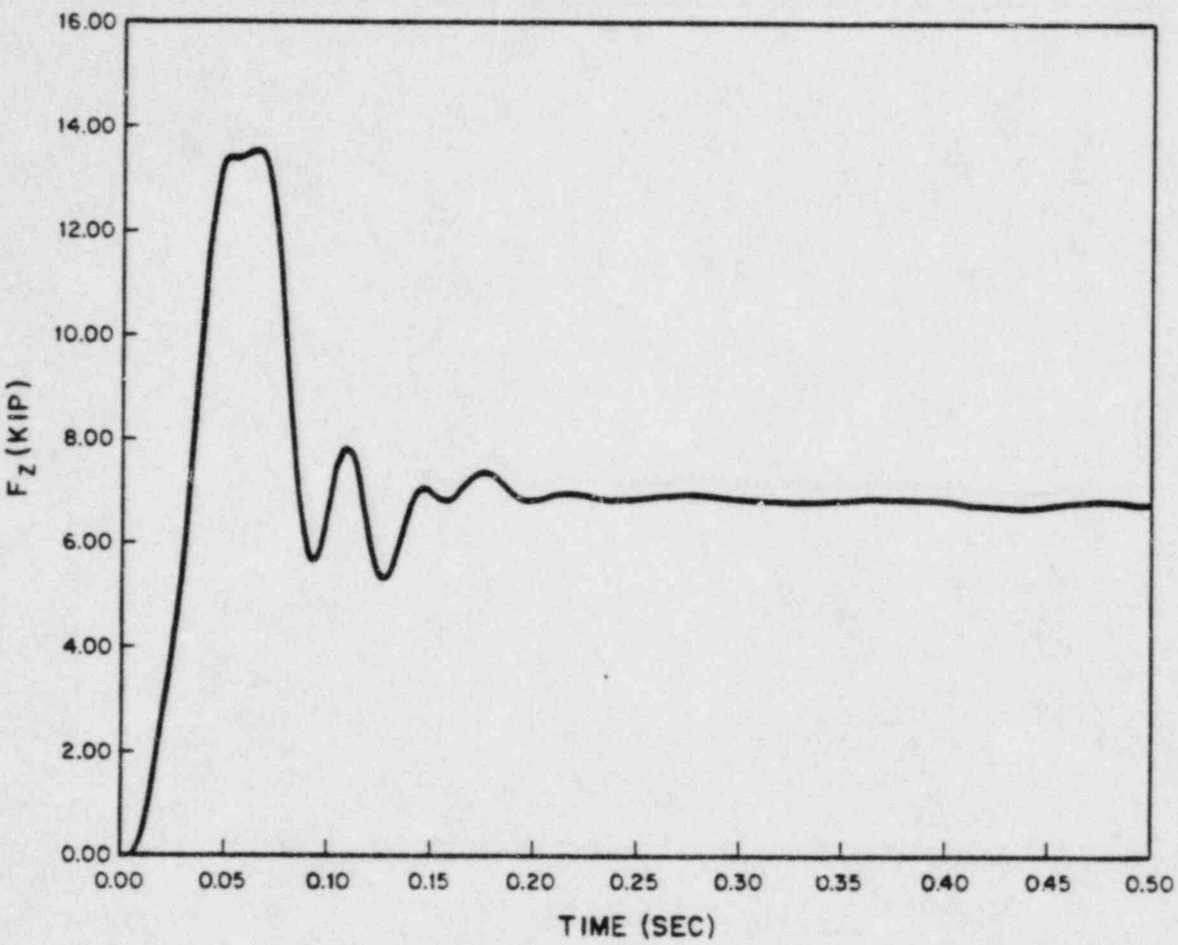

FIGURE Q480.37-29
NET FORCE IN GLOBAL Z
DIRECTION ON RCP-BREAK 7
MILLSTONE NUCLEAR POWER STATION
UNIT 3
FINAL SAFETY ANALYSIS REPORT

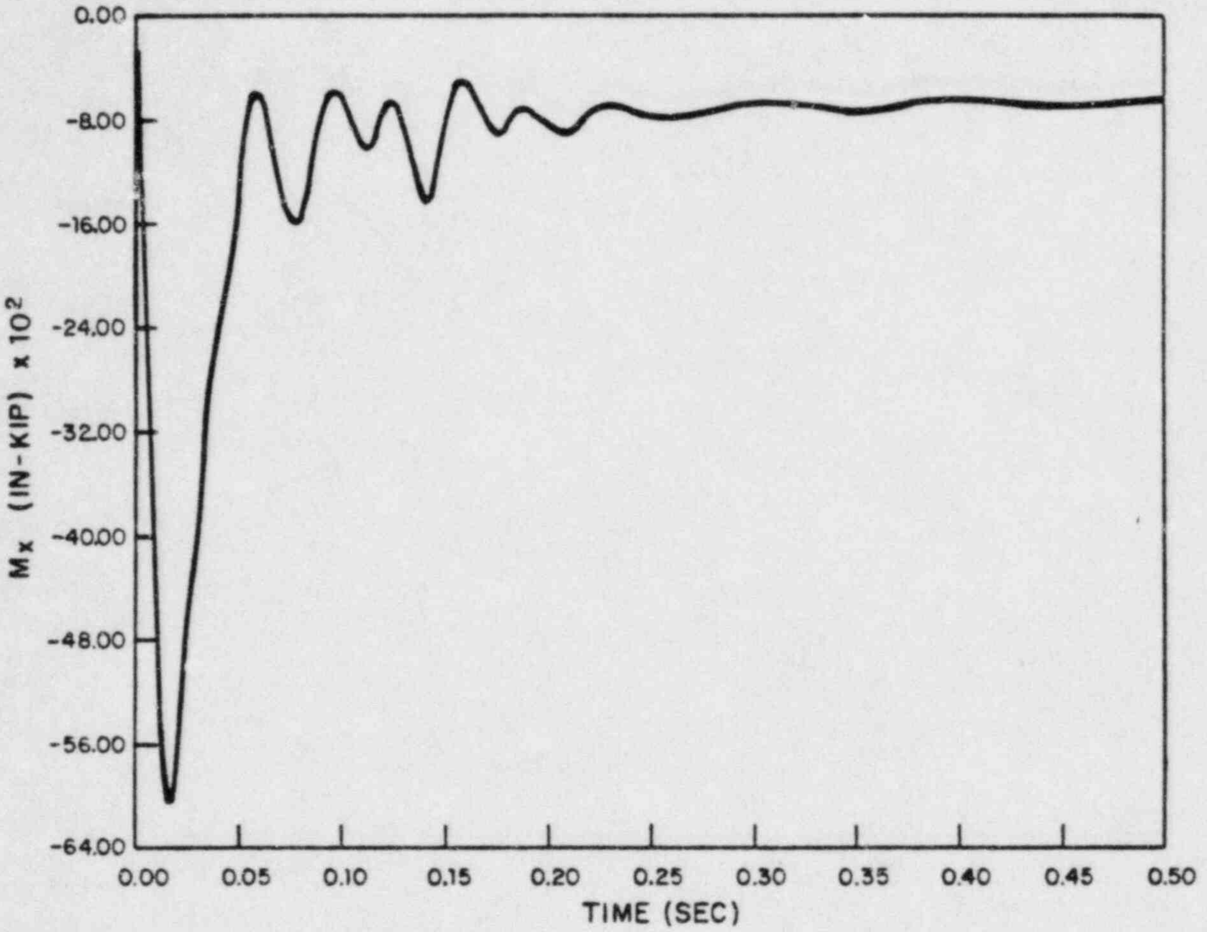

FIGURE Q480.37-30

NET MOMENT ABOUT GLOBAL X AXIS AT RCP NODE 24- BREAK 7

MILLSTONE NUCLEAR POWER STATION
UNIT 3
FINAL SAFETY ANALYSIS REPORT

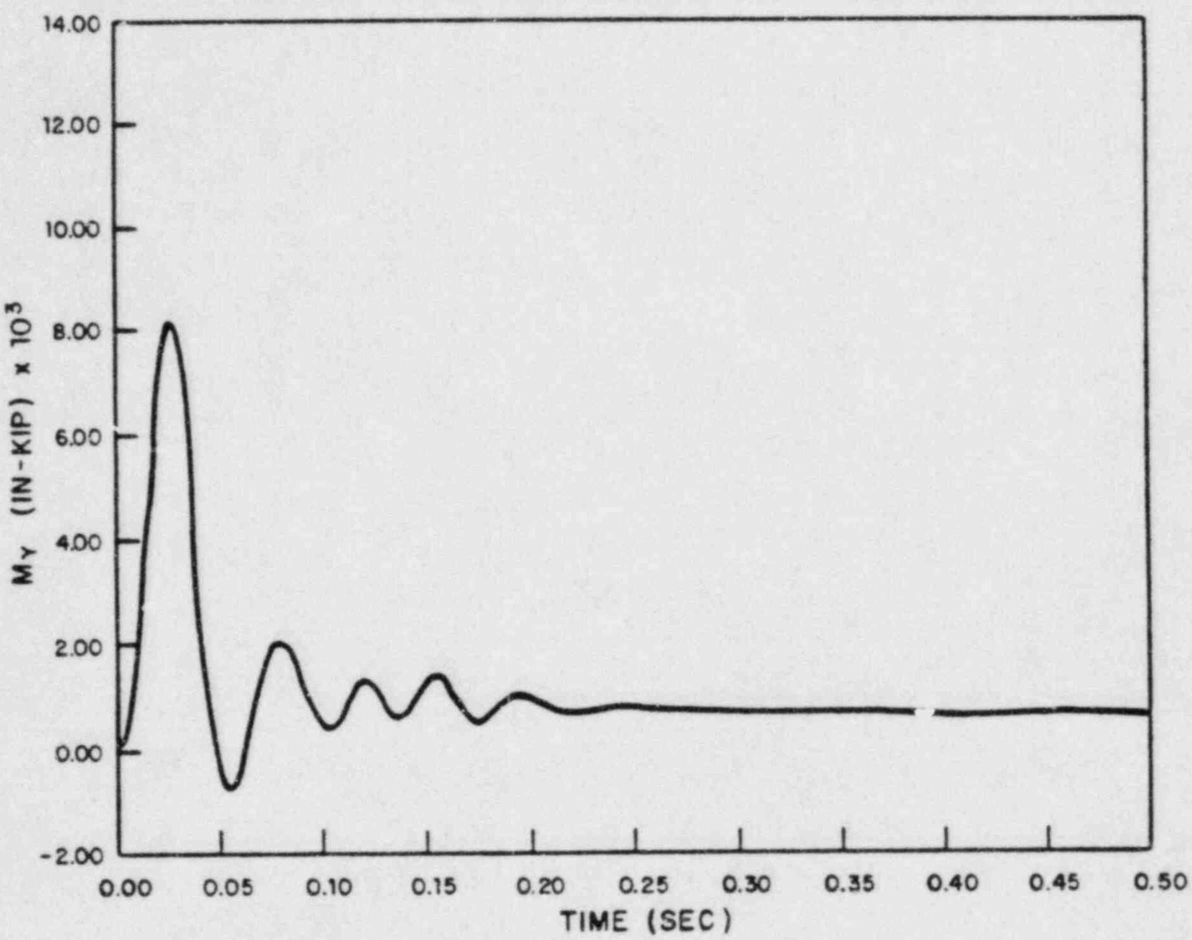

FIGURE Q480.37-31

NET MOMENT ABOUT GLOBAL Y AXIS AT RCP NODE 24 - BREAK 7

MILLSTONE NUCLEAR POWER STATION
UNIT 3
FINAL SAFETY ANALYSIS REPORT

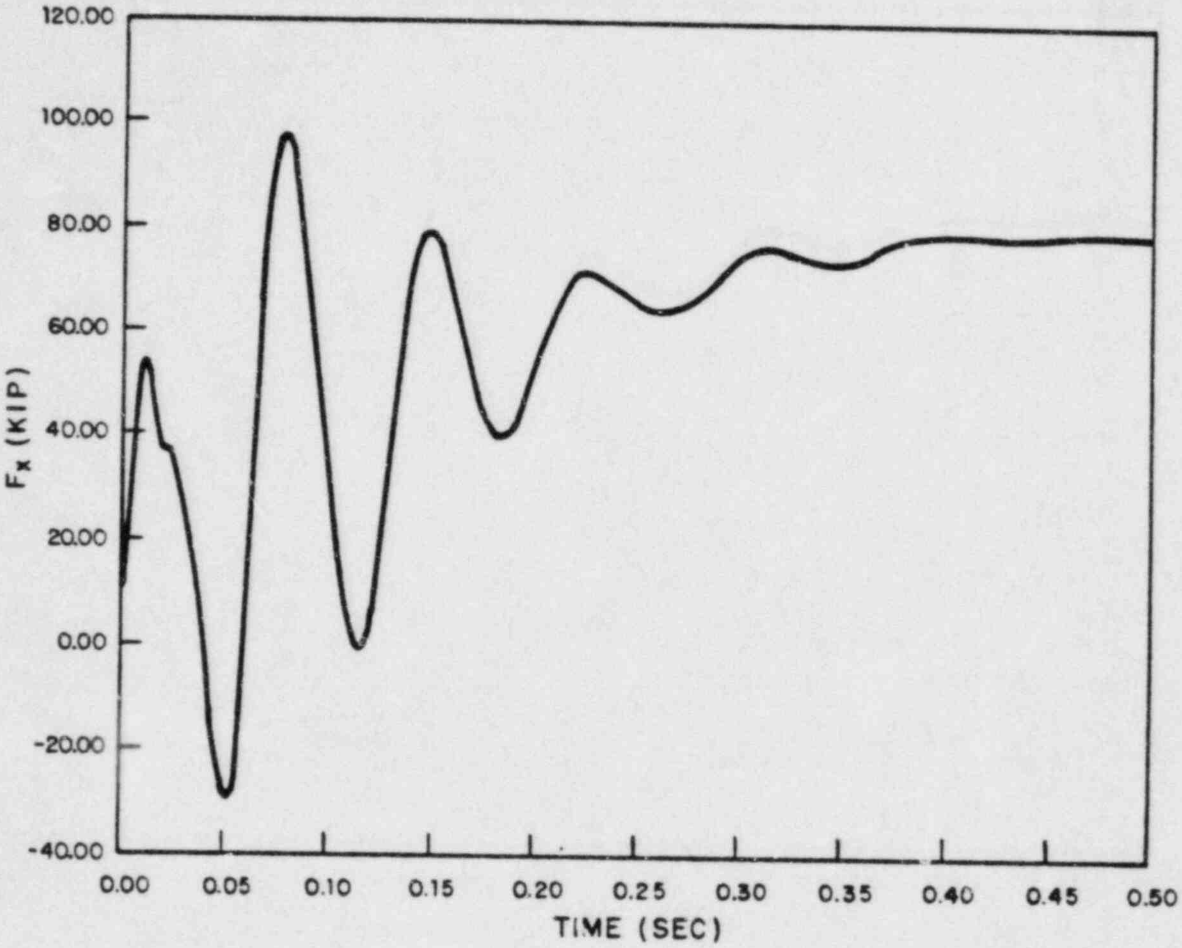

FIGURE Q480.37-32

NET FORCE IN GLOBAL X DIRECTION ON SG - BREAK 4

MILLSTONE NUCLEAR POWER STATION
UNIT 3
FINAL SAFETY ANALYSIS REPORT

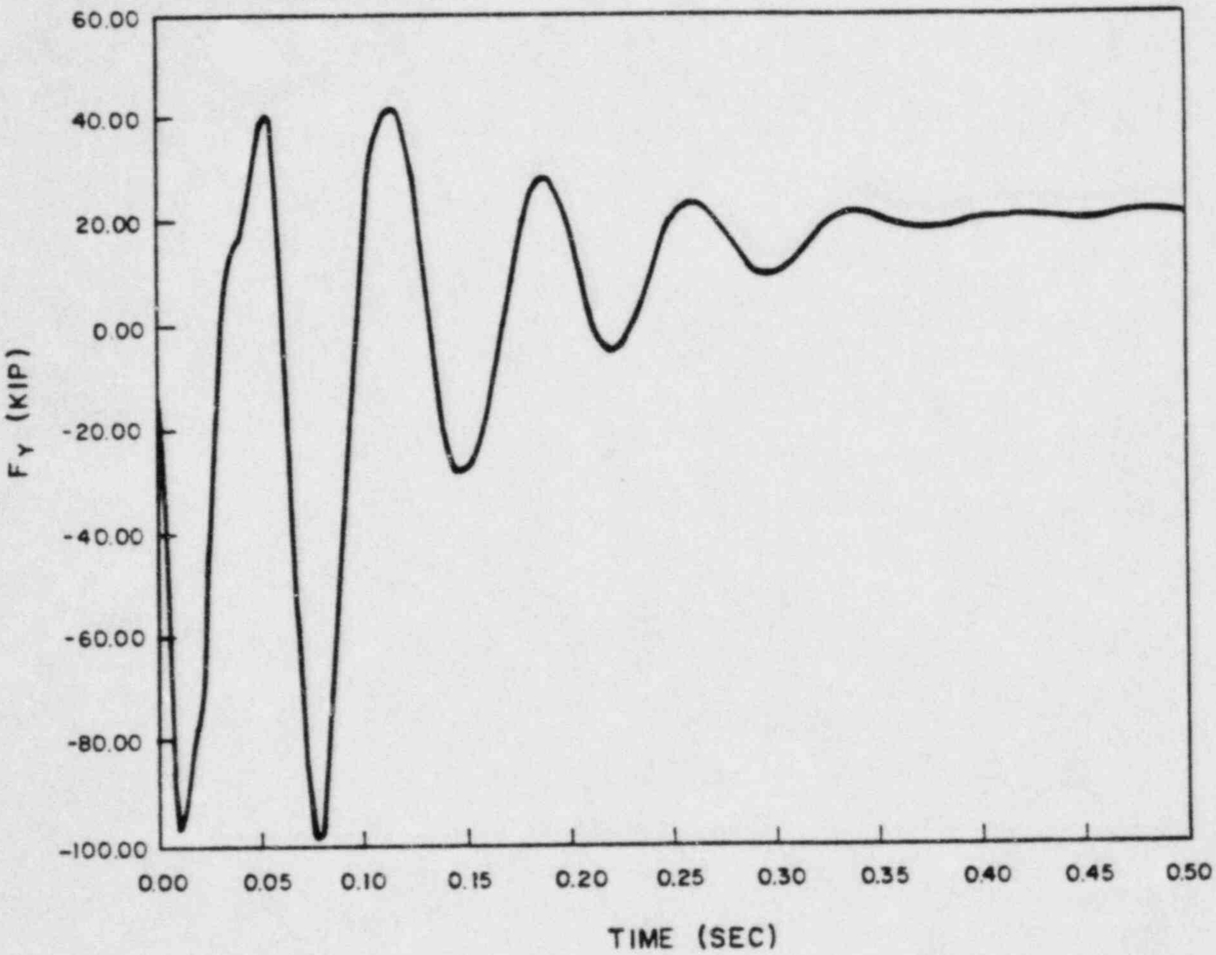

FIGURE Q480.37-33
NET FORCE IN GLOBAL Y
DIRECTION ON SG - BREAK 4
MILLSTONE NUCLEAR POWER STATION
UNIT 3
FINAL SAFETY ANALYSIS REPORT

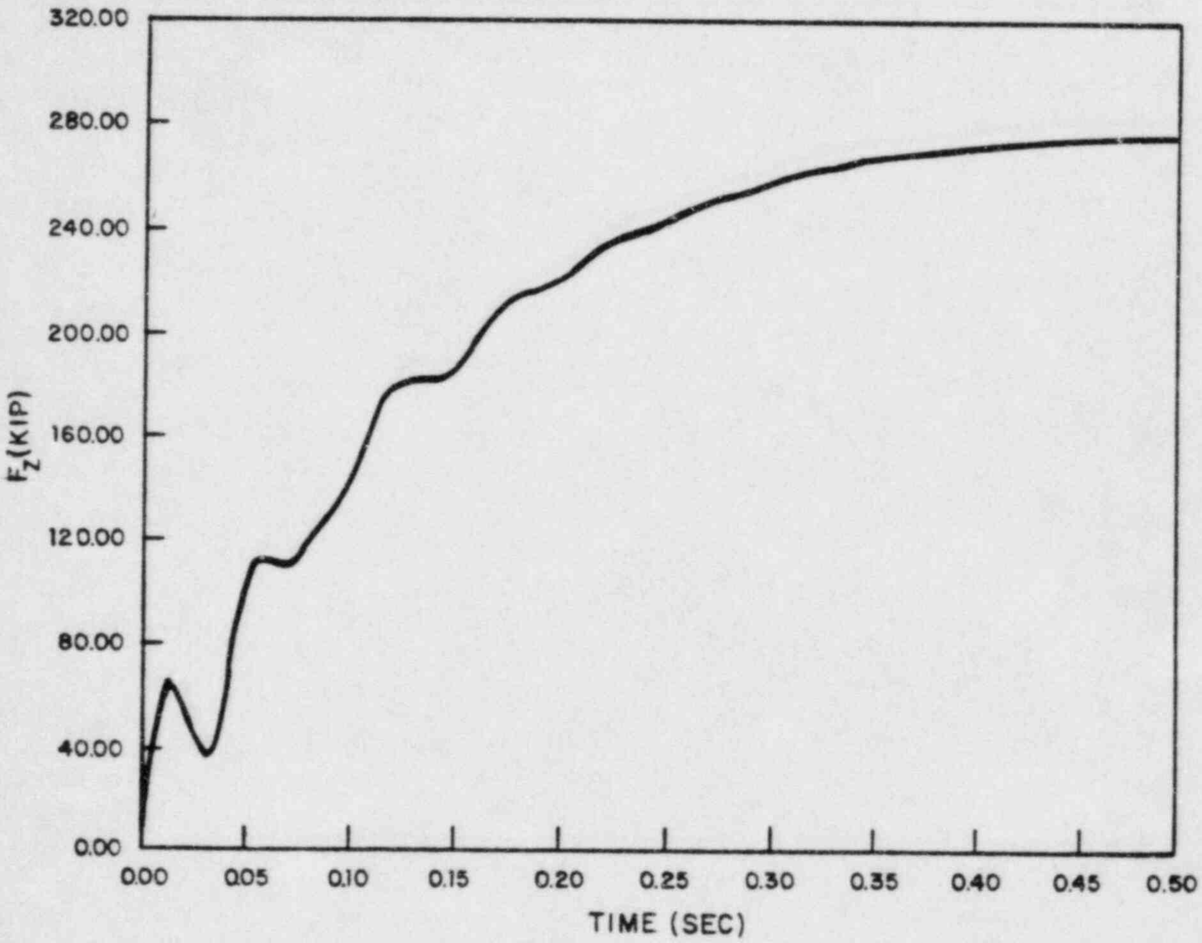

FIGURE Q480.37-34

NET FORCE IN GLOBAL Z DIRECTION ON SG - BREAK 4

MILLSTONE NUCLEAR POWER STATION
UNIT 3
FINAL SAFETY ANALYSIS REPORT

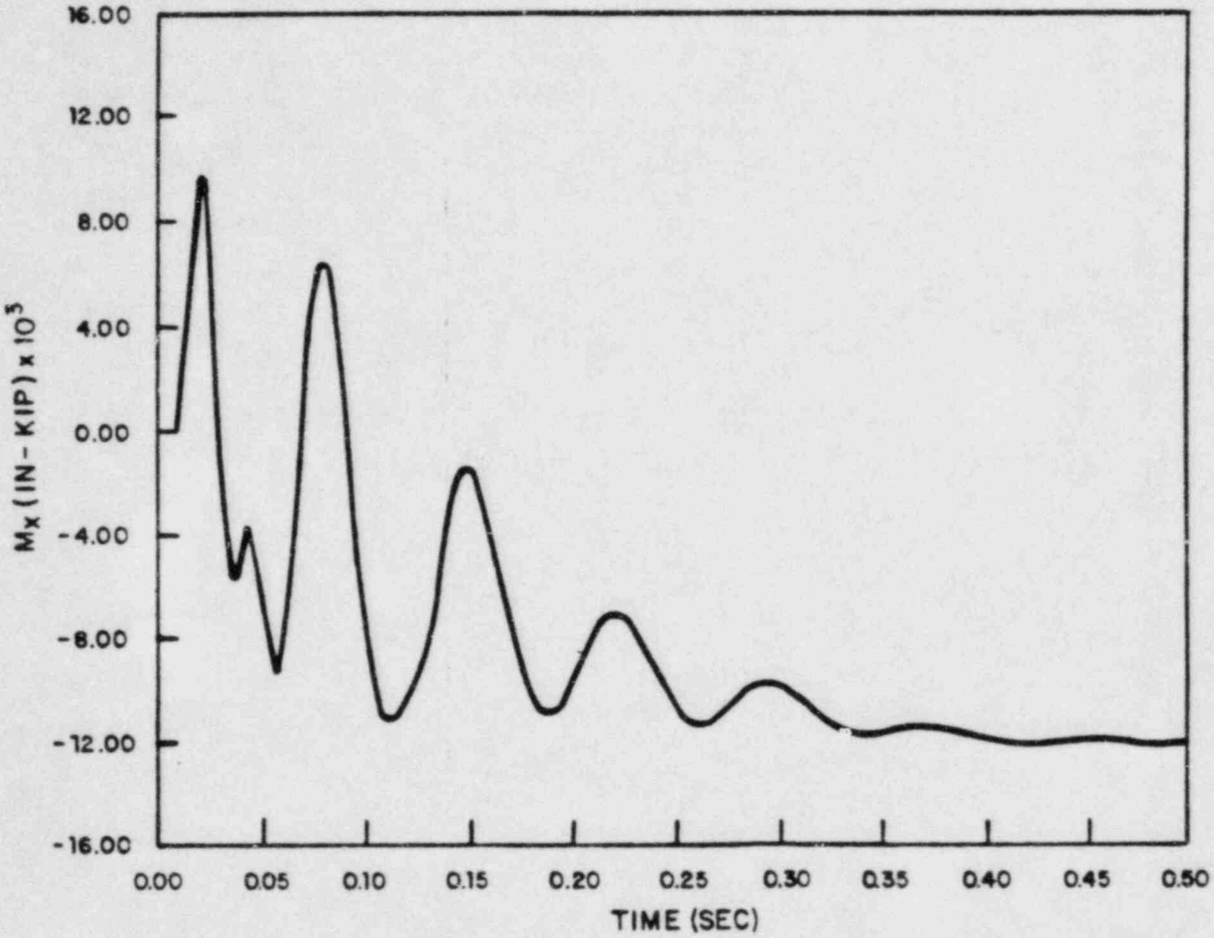

FIGURE Q480.37-35

NET MOMENT ABOUT GLOBAL X AXIS AT SG NODE 12 - BREAK 4

MILLSTONE NUCLEAR POWER STATION
UNIT 3
FINAL SAFETY ANALYSIS REPORT

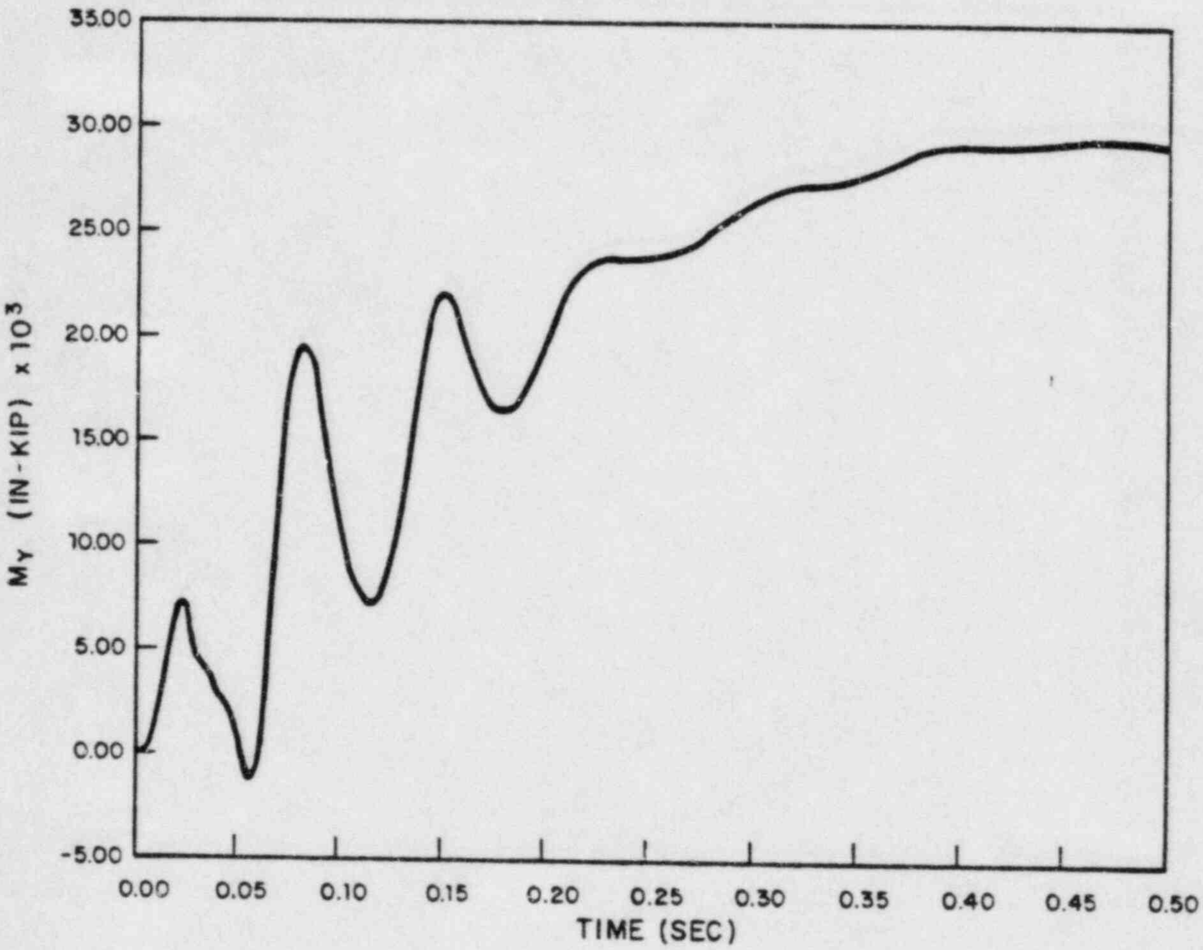

FIGURE Q480.37-36

NET MOMENT ABOUT GLOBAL Y AXIS AT SG NODE 12 - BREAK 4

MILLSTONE NUCLEAR POWER STATION
UNIT 3
FINAL SAFETY ANALYSIS REPORT

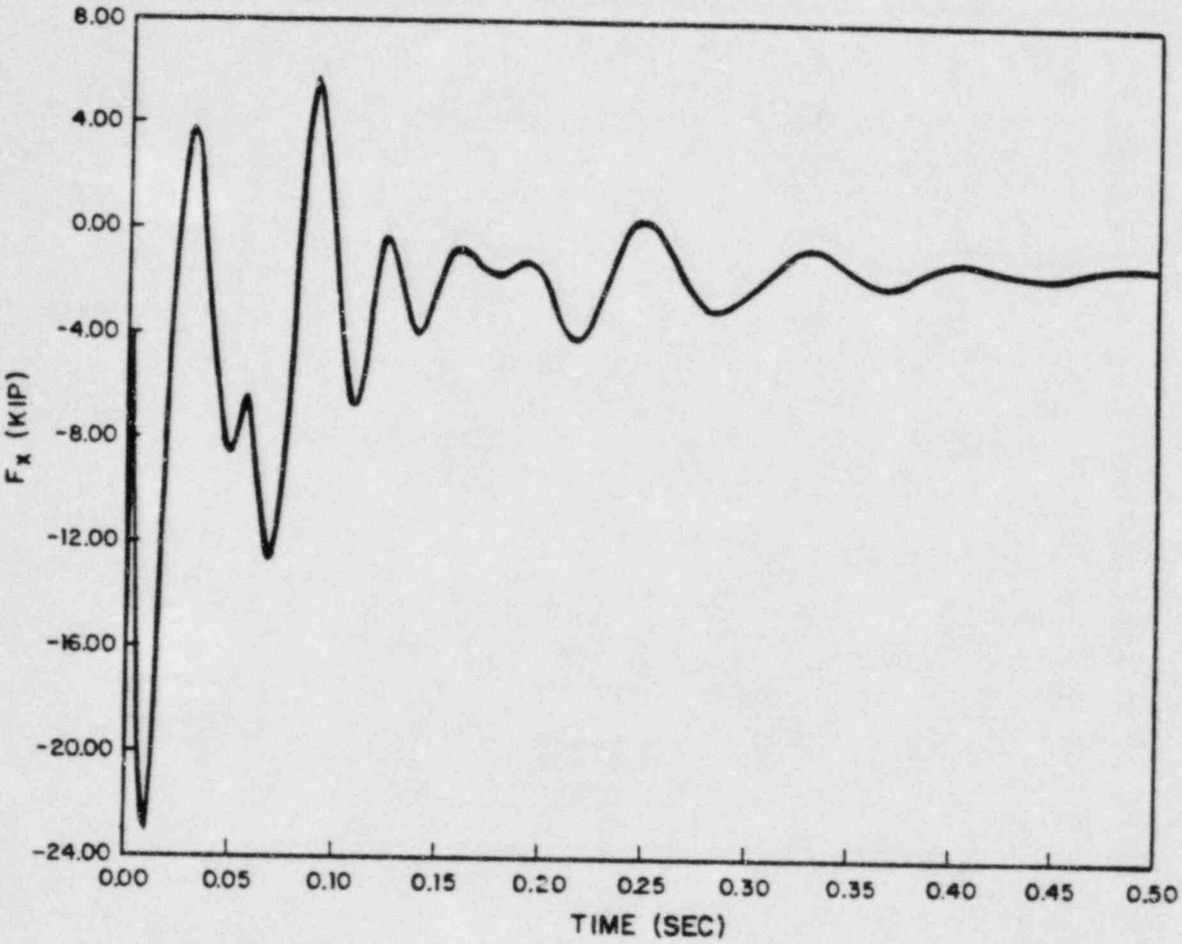

FIGURE Q480.37-37

NET FORCE IN GLOBAL X DIRECTION ON RCP - BREAK 4

MILLSTONE NUCLEAR POWER STATION UNIT 3

FINAL SAFETY ANALYSIS REPORT

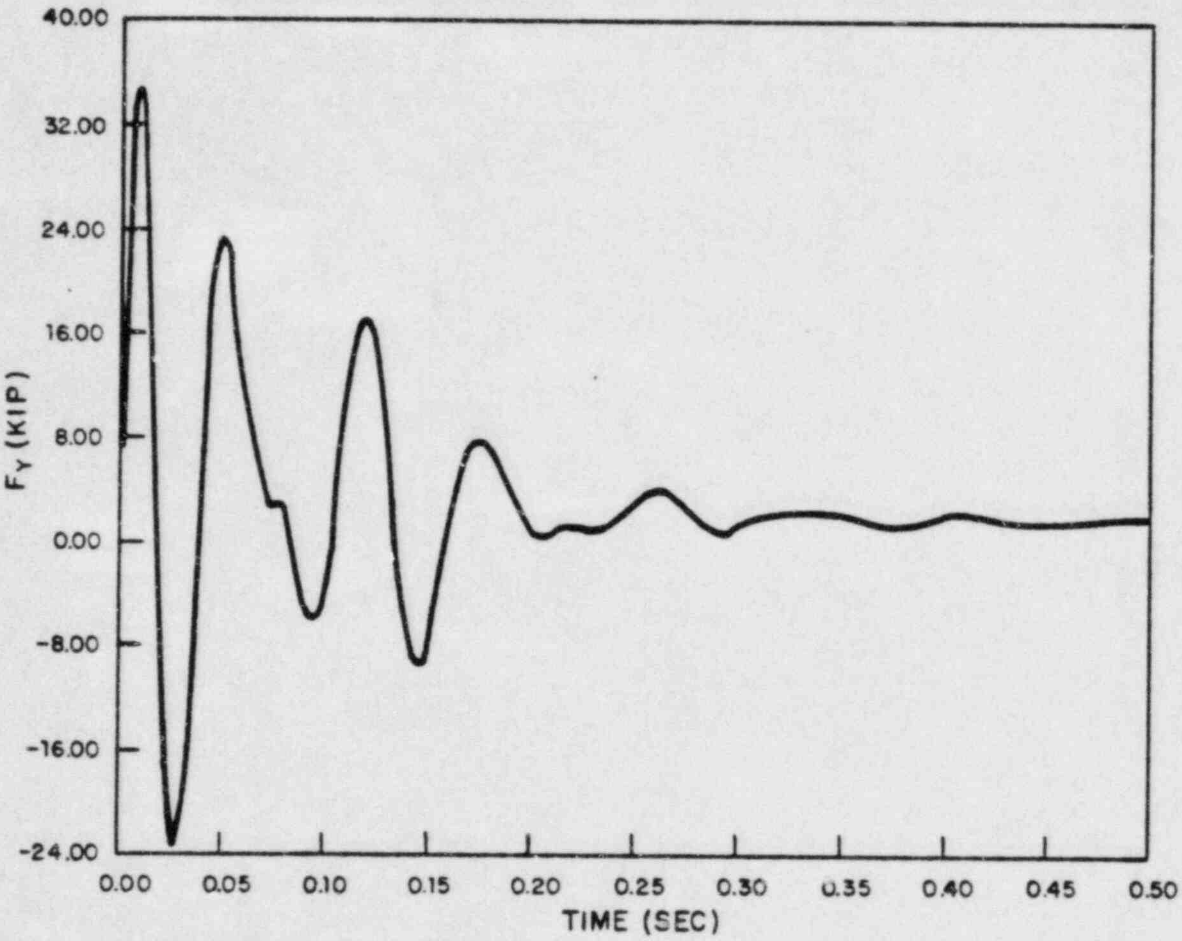

FIGURE Q480.37-38

NET FORCE IN GLOBAL Y DIRECTION ON RCP-BREAK 4

MILLSTONE NUCLEAR POWER STATION UNIT 3

FINAL SAFETY ANALYSIS REPORT

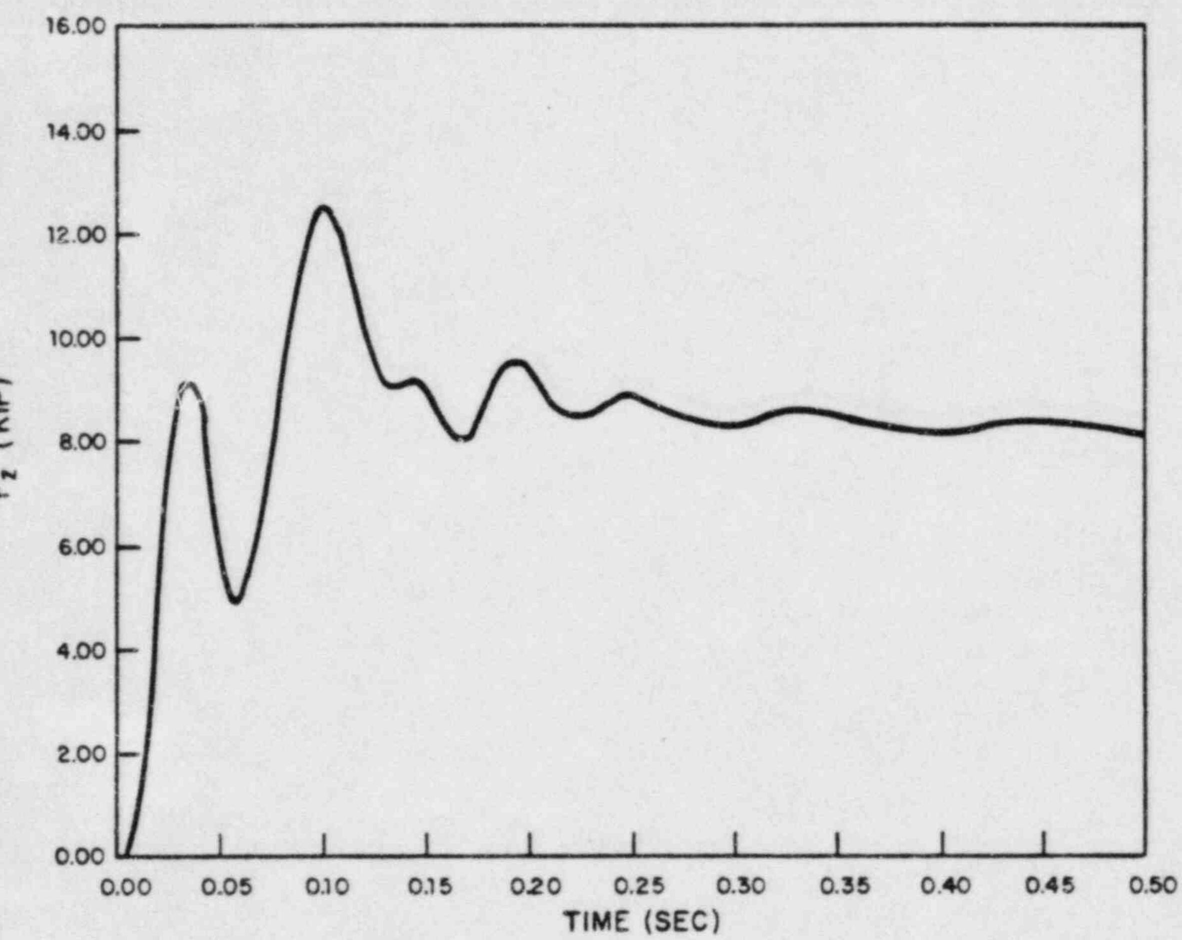

FIGURE Q480.37-39
NET FORCE IN GLOBAL Z
DIRECTION ON RCP-BREAK 4
MILLSTONE NUCLEAR POWER STATION
UNIT 3
FINAL SAFETY ANALYSIS REPORT

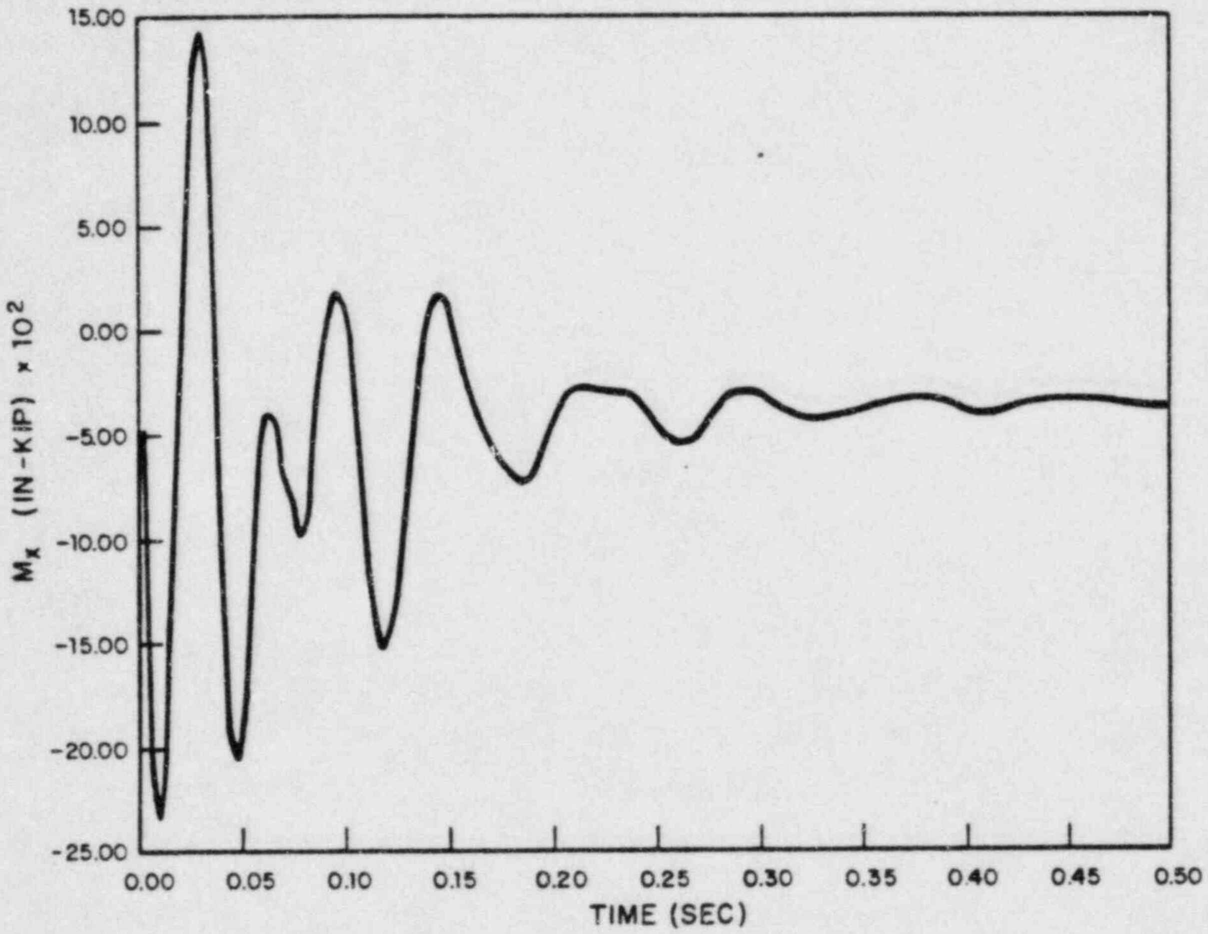

FIGURE Q480.37-40

NET MOMENT ABOUT GLOBAL X AXIS AT RCP NODE 24 - BREAK 4

MILLSTONE NUCLEAR POWER STATION
UNIT 3
FINAL SAFETY ANALYSIS REPORT

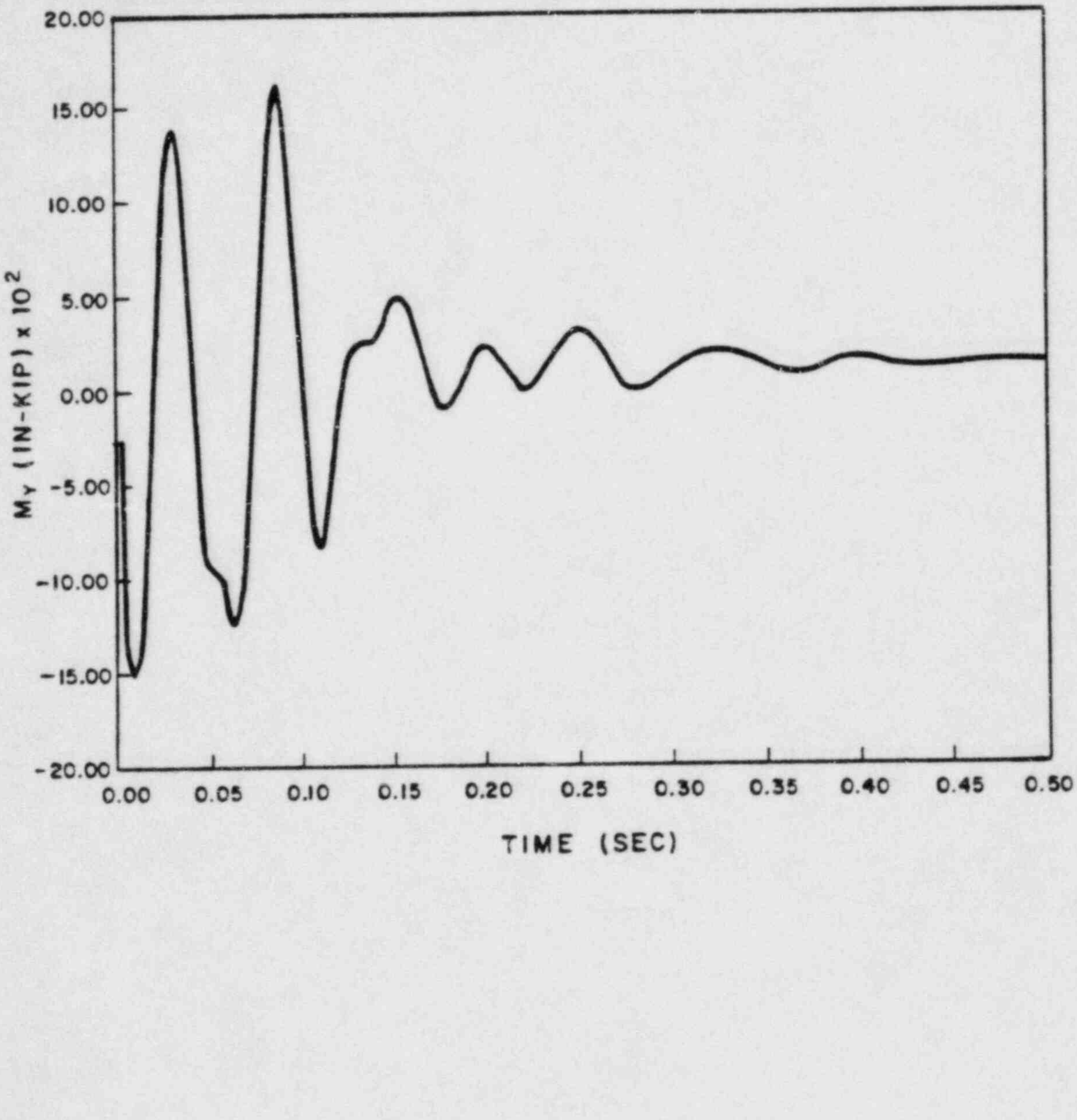

FIGURE Q480.37-41
NET MOMENT ABOUT GLOBAL Y
AXIS AT RCP NODE 24 - BREAK 4
MILLSTONE NUCLEAR POWER STATION
UNIT 3
FINAL SAFETY ANALYSIS REPORT

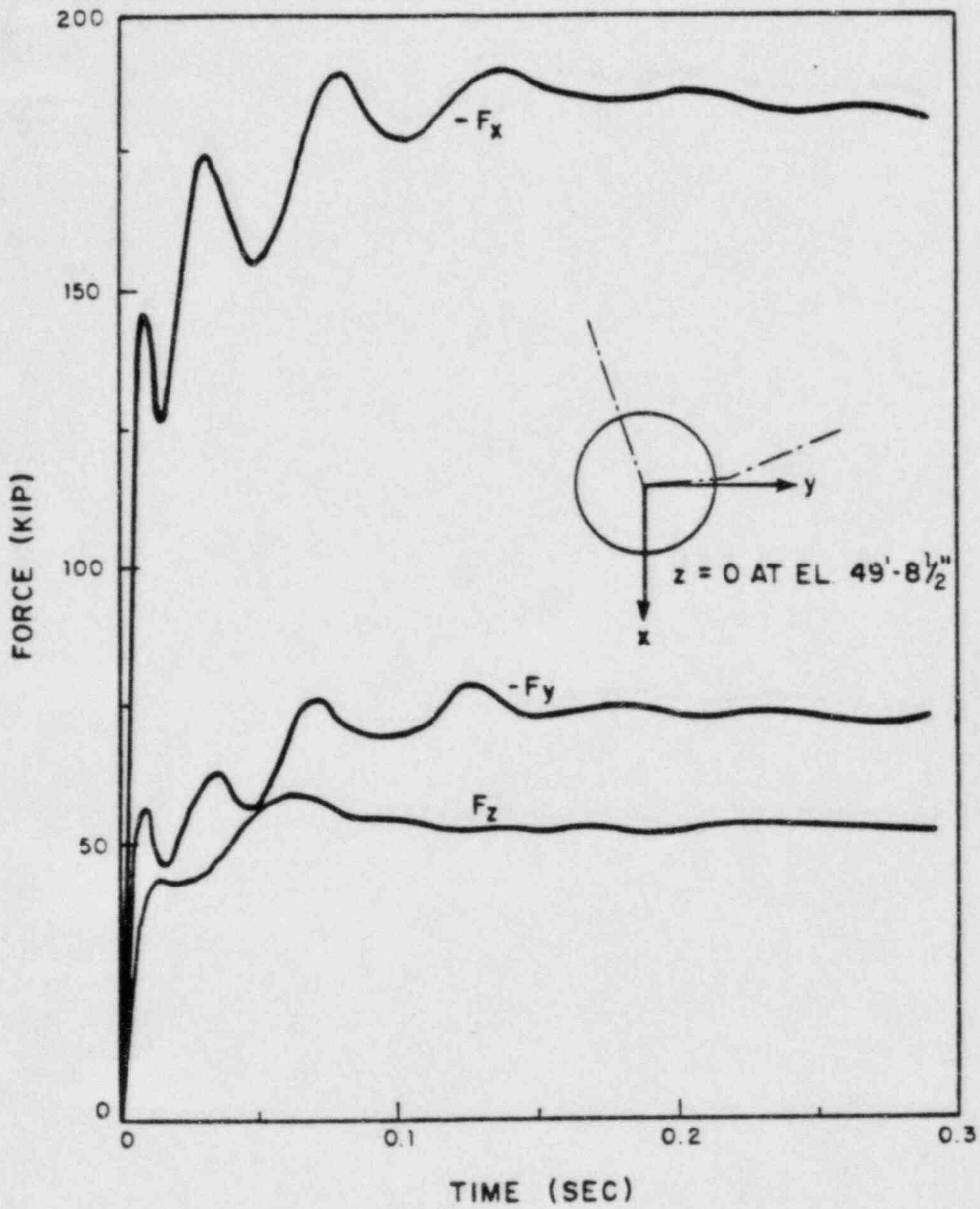

FIGURE Q480.37-42
NET FORCES ON SG-FEEDWATER
LINE BREAK (CUBICLE B)
MILLSTONE NUCLEAR POWER STATION
UNIT 3
FINAL SAFETY ANALYSIS REPORT

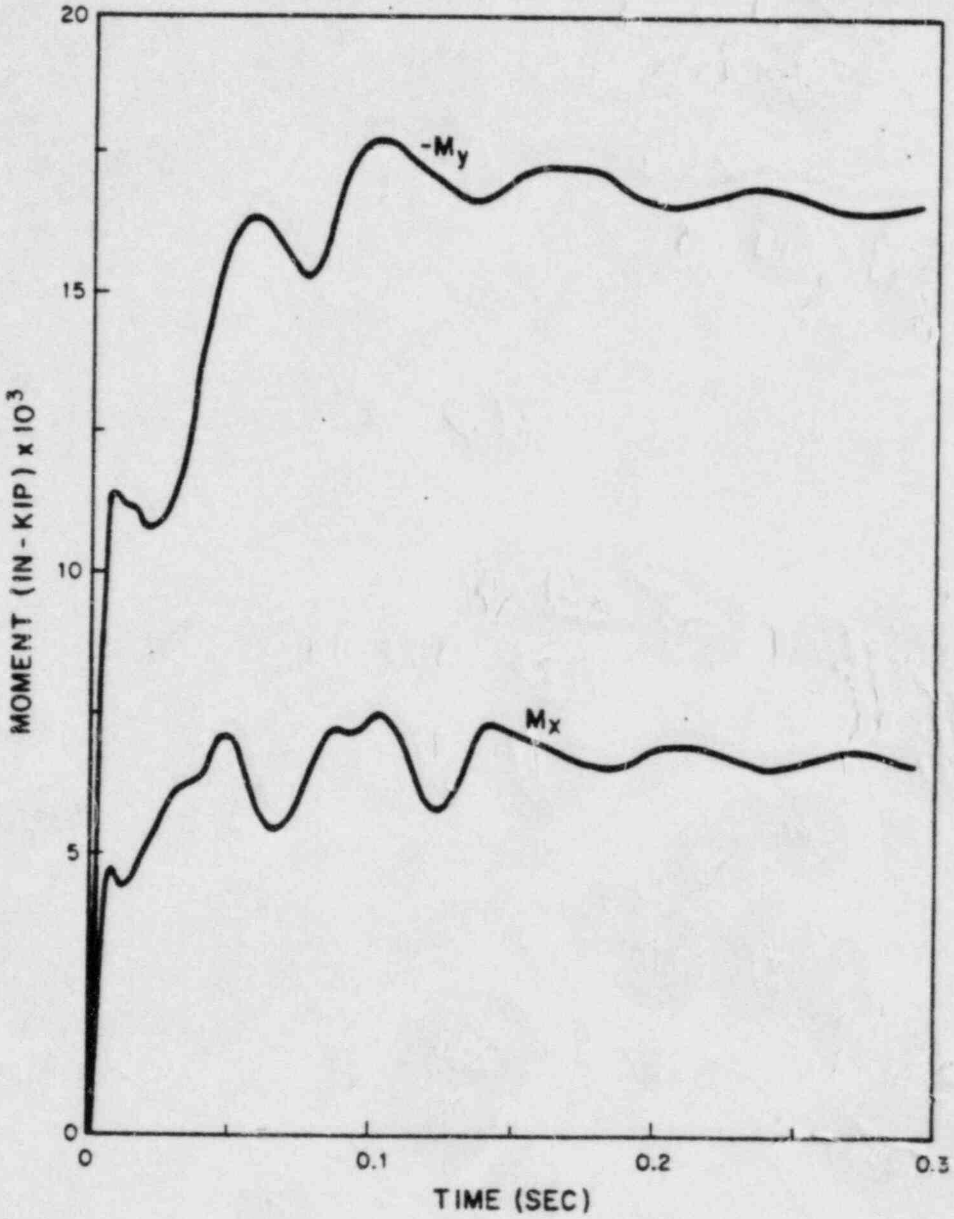

FIGURE Q480.37-43
NET MOMENTS ON SG-
FEEDWATER LINE BREAK
MILLSTONE NUCLEAR POWER STATION
UNIT 3
FINAL SAFETY ANALYSIS REPORT

336°F. For this accident, the peak calculated containment liner is 1.10
236.3°F. The liner temperature shown is the inside surface 1.11
temperature.

The qualification of safety related equipment inside the containment 1.12
to the pressure and temperature resulting from a steam line break is 1.13
discussed in Section 3.11.

A chronology of events for the limiting containment pressure and 1.14
temperature cases is given in Tables 6.2-24 and 6.2-25, respectively. 1.15

6.2.1.1.3.8 Feedwater Pipe Break Results 1.17

The feedwater pipe break is not as severe as the main steam pipe 1.18
break, since the break effluent is at a lower specific enthalpy. The 1.21
feedwater pipe break analysis is, therefore, not analyzed.

6.2.1.2 Containment Subcompartments 1.24

6.2.1.2.1 Design Basis 1.25

The containment subcompartments are designed in accordance with 1.26
General Design Criteria 4 and 50.

Break locations and types (Section 3.6.2) are chosen as follows for 1.28
the various subcompartments:

1. Upper pressurizer cubicle - Spray line doubled ended rupture 1.30
(DER) in the upper pressurizer cubicle is the largest break 1.31
that can occur in the upper pressurizer cubicle.
Section 6.2.1.2.3 describes the break types. 1.32

2. Lower pressurizer cubicle - Surge line DER in the lower 1.33
pressurizer cubicle. This is the largest break which can 1.34
occur within the pressurizer cubicle.

3. Lower steam generator subcompartments - Reactor coolant 1.35
system (RCS) 707 sq in. hot leg intrados split break in the 1.36
lower steam generator subcompartment. This is the largest 1.37
area break which can occur in the steam generator
subcompartment.

4. Upper steam generator subcompartments - A feedwater line 1.38 | 480.37
DER.

5. Upper reactor cavity - RCS 100 sq in. cold leg limited 1.39
displacement break inside the upper reactor cavity. This 1.40
break area exceeds the maximum which can occur inside the
upper reactor cavity.

Additional smaller breaks used for the major component support 1.42
evaluation are identified in the discussion of the results in 1.43 | 480.37
Section 6.2.1.2.3.

A full power condition with hot leg equal to 616.4°F and cold leg 1.44
equal to 555.9°F yields the maximum mass and energy release rates. 1.45

The RCS mass and energy release rates are computed by SATAN V Program 1.46
(Section 6.2.1.5.1). For subcompartment analysis, 110 percent of the 1.47
SATAN V mass and energy release rates is used.

The initial containment conditions selected to maximize the resultant 1.48
differential pressure within the subcompartments are: 1.49

1. Maximum temperature 120°F 1.51

2. Minimum air partial pressure 9.00 psia 1.52

3. Minimum relative humidity 50 percent 1.53

Subcompartment nodalization schemes are chosen to provide a 1.55
conservative load and moment on a given component and structure. All 1.57
vent flow paths used in the analysis are unobstructed by moveable
objects throughout the transient. These flow path areas are 1.58
conservatively calculated. Nominal reductions to the net vent areas 1.59
are typically made to account for building tolerances and blockages
that may occur from insulation displaced from the ruptured pipe. 1.60
Insulation and associated materials are the only moveable 2.1
obstructions to flow. Vent areas in the steam generator and 2.2
pressurizer subcompartments are relatively large, and accordingly,
the likelihood of significant blockage by displaced insulation is 2.3
remote. Vent areas local to the break location in the upper reactor 2.4
cavity subcompartment are, in general, significantly smaller than in 2.6
other subcompartments and are, therefore, more susceptible to
blockage. According to the Subcompartment Analysis Procedures 2.7
(Gido 1979), it is conservative to assume blockage of some vent areas 2.8
local to the break. However, it is unlikely that the blockage will 2.9
sustain itself because the high local pressures would immediately
dislodge the debris. 2.10

The flows through all flow paths with the nodalized subcompartment 2.11
model are based on a homogeneous mixture in thermal equilibrium with 2.12
the assumption of 100 percent liquid carryover (Section 6.2.1.2.3.3).

The subcompartment design differential pressure is equal to or 2.13
greater than the calculated differential pressure in that 2.14
subcompartment (Table 6.2-26). Multinode schemes providing a 2.15
conservative load and moment on a given component and structure are
considered in the subcompartment design. 2.16

6.2.1.2.2 Design Features 2.18

Figures 3.8-59 and 3.8-60 provide detailed plan and section drawings 2.19
of the containment subcompartments. They show the arrangement of 2.21
structures and components within the containment. Views of the 2.22
subcompartment are shown on Figures 6.2-17 and 6.2-18, 6.2-19 through
6.2-22, and 6.2-23 for the upper and lower pressurizer cubicle, the 2.25
most limiting steam generator subcompartment, and the upper reactor

cavity. Schematic nodalization models of the upper and lower 2.26
pressurizer cubicle, the most limiting steam generator
subcompartment, and the upper reactor cavity are given on 2.27
Figures 6.2-24, 6.2-25, and 6.2-23, respectively. The corresponding 2.28
subcompartment vent path and nodal descriptions are given in
Tables 6.2-27 through 6.2-30.

6.2.1.2.3 Design Evaluation 2.30

Conditions considered in the subcompartment analyses are the 2.31
development of pressure gradients across the walls, major equipment, 2.32
and supports. The resulting asymmetric pressures are used to 2.34
calculate loads and moments applied to the equipment and its
supports. The maximum differential pressure across the walls is used 2.35
as the design basis for the subcompartment structures.

The volume of the subcompartment is divided into a series of nodes 2.36
with as many connecting vents as there are significant flow 2.37
resistances. A model that provides a conservative load and moment on 2.38
the given component and structure is used.

Break Type Definitions and Areas 2.41

Two types of breaks are used to analyze containment subcompartments. 2.43
The first is a guillotine break. A guillotine break, which results 2.46
in a break flow area of two pipe cross sections, is called a double-
ended rupture (DER). In some subcompartments, pipe restraints limit 2.48
the displacement of the two broken ends of the pipe so that the break
flow area is less than two pipe cross-sectional areas. This type 2.50
break is called a limited displacement rupture (LDR). The special 2.51
case of a LDR of one pipe cross-sectional area is called a single
ended rupture (SER).

The second type of break is a longitudinal split which is equivalent 2.52
to a hole in the wall of the pipe. A split which results in a break 2.53
flow area of one pipe cross section is called a single ended split
(SES).

The containment subcompartment analysis results describe all breaks 2.54
analyzed within a particular subcompartment. Pipe restraints are 2.55
provided to limit the break areas to those analyzed. Break areas are 2.56
determined by the NSSS vendor.

A DER is considered in the analyses for the pressurizer cubicle and 2.57
upper steam generator subcompartment. Breaks with less than two 2.58 480.37
cross-sectional flow areas are used in the analysis for the reactor
cavity and steam generator subcompartment. The analytical model used 2.60
for predicting the mass and energy release rates for the primary
coolant system breaks is given in WCAP-8264-P-A (1975) and 3.2
WCAP-8312-A, Revision 2 (1975).

480.37

The mass and energy releases for the feedwater line full DER 3.3
(Table 6.2-36A) were determined by a manual calculation using the 3.4
frictionless Moody correlation for a saturated liquid. The initial 3.6

temperature and pressure of the feedwater were taken at 102 percent reactor power with valves wide open (Figure 10.1-3). These conditions produce the limiting releases for this break. As the reactor power decreases, the pressure and temperature of the steam generator inventory increases slightly. However, the pressure and temperature of the feedwater line inventory decreases significantly. Accordingly, the total calculated release is maximum at the 102 percent reactor power level. 480.37

Vent Loss Coefficient

The vent loss coefficients used in the subcompartment analyses depend on the geometry of the particular vent. The basis for the coefficients is the Handbook of Hydraulic Resistance (Idelchik 1960). Tables 6.2-27, thru 6.2-30 give the values of the loss coefficients utilized in subcompartment analyses.

Subcompartment Analytical Model

1. Functional Description of THREED Code

The THREED computer program is used to calculate the transient conditions of pressure, temperature, and humidity in various subcompartments following a postulated rupture in a moderate or high energy pipeline. The results obtained from such an analysis are used to calculate loads on structures and to define environmental conditions for equipment qualification.

The THREED computer program is similar to RELAP4 (Aerojet Nuclear Company 1976; Moore and Rettig 1974) and will give the same results as RELAP4 if similar options are chosen. THREED performs subcompartment analyses with capabilities and options extended beyond those available in RELAP4. A significant improvement in THREED is that the homogeneous equilibrium mode (HEM) has been extended to include two-phase, two-component flow which is encountered in subcompartment analysis.

The current THREED computer program was put into use in October 1978, and has been used in the design of Beaver Valley Power Station Unit 2, River Bend Station, and Nine Mile Point Nuclear Station Unit 2. 480.8

2. Description of the Model

The THREED computer code can be viewed as a numerical integrator for the macroscopic form of the basic field equations describing the conservation of mass, energy, and momentum. The conservation equations, along with the equation of state for the fluid, give a complete solution to the fluid flow phenomena. THREED solves a stream tube form of the field equations based on the assumptions of one-dimensional, homogeneous, thermal-equilibrium flow.

Although THREED does not prohibit the use of 3.55
multidimensional flow paths, the flow paths are modeled to
approximate a one-dimensional equation. Subcompartments are 3.58
modeled in THREED as a hydraulic network which consists of a
series of interconnecting user defined nodes (mass and 3.59
energy control volumes). Nodes are connected by internal 3.60
junctions (momentum control volumes) with the internodal
flow rates being determined by the solution of the momentum 4.1
equation. An internal junction control volume is defined as 4.2
the composite volume between the centers of adjacent nodes.
This inconsistency in control volumes (different control 4.3
volume for momentum than for mass and energy) is illustrated
on Figure 6.2-26. This "staggered mesh" approximation is 4.5
necessary for purposes of solving the equations.

Fill junctions are dissimilar to internal junctions in that 4.6
they have no initial node and their flow rate is dependent
only on the junction area and time. These junctions are 4.8
used to simulate flow originating external to the network
(blowdown). Mathematically, they are treated as boundary 4.9
conditions.

THREED numerically solves finite difference equations which 4.10
account for mass and energy flows into and out of a node.
Figure 6.2-27 summarizes the computational approach used in 4.11
THREED.

The fluid conservation equations used by THREED can be 4.12
obtained by integrating the stream tube equations over a
fixed volume, V. The mass and energy equations are 4.14
developed for the generalized ith node, while the momentum
equation is developed for the generalized jth internal 4.15
junction connecting nodes K and L. Neglecting kinetic 4.16
energy affects the resulting equations as follows:

7. Incompressible form of the momentum equation. 1.9

8. Kinetic energy effects are neglected. 1.10

9. For the choked flow models, the static properties in the 1.11
nodes are considered to be stagnation properties.

10. Valves open/close instantaneously. 1.12

<u>Containment Subcompartment Analysis Results</u> 1.15

1. Pressurizer Cubicle 1.16

The pressurizer cubicle is analyzed according to the 1.18
nodalization diagram of Figure 6.2-24.

A spray line DER in the upper cubicle and a surge line DER 1.20
in the lower cubicle are considered for the pressurizer
cubicle analysis. The pressurizer is supported from the 1.22
floor at elevation 51 ft-4 in. which defines the boundary
between the upper and lower cubicles. 1.23

The mass and energy release for a spray line DER are given 1.24
in Table 6.2-31 and for a surge line DER in Table 6.2-32. 1.25

Pressurizer cubicle subcompartment nodal volumes, vent 1.26
areas, K-factors, and inertias for the THREED analysis are
listed in Table 6.2-27. 1.27

The pressure response for the pressurizer cubicle (maximum 1.28
pressure differential) is shown on Figures 6.2-28 and 6.2-29 1.29
for both the spray line and surge line DER, respectively.

The peak calculated differential pressures between 1.30
contiguous nodes for the pressurizer cubicle are given in
Table 6.2-33. The time of peak differential pressure is 1.32
given with the peak calculated differential pressure.

2. Steam Generator Compartment 1.35

The nodalization schematic used in the steam generator 1.37
compartment analysis is shown on Figure 6.2-25. Seven 1.39 | 480.37
postulated breaks are considered for the steam generator
analysis. They are as follows. 1.40

1. Steam generator inlet nozzle with a 196.6 sq in. LDR 1.42
(Break 3).

2. Pressurizer surge line with a 196.6 sq in. LDR 1.43
(Break 11). 480.37

3. Residual heat removal line with 196.6 sq in. LDR 1.44
(Break 9).

4. RCS hot leg intrados split break with 707 sq in. 1.45
opening (Break 7).

5. Feedwater line 477.6 sq in. DER. 1.46

6. Steam generator outlet nozzle LDR with 500 sq in. 1.47
opening (Break 4). 480.37

7. Pump suction loop closure weld LDR with 500 sq in. 1.48
opening (Break 12).

Refer to Figure Q480.37-21 which shows the locations of the 1.50
various breaks.

The steam generator cubicle subcompartments (cubicles A and 1.51
B) nodal volumes, vent areas, K-factors, and inertias for 1.52
the THREED analysis are listed in Tables 6.2-28 and 6.2-29.
Cubicle B was used for analysis of breaks that can occur in 1.53
either cubicle. This is conservative because the K-factors 1.54
and inertia values are larger and the node volumes and vent
areas in cubicle B are smaller. 1.55

The peak nodal pressures and time at which it occurred for 1.56
each of the above-listed breaks are shown in Table 6.2-34. 1.57
Tables 6.2-35, 6.2-36, 6.2-36A, and 6.2-36B give the mass 1.58
and energy release rates for the 196.6 sq in. LDR, the 1.59
707 sq in. intrados split break, the 477.6 sq in. feedwater 1.60 480.37
line DER, and the 500 sq in. outlet nozzle LDR,
respectively.

Figures 6.2-30 through 6.2-34D show the pressure response 2.1
for the steam generator cubicle (maximum pressure
differential across the steam generator and the cubicle 2.2
walls for each break).

The main steam line is not routed through any portion of the 2.3
compartment and is not considered in the analysis. 2.4

Tables 6.2-37 through 6.2-40 and 6.2-26 list the peak 2.5 10
calculated differential pressures between contiguous nodes
of each of the above-listed breaks. The time of peak 2.9
differential pressure is given with the peak calculated
differential pressure.

3. Upper Reactor Cavity 2.12

The design of the neutron shield tank and the reactor vessel 2.14
insulation prevent venting downward below the upper reactor 2.15
cavity. Thus, the reactor cavity analysis considers 2.17
pressurization of the upper cavity and the refueling cavity
which is directly above the upper reactor cavity. 2.18

The upper reactor cavity and the refueling cavity is 2.19
analyzed according to the nodalization schematic shown on

Figure 6.2-23. The minimum number of nodes required to predict the peak local pressure is determined by performing a nodalization sensitivity study. Since the reactor cavity is symmetrical, only one-half of the cavity was analyzed. 2.21 2.23

The design nodal configuration for the reactor cavity 2.24
employs a vertical plane through each reactor vessel nozzle
centerline. Thus, the number of circumferential nodes is 2.26
equal to the number of reactor vessel nozzles. A horizontal 2.27
plane is also passed through the centerline of the nozzle
where the break is assumed and the centerline of two nozzles 2.28
on both sides of this nozzle. Thus, the total number of 2.29
nodes inside the reactor cavity is 12. Based on symmetry, 2.30 | 10
six nodes were analyzed plus four nodes in the refueling
cavity and the remainder of the containment for a total of 2.31
11 nodes with this configuration. All node boundaries 2.32 | 10
inside the upper reactor cavity are placed at the minimum
flow area available for internodal flow. This results in 2.33
the most conservative configuration for reactor cavity
pressurization calculations.

Table 6.2-30 lists the node, volumes, vent areas, K-factors, 2.34
and inertias used for the THREED analysis.

Table 6.2-41 gives the resultant peak calculated 2.35
differential pressures. The time of peak differential 2.36
pressure is given with the peak calculated differential
pressure. Table 6.2-42 gives the mass and energy releases 2.37
for the cold leg LDR (100 sq in. area).

Table 6.2-43 summarizes the subcompartment differential 2.38
pressures (design and maximum calculated).

4. Reactor Cavity Nodalization Sensitivity Study 2.41

A total of six different nodal configurations were analyzed 2.43
inside the reactor cavity. The different configurations 2.45
consist of 1, 4, 8, 16, 24, and 48 node models. The 2.46
remainder of the containment is represented by an additional
node in these analyses. A 100 sq in. pump discharge LDR is 2.47
postulated in the nodalization study.

The 1 node model considers the entire upper reactor cavity 2.48
pressurization to be uniform.

The nodes in the 4 node model are bounded by vertical planes 2.49
through the centerline of the broken pipe and every second 2.50
pipe from the broken pipe. The resultant differential 2.51
pressure is higher than the one node model. In the 8 node 2.52
model, the nodes are bounded by vertical planes through the
centerline of every pipe.

In the 16 node model, the nodes are bounded by vertical and 2.53
horizontal planes through the centerline of every pipe. In 2.54

models with a large number of nodes (16 node model and larger), several of the nodes located relatively far from the break were combined into a single node. This did not influence the results significantly since these nodes would have nearly equal pressure if kept separate. This model results in a higher calculated differential pressure than any of the other models using lesser nodes. The results indicate that the peak differential pressure is nearly constant for all models with sixteen or more nodes, so the 16-node model was used as the limiting model.

In the 24 node model, the nodes are bounded by vertical and horizontal planes through the centerline of every pipe plus a horizontal plane 4 ft-1/2 in. above the pipe centerline. The resultant differential pressure is essentially equal to that calculated using the 16 node model.

5. Primary Shield Wall Pipe Penetrations

There are no breaks postulated inside the primary shield wall pipe penetrations. The penetrations are conservatively designed to withstand with maximum design pressure within the upper reactor cavity.

6.2.1.3 Mass and Energy Release Analyses for Postulated Loss-of-Coolant Accidents

This analysis presents the mass and energy releases to the containment subsequent to a hypothetical loss-of-coolant accident (LOCA). The release rates are calculated for pipe failure at three distinct locations:

1. Hot leg (between vessel and steam generator)
2. Pump suction (between steam generator and pump)
3. Cold leg (between pump and vessel)

During the reflood phase, these breaks have the following different characteristics. For a cold leg pipe break, all of the fluid which leaves the core must vent through a steam generator and becomes superheated. However, relative to breaks at the other locations, the core flooding rate (and therefore the rate of fluid leaving the core) is low, because all the core vent paths include the resistance of the reactor coolant pump. For a hot leg pipe break, the vent path resistance is relatively low, which results in a high core flooding rate, but the majority of the fluid which exits the core bypasses the steam generators in venting to the containment. The pump suction break combines the effects of the relatively high core flooding rate, as in the hot leg break, and steam generator heat addition, as in the cold leg break. As a result, the pump suction breaks yield the highest energy flow rates during the post-blowdown period.

The spectrum of breaks analyzed includes the largest cold and hot leg 3.33
breaks, reactor inlet and outlet, respectively, and a range of pump 3.34
suction breaks from the largest (10.48 sq ft) to a 3.0 sq ft break. 10
Because of the phenomena of reflood as discussed above, the pump 3.35
suction break location is the worst case for long term containment 3.36
depressurization. This conclusion is supported by studies of smaller 3.37
hot leg breaks which have been shown on similar plants to be less
severe than the double-ended hot leg. Cold leg breaks, however, are 3.39
lower both in the blowdown peak and in the reflood pressure rise.
Thus, an analysis of smaller pump suction breaks is representative of 3.40
the spectrum of break sizes. The hot leg break is the worst case for 3.41
containment pressure.

The LOCA transient is typically divided into four phases: 3.42

1. Blowdown - which includes the period from accident 3.47
occurrence (when the reactor is at steady state operation)
to the time when the total break flow stops. 3.48

2. Refill - the period of time when the lower plenum is being 3.49
filled by accumulator and safety injection water. (This 3.50
phase is conservatively neglected in computing mass and
energy releases for containment evaluations.)

3. Reflood - begins when the water from the lower plenum enters 3.51
the core and ends when the core is completely quenched. 3.52

4. Post-Reflood - describes the period following the reflood 3.53
transient. For the pump suction and cold leg breaks, a two- 3.54
phase mixture exits the core, passes through the hot legs,
and is superheated in the steam generators. After the 3.56
broken loop steam generator cools, the break flow becomes
two phase.

6.2.1.3.1 Mass and Energy Release Data 3.59

Blowdown Mass and Energy Release Data 4.1

Tables 6.2-7, 6.2-12, 6.2-18, 6.2-45, and 6.2-46 present the 4.3
calculated mass and energy releases for the blowdown phase of the 4.5
various breaks analyzed. 4.6

The mass and energy releases for the hot leg double-ended break, 4.8
given in Table 6.2-7, terminate 25.2 seconds after the postulated 4.10
accident. Since safety injection does not become effective until 4.11
about the time blowdown terminates, these releases apply for both 4.12
maximum and minimum safety injection.

Reflood Mass and Energy Release Data 4.15

Tables 6.2-13, 6.2-19, 6.2-47, 6.2-48, and 6.2-49 present the 4.17 10
calculated mass and energy releases for the reflood phase of the 4.19
various breaks analyzed along with the corresponding safety injection 4.22
assumption (maximum or minimum). The release data for the 3.0 sq ft 4.23 10

pump suction split and the cold leg double-ended rupture also include
the dry steam post-reflood mass and energy release data. 4.25

Two Phase Post-Reflood Mass and Energy Release Data 4.28

Tables 6.2-50 and 6.2-20 present the two phase (froth) mass and 4.30
energy release data for a double-ended pump suction break using 4.33
maximum and minimum safety injection assumptions, respectively. The 4.34
data was generated using an assumed 3,600 second containment
depressurization transient.

A sensitivity analysis was performed utilizing the release data 4.35
presented in Tables 6.2-50 and 6.2-20 and a second set of release 4.36
data generated with an assumed 1,800-second containment
depressurization transient. The data presented produced the worst 4.37
case for containment depressurization (Section 6.2.1.1).

Table 6.2-14 presents the post-reflood mass and energy release data 4.38
for 0.6 double-ended pump suction break using minimum safety 4.39
injection.

leak-rate test described in Section 6.2.6.1 adequately demonstrates 1.10
the leak tightness of the containment. 1.11

An evaluation of in-leakage following a LOCA shows the containment 1.12
pressure to be effecti ely subatmospheric at -0.5 psig 30 days 1.13
following the accident. The inleakage analysis is based on the 1.14
max: um specified out-leakage rate of 0.9 percent per day at
approximately 45 psig adjusted to the pressure differences determined 1.15 480.22
to be present following a LOCA.

The maximum in-leakage rate to the subatmospheric containment during 1.16
normal operation is approximately 14 scfm at 9.5 psia, the lowest 1.17
normal operating containment pressure. This corresponds to the 1.18
out-leakage rate of 0.9 percent per day at 45 psig adjusted for the
pressure differential and other important flow paramaters. 1.19

The containment structure enclosure will be evacuated by the 1.20
supplementary leak collection and release system (SLCRS) to slightly 1.21
negative pressure immediately following the design bases accident
initiation of the engineered safety features actuation system 1.22
(ESFAS). This will ensure all leakage from the primary containment 1.23
(0.9 percent per day) is passed through the high-efficiency
particulate air (99-percent efficient) filters of the SLCRS prior to 1.25
release from the containment structure enclosure, engineered safety 1.26
feature building, main steam valve building, hydrogen recombiner
building or auxiliary building which are all connected to the SLCRS. 1.28

This filtration will ensure the reduction of primary leakage from 1.29
0.9 percent per day to less than 0.1 percent per day released to the 1.30
environment. The SLCRS will be tested prior to loading fuel to 1.31
verify that a slightly negative pressure can be obtained and
maintained following an ESFAS actuation in the areas mentioned above. 1.32
This test will be conducted again at each refueling or at intervals 1.33
not to exceed 18 months. Some leakage through piping systems may 1.34
bypass the secondary containment. This leakage is limited to the 1.35
design leak rates through these piping systems. The bypass leakage 1.36
penetrations, identified in Table 6.2-65, are tested in accordance
with Section 6.2.6.3, and the combination of their leakage rates is 1.38
compared with the maximum allowable rate (9 scfh). When the actual 1.39
leakage rate approaches this limit, corrective action will be taken.

6.2.7 References for Section 6.2 1.41

Aerojet Nuclear Company, 1976. RELAP4/MOD5: A Computer Program for 1.43
Transient Thermal Hydraulic Analysis of Nuclear Reactors and Related
Systems. User's Manual Vol I-III, Report ANCR-NUREG-1335. Aerojet 1.45
Nuclear Company.

American Nuclear Society (ANS) 1978. Decay Heat Power in Light Water 1.48
Reactors. ANS Standard, June 1, 1978, Revised September 1978. 1.49

Atomics International Division Rockwell International. Test 1.51
Procedure - Hydrogen Analyzer Systems, No. N019DTP120003.

Baer, Robert L. (Office of Reactor Regulation Division of Project Management, (USNRC) 1978. Letter to Mr. Gordan Pinsky (Owens-Corning Fiberglass Corporation).

Bloom, G.R., et al. Hydrogen Distribution in a Containment with a High Velocity Hydrogen-Steam Source. Presented at the Second International Workshop on the Impact of Hydrogen on Water Reactor Safety, Albuquerque, New Mexico, October 3-7, 1982. 480.19

Brocard, D.N. Buoyancy, Transport and Head Loss of Fibrous Reactor Insulation. NUREG/CR-2982, U.S. Nuclear Regulatory Commission. Prepared by Alden Research Laboratory, Worcester Polytechnic Institute, Holden, Massachusetts. November 1982. 480.18

CONTEMPT - A Computer Program for Predicting the Containment Pressure-Temperature Response to a Loss-of-Coolant Accident (LOCA), IDO-17220 1967.

Crank, J. The Mathematics of Diffusion. Oxford University Press, 1956, pp 186-199. 480.16

Gido, R.G. Liner-Concrete Heat Transfer Study for Nuclear Power Plant Containments, Los Alamos Scientific Laboratory, LA-7089-MS Informal Report NRC-4, issued January 1978.

Gido, R.G. Subcompartment Analysis Procedures. Los Alamos Scientific Laboratory. NUREG/CR-1199, LA-8169-MS, Informal Report R-4. December 1979. 480.37

Hanover, Stephen H. (Chairman Advisory Committee of Reactor Safeguards) 1969. Letter to Hon. Glenn T. Seaborg (Chairman USAEC) Report on Brunswick Steam Electric Plant.

Hanover, Stephen H. (Chairman Advisory Committee of Reactor Safeguards) 1969. Letter to Hon. Glenn T. Seaborg (Chairman USAEC) Report on Edwin I. Hatch Nuclear Plant.

Hilliard, R.K., et al. 1970. Removal of Iodine and Particles from Containment Atmosphere by Sprays. Battelle-Northwest, Richland, Wash. BNWL-1244.

Hilliard, R.K. and Coleman, L.F. Natural Transport Effects on Fission Product Behavior in the Containment Systems Experiment. BNWL-1457, Battelle Pacific Northwest Laboratories, Richland, Washington. December 1970. 480.19

IDCOR Program Report, Technical Report 12.2, Hydrogen Distribution in Reactor Containment Building. September 1983.

Idel'chik, I.E 1960. Handbook of Hydraulic Resistance, Published persuant to an agreement with the U.S. Atomic Energy Commission and the National Science Foundation, Washington, D.C.

Knudsen, J.G. and Hilliard, R.K. 1969. Fission Product Transport by Natural Processes in Containment Vessels. Battelle-Northwest, Richland, Wash. BNWL-943.

LOCTIC - A Computer Code to Determine the Pressure and Temperature Response of Dry Containments to a Loss-of-Coolant Accident, SWND-1, (SWEC), 1971. Letter from W.J.L. Kennedy to P.A. Morris et al.

Los Alamos Scientific Laboratory Reactor Safety and Technology Quarterly Progress Report, 1976. LA-NUREG-6447-PR, p 53.

McAdams, W.H. 1954. Heat Transmission, Third Edition, p 44.

Moody, L.J. 1965. Maximum Flow Rate of a Single Component, Two-Phase Mixture. Journal of Heat Transfer Transactions, ASME Vol. 87, p 134-142.

Moore, K.V. and Rettig, W.H. 1974. RELAP4 - A Computer Program for Thermal Hydraulic Analysis. Report ANCR-1127 Aerojet Nuclear Company.

Norberg, J.A. et al 1969. Simulated Design Basis Accident Tests of the Carolinas Virginia Tube Reactor Containment - Preliminary Results, IN-1324. Idaho Nuclear Corporation.

NS-TMA-2075. 1979. A letter from T.M. Anderson, Westinghouse, to J.F. Stolz, 1979. Westinghouse LOCA Mass and Energy Release Model for Containment Design - March 1979 Version.

Nystrom, J.B. Experimental Evaluation of a Reactor Containment Sump, MNPS-3, Alden Research Laboratory, Report No. 114-82/M10XXF, October 1982.

ORNL - TM 2412. Parsly, L.F. 1970 Design Considerations of Reactor Containment Spray Systems - Part VI, the Heating of Spray Drops in Air/Steam Atmosphere.

Sandia National Laboratory and General Physics Corporation. NUREG/CR-2726, SAND 82-1137, R3, Light Water Reactor Hydrogen Manual. June 1983. 440.19

Schmidt, R.C., et al 1970. Simulated Design Basis Accident Tests of the Carolinas Virginia Tube Reactor Containment - Final Report. UC-80, Idaho Nuclear Corporation.

Slaughterbeck, D.C. 1970. A Review of Heat Transfer Coefficients for Condensing Steam in a Containment Building Following a Loss-of-Coolant Accident. Interim Task Report, Subtask 4.2.2.1, Idaho Nuclear Corp.

Spray Engineering Company. Spray Analysis on SPRACo Model 1713A Nozzles. Nashua, New Hampshire.

Uchida, H.; Oyama, A.; and Togo, Y. 1964. Evaluation of Post-Incident Cooling Systems of Light-Water Power Reactors. Proceedings of the Third International Conference on the Peaceful Uses of Atomic Energy held in Geneva. Vol. 13, New York: United Nations 93-104, (A/CONF 28/P/436). 3.11 3.12 3.13

USAEC, Division of Reactor Licensing 1970. Safety Evaluation Report for Virginia Electric and Power Company, North Anna Power Station Units 1 and 2. Docket 50-338 and 50-339. 3.15 3.16

|480.19

USAEC, Directorate of Licensing 1972a. Safety Evaluation Report for Virginia Electric and Power Company, North Anna Power Station Units 3 and 4. Dockets 50-404 and 405. 3.18 3.19

USAEC, Division of Reactor Licensing 1972b. Safety Evaluation Report for Virginia Electric Power Company, Surry Power Station Units 1 and 2. Docket 50-280 and 50-281. 3.21 3.22

USAEC, Division of Reactor Licensing 1972c. Safety Evaluation Report for Maine Yankee Atomic Power Station. Docket 50-309. 3.24 3.25

USAEC, Directorate of Licensing 1974a. Safety Evaluation Report Supplement No. 2 for the Cleveland Electric Illuminating Company, Duquesne Light Company, Ohio Edison Company, Pennsylvania Power Company, and Toledo Edison Company, Beaver Valley Power Station Unit 2. Docket 50-412. 3.27 3.28 3.29

USAEC 1974b. Evaluation of LOCA Hydrodynamics. Regulatory Staff: Technical Review. 3.32

USAEC, Directorate of Licensing 1974c. Safety Evaluation Report for the Duquesne Light Company, Toledo Edison Company, Pennsylvania Power Company, Beaver Valley Power Station Unit 1. Docket 50-334. 3.34 3.36

WCAP-6174, 1974. Bordelon, F.M. et al. SATAN-VI Program: Comprehensive Space-Time Dependent Analysis of Loss-of-Coolant. 3.39

WCAP-8170, 1974. Collier, G. et al. 1974. Calculational Model for Core Reflooding After a Loss-of-Coolant Accident (WREFLOOD Code). 3.42

WCAP-8264-P-A (Proprietary) and WCAP-8312-A (Non-proprietary), Revision 2, Westinghouse Corp. 1975. Westinghouse Mass Energy Release for Containment Design. 3.43 3.44

WCAP-8339, 1974. Burdelon, F.M.; Massie, H.W.; Zordum, J.A. Westinghouse Emergency Core Cooling System Evaluation Model - Summary. 3.46

WCAP-8859. Land, R.E. TRANFLO Steam Generator Code Description. 3.48

WCAP-8860. Land, R.E. Mass and Energy Release Following a Steam Line Rupture. 3.50

WCAP-9220, 1978. Westinghouse ECCS Evaluation Model. 3.52

TABLE 6.2-34

STEAM GENERATOR CUBICLE PEAK PRESSURES

Node	Steam Generator Inlet Nozzle		Pressurizer Surge Line		Residual Heat Removal Line		RCS Hot Leg Intrados Split		Feedwater Line	
(No.)	Pressure (psia)	Time (sec)	Pressure (psia)	Time (sec)	Pressure (psia)	Time (sec)	Pressure (psia)	Time (sec)	Pressure (psia)	Time (sec)
1	13.79	0.064	14.07	0.062	13.80	0.046	26.78	0.501	10.64	0.501
2	13.59	0.044	13.76	0.072	13.53	0.052	26.65	0.501	10.64	0.501
3	13.71	0.066	14.30	0.066	13.58	0.068	26.64	0.501	10.64	0.501
4	14.42	0.030	15.12	0.026	15.35	0.024	26.83	0.501	10.63	0.501
5	13.62	0.086	14.03	0.072	16.25	0.010	26.84	0.501	10.63	0.501
6	13.94	0.094	13.85	0.028	14.54	0.020	26.88	0.501	10.63	0.501
7	14.21	0.048	14.86	0.052	13.83	0.058	26.78	0.501	10.64	0.501
8	14.66	0.054	14.40	0.054	13.30	0.070	26.62	0.501	10.64	0.501
9	14.07	0.056	14.59	0.094	14.48	0.068	26.64	0.501	10.64	0.501
10	14.70	0.070	16.78	0.016	16.19	0.026	27.24	0.501	10.63	0.501
11	15.42	0.012	18.36	0.010	13.63	0.088	27.67	0.501	10.63	0.501
12	17.77	0.010	13.75	0.046	14.50	0.054	29.29	0.014	10.64	0.501
13	12.76	0.146	13.18	0.062	13.22	0.058	25.26	0.501	10.72	0.031
14	12.95	0.102	13.07	0.102	13.07	0.056	25.25	0.501	10.66	0.501
15	12.99	0.106	13.14	0.094	13.24	0.070	25.14	0.501	10.65	0.501
16	13.65	0.030	13.70	0.086	13.51	0.082	25.48	0.501	10.65	0.501
17	13.00	0.074	13.40	0.076	13.67	0.078	25.50	0.501	10.65	0.501
18	13.37	0.020	13.22	0.030	13.20	0.064	25.52	0.501	10.65	0.501
19	10.77	0.501	10.98	0.601	11.65	1.001	13.31	0.501	16.66	0.010
20	10.77	0.501	10.98	0.601	11.65	1.001	13.31	0.501	16.67	0.010
21	11.25	0.501	11.53	0.601	12.06	1.001	17.17	0.501	11.37	0.013
22	11.24	0.501	11.52	0.601	12.06	1.001	17.16	0.501	11.51	0.013
23	10.56	0.501	10.74	0.601	11.47	1.001	11.89	0.501	10.46	0.501
24	11.80	0.064	12.12	0.114	12.38	1.001	23.37	0.501	14.77	0.010
25	11.92	0.104	12.06	0.074	12.37	1.001	23.34	0.501	14.36	0.010
26	12.29	0.026	12.34	0.074	12.42	1.001	23.46	0.501	11.41	0.016
27	12.19	0.096	12.32	0.032	12.43	1.001	23.48	0.501	12.17	0.017
28	13.16	0.090	13.43	0.032	13.51	0.096	25.88	0.501	10.61	0.501

TABLE 6.2-34 (Cont)

Node (No.)	Steam Generator Outlet Nozzle Pressure (psia)	Steam Generator Outlet Nozzle Time (sec)	Steam Generator Pump Suction Loop Closure Weld Pressure (psia)	Steam Generator Pump Suction Loop Closure Weld Time (sec)
1	26.32	0.630	26.59	0.628
2	26.69	0.618	26.93	0.608
3	26.67	0.622	26.82	0.622
4	26.32	0.622	26.82	0.626
5	26.33	0.642	26.90	0.640
6	26.30	0.642	26.58	0.626
7	26.33	0.652	26.59	0.632
8	26.79	0.608	26.76	0.610
9	26.67	0.612	26.78	0.618
10	26.67	0.614	26.39	0.632
11	26.93	0.606	26.35	0.636
12	26.24	0.648	26.37	0.636
13	24.84	0.632	24.74	0.618
14	24.84	0.616	24.74	0.650
15	24.72	0.622	24.61	0.612
16	24.92	0.620	24.77	0.608
17	24.94	0.632	24.79	0.636
18	24.94	0.628	24.80	0.618
19	13.91	0.751	13.89	0.751
20	13.91	0.751	13.89	0.751
21	17.17	0.751	17.11	0.751
22	17.17	0.751	17.11	0.751
23	12.65	0.751	12.64	0.751
24	23.90	0.642	22.89	0.630
25	22.97	0.660	22.86	0.644
26	23.03	0.642	22.90	0.616
27	23.05	0.638	22.92	0.614
28	25.40	0.640	25.87	0.630

480.37

TABLE 6.2-36 (Cont)

Time (sec)	Mass (lb/sec)	Energy (Btu/sec)	Average Enthalpy (Btu/lb)	
2.10001	36,858.204	24,656,318	668.95	1.19
2.30009	36,048.665	24,068,766	667.67	1.20
2.50025	35,210.472	23,501,169	667.45	1.21
2.70019	34,537.213	23,028,338	666.77	1.22
3.00027	36,798.127	24,517,748	666.28	1.23

480.37

TABLE 6.2-36A

MASS AND ENERGY RELEASE RATES FOR A FEEDWATER LINE FULL DER IN THE STEAM GENERATOR CUBICLE

Time (sec)	Mass Flow SG Side (lb/sec)	Mass Flow Piping Side (lb/sec)	Energy SG Side (Btu/lb)	Energy Piping Side (Btu/lb)	Total Mass Flow (lb/sec)	Total Energy (Btu/sec)
0.0	13101.	8623.	7.048E6	3.622E6	21724.	10.67E6
2.0	13101.	8623.	7.048E6	3.622E6	21724.	10.67E6

TABLE 6.2-36B

MASS AND ENERGY RELEASE RATES FOR A 500 SQUARE INCH COLD LEG LDR IN THE STEAM GENERATOR CUBICLE

Time (sec)	Mass (lb/sec)	Energy (Btu/sec)	Average Enthalpy (Btu/lb)
0.0	0.0	0.0	0.00
0.00300	2.7553554E4	1.5365431E7	557.62
0.00762	3.5126475E4	1.9615838E7	558.44
0.01101	3.5272477E4	1.9668454E7	557.61
0.01504	4.0481375E4	1.8815784E7	557.54
0.01901	3.5526048E4	1.9804758E7	557.47
0.02302	3.4149137E4	1.9031251E7	557.30
0.02704	3.2223069E4	1.7947655E7	557.00
0.03105	3.1357026E4	1.7463354E7	556.92
0.03500	3.1173067E4	1.7360838E7	556.90
0.03901	3.1572734E4	1.7587118E7	556.87
0.04301	3.2089701E4	1.7872020E7	556.94
0.04701	3.2943141E4	1.8348849E7	556.99
0.05101	3.2957101E4	1.8356301E7	556.97
0.05501	3.3752582E4	1.8800311E7	557.06
0.05902	4.3581443E4	2.4295982E7	557.48
0.06303	4.6559619E4	2.5966536E7	557.71
0.06703	5.0176752E4	2.7997336E7	557.97
0.07102	5.1474565E4	2.8126708E7	558.08
0.07504	5.5649593E4	3.1082255E7	558.47
0.07906	5.5871919E4	3.1176204E7	558.01
0.08302	5.4253849E4	3.0266530E7	557.87
0.08707	5.2995360E4	2.9556141E7	557.71
0.09109	5.2667082E4	2.9373640E7	557.72
0.09506	5.1601936E4	2.8767941E7	557.50
0.09905	4.9847279E4	2.7788070E7	557.46
0.11501	5.1517896E4	2.8730435E7	557.68
0.13502	5.4052551E4	3.0150688E7	557.90
0.15505	5.1675352E4	2.8820766E7	557.73
0.17501	5.2674332E4	2.9387760E7	557.91
0.19510	5.2804854E4	2.9465270E7	558.00
0.23013	5.2756783E4	2.9445480E7	558.14
0.27008	5.2125022E4	2.9105085E7	558.37
0.31003	5.2666673E4	2.9427243E7	558.75
0.35007	5.2049310E4	2.9097595E7	559.04

TABLE 6.2-36B (Cont)

Time (sec)	Mass (lb/sec)	Energy (Btu/sec)	Average Enthalpy (Btu/lb)	
0.39030	5.1629608E4	2.8883611E7	559.44	2.11
0.43075	5.1939759E4	2.9081424E7	559.91	2.12
0.47007	5.1562917E4	2.8895244E7	560.39	2.13
0.51007	5.1387973E4	2.8827092E7	560.97	2.14
0.55001	5.1343287E4	2.8833112E7	561.58	2.15
0.59013	5.0769706E4	2.8544503E7	562.23	2.17
0.63001	5.0486202E4	2.8420679E7	562.94	2.18
0.67003	5.0033919E4	2.8201396E7	563.65	2.19
0.71008	4.9638937E4	2.8017887E7	564.43	2.20
0.75010	4.9336961E4	2.7886235E7	565.22	2.21
0.79004	4.8769620E4	2.7603714E7	568.00	2.23
0.83007	4.8204470E4	2.7322395E7	566.80	2.24
0.87003	4.7848952E4	2.7158782E7	567.59	2.25
0.91006	4.7389542E4	2.6935723E7	568.39	2.26
0.95011	4.6948187E4	2.6721463E7	569.17	2.27
0.99002	4.6504795E4	2.6503781E7	569.92	2.29
1.00012	4.6372995E4	2.6437194E7	570.10	2.30

TABLE 6.2-37A

STEAM GENERATOR CUBICLE PEAK DIFFERENTIAL PRESSURES,
STEAM GENERATOR OUTLET NOZZLE LDR

Vent Path (No.)	Vent Path Connecting Nodes From	To	Pressure (psid)	Time (sec)	Vent Path (No.)	Vent Path Connecting Nodes From	To	Pressure (psid)	Time (sec)
1	1	2	-3.64	0.082	36	16	17	1.28	0.029
2	2	3	-2.18	0.033	37	17	18	1.55	0.080
3	3	4	3.11	0.034	38	14	17	-0.84	0.041
4	4	5	1.62	0.028	39	13	18	1.21	0.047
5	5	6	1.72	0.018	40	13	23	13.06	0.488
6	2	5	2.26	0.027	41	13	24	1.86	0.566
7	1	6	2.02	0.042	42	14	23	13.03	0.472
8	1	7	3.15	0.036	43	14	25	1.88	C.615
9	1	23	14.58	0.479	44	15	23	12.91	0.476
10	2	8	-5.75	0.010	45	17	25	2.01	0.079
11	3	9	4.67	0.033	46	16	23	13.12	0.476
12	3	23	14.93	0.471	47	16	23	13.12	0.476
13	4	10	-4.59	0.015	48	17	26	1.93	0.079
14	4	28	2.23	0.025	49	17	23	13.13	0.486
15	5	11	-6.28	0.009	50	17	23	13.13	0.486
16	5	28	2.01	0.019	51	18	27	1.90	0.562
17	6	12	2.87	0.032	52	18	23	13.15	0.481
18	6	28	1.60	0.058	53	19	20	-0.28	0.070
19	7	8	-5.85	0.010	54	20	21	-3.75	0.474
20	8	9	4.65	0.009	55	21	22	0.31	0.079
21	9	10	-1.32	0.123	56	19	22	-3.75	0.474
22	10	11	-5.12	0.008	57	19	23	1.37	0.489
23	11	12	5.80	0.009	58	20	23	1.37	0.503
24	8	11	-0.95	0.007	59	21	23	5.12	0.480
25	7	12	1.47	0.048	60	22	23	5.12	0.479
26	7	13	3.07	0.051	61	24	25	-1.55	0.081
27	8	14	6.06	0.011	62	25	26	-0.77	0.040
28	9	15	4.93	0.019	63	26	27	1.14	0.086
29	14	23	13.03	0.472	64	27	24	0.79	0.033
30	10	16	4.88	0.017	65	24	19	9.84	0.488
31	11	17	6.52	0.010	66	25	20	9.80	0.472
32	12	18	2.93	0.053	67	26	21	6.13	0.561
33	13	14	-2.04	0.023	68	27	22	6.17	0.568
34	14	15	1.38	0.049	69	28	23	13.63	0.479
35	15	16	-1.11	0.084					

420.37

TABLE 6.2-37B

STEAM GENERATOR CUBICLE PEAK DIFFERENTIAL PRESSURES,
PUMP SUCTION LOOP CLOSURE WELD LDR

Vent Path (no.)	Vent Path Connecting Nodes From	To	Pressure (psid)	Time (sec)	Vent Path (no.)	Vent Path Connecting Nodes From	To	Pressure (psid)	Time (sec)
1	1	2	-5.94	0.013	35	15	16	-0.92	0.056
2	2	3	4.65	0.010	36	16	17	-0.41	0.113
3	3	4	2.51	0.073	37	17	18	-0.64	0.056
4	4	5	-4.30	0.009	38	14	17	-0.73	0.052
5	5	6	4.49	0.009	39	13	18	-0.52	0.094
6	2	5	2.34	0.019	40	13	23	12.97	0.491
7	1	6	1.91	0.038	41	13	24	1.86	0.568
8	1	7	1.71	0.021	42	14	23	12.93	0.505
9	1	23	14.86	0.476	43	14	25	1.89	0.584
10	2	8	5.20	0.011	44	15	23	12.79	0.512
11	3	9	3.31	0.018	45	17	25	2.11	0.114
12	3	23	15.09	0.445	46	16	23	12.97	0.489
13	4	10	2.55	0.018	47	16	23	12.97	0.489
14	4	28	2.18	0.022	48	17	26	1.89	0.581
15	5	11	4.51	0.009	49	17	23	12.99	0.490
16	5	28	4.26	0.009	50	17	23	12.99	0.490
17	6	12	2.61	0.019	51	18	27	1.88	0.559
18	6	28	1.36	0.053	52	18	23	13.02	0.486
19	7	8	-3.17	0.021	53	19	20	0.23	0.049
20	8	9	-3.60	0.032	54	20	21	-3.68	0.489
21	9	10	3.04	0.034	55	21	22	-0.20	0.068
22	10	11	2.64	0.028	56	19	22	-3.67	0.486
23	11	12	1.70	0.017	57	19	23	1.36	0.496
24	8	11	1.76	0.026	58	20	23	1.36	0.504
25	7	12	1.98	0.040	59	21	23	5.03	0.492
26	7	13	4.12	0.035	60	22	23	5.03	0.489
27	8	14	4.03	0.023	61	24	25	1.22	0.118
28	9	15	6.97	0.030	62	25	26	-0.61	0.058
29	14	23	12.93	0.505	63	26	27	-0.73	0.052
30	10	16	4.76	0.027	64	27	24	-0.44	0.065
31	11	17	2.59	0.023	65	24	19	9.76	0.492
32	12	18	3.22	0.029	66	25	20	9.70	0.499
33	13	14	-1.46	0.085	67	26	21	6.08	0.551
34	14	15	0.64	0.035	68	27	22	6.13	0.487
					69	28	23	14.14	0.466

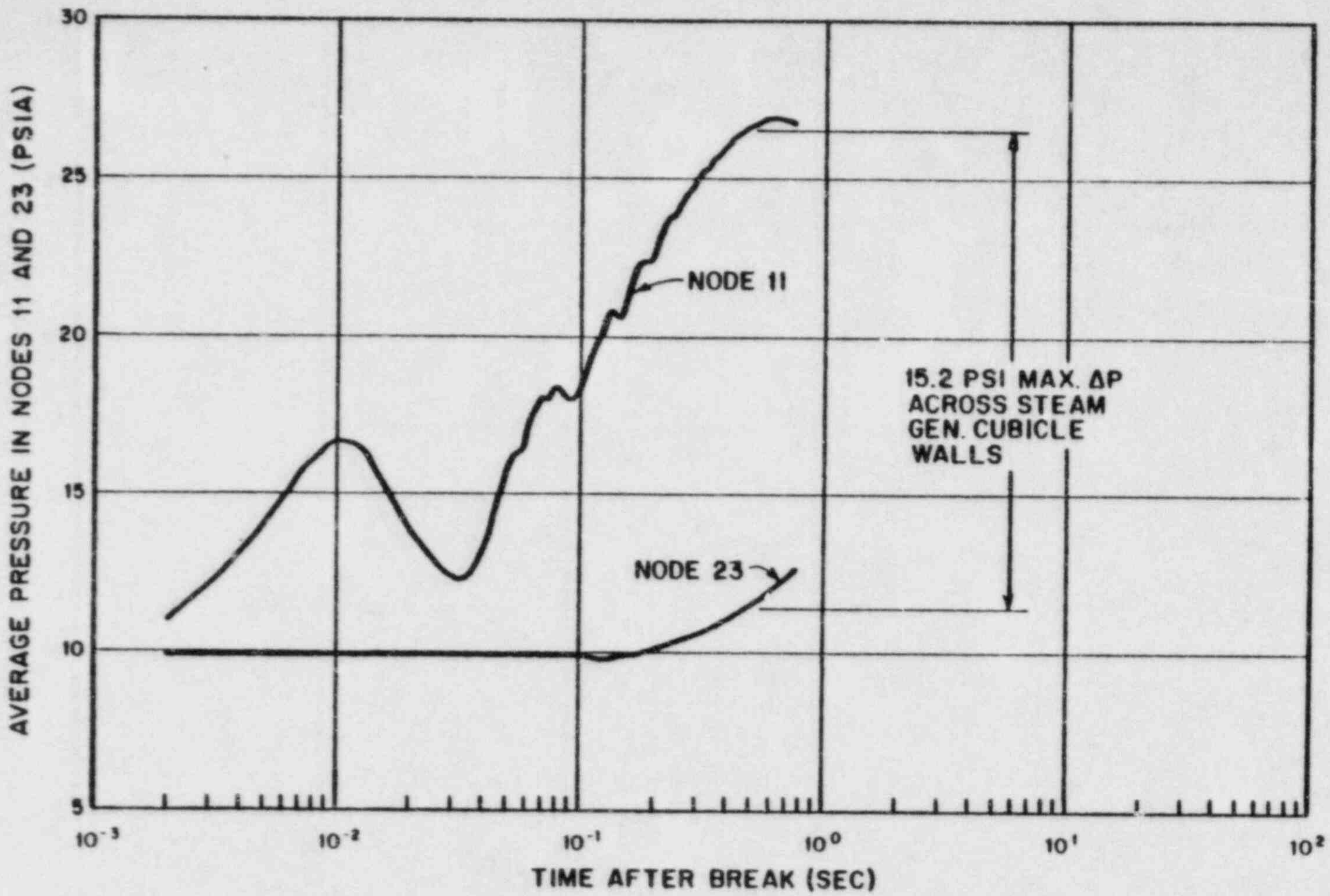

NOTE
STEAM GENERATOR OUTLET NOZZLE
LDR IN NODES 8 AND 11.

FIGURE 6.2.-34A
PRESSURE RESPONSE
STEAM GENERATOR CUBICLE
MILLSTONE NUCLEAR POWER STATION
UNIT 3
FINAL SAFETY ANALYSIS REPORT

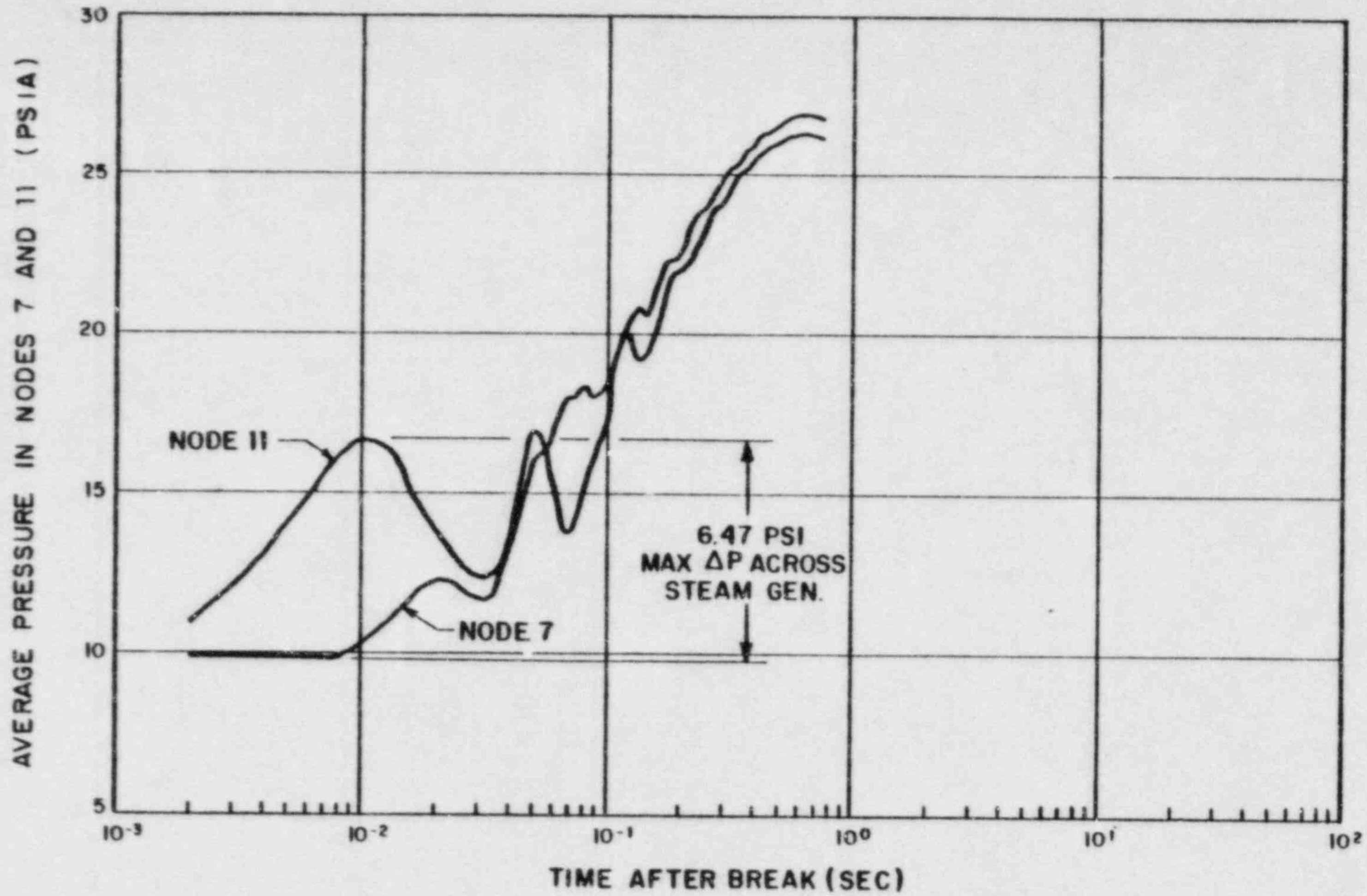

NOTE:

STEAM GENERATOR OUTLET NOZZLE
LDR IN NODES 8 AND 11

FIGURE 6.2-34B

PRESSURE RESPONSE
STEAM GENERATOR CUBICLE

MILLSTONE NUCLEAR POWER STATION
UNIT 3
FINAL SAFETY ANALYSIS REPORT

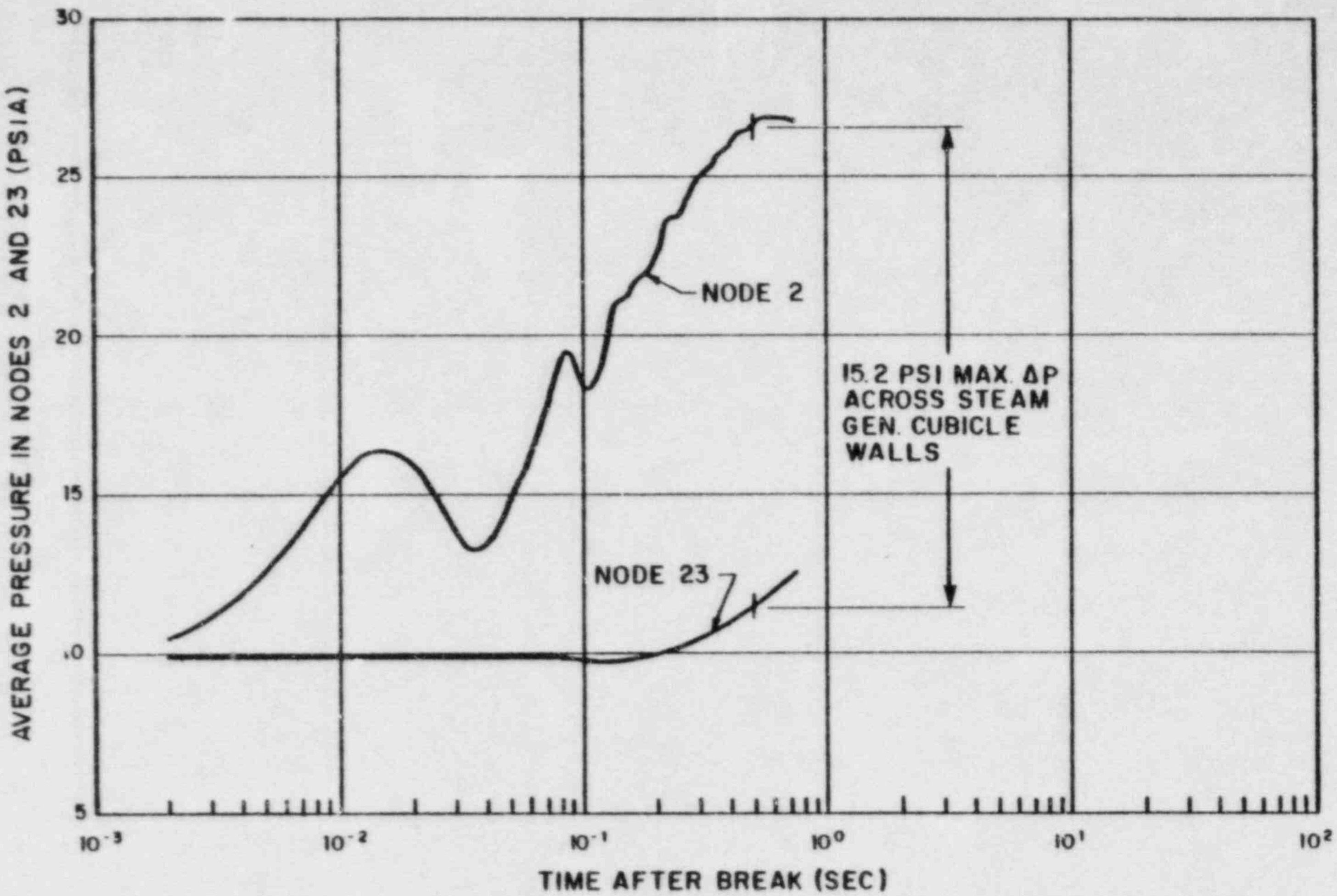

NOTE

STEAM GENERATOR PUMP SUCTION LOOP CLOSURE WELD LDR IN NODES 2 AND 5.

FIGURE 6.2-34C
PRESSURE RESPONSE
STEAM GENERATOR CUBICLE
MILLSTONE NUCLEAR POWER STATION
UNIT 3
FINAL SAFETY ANALYSIS REPORT

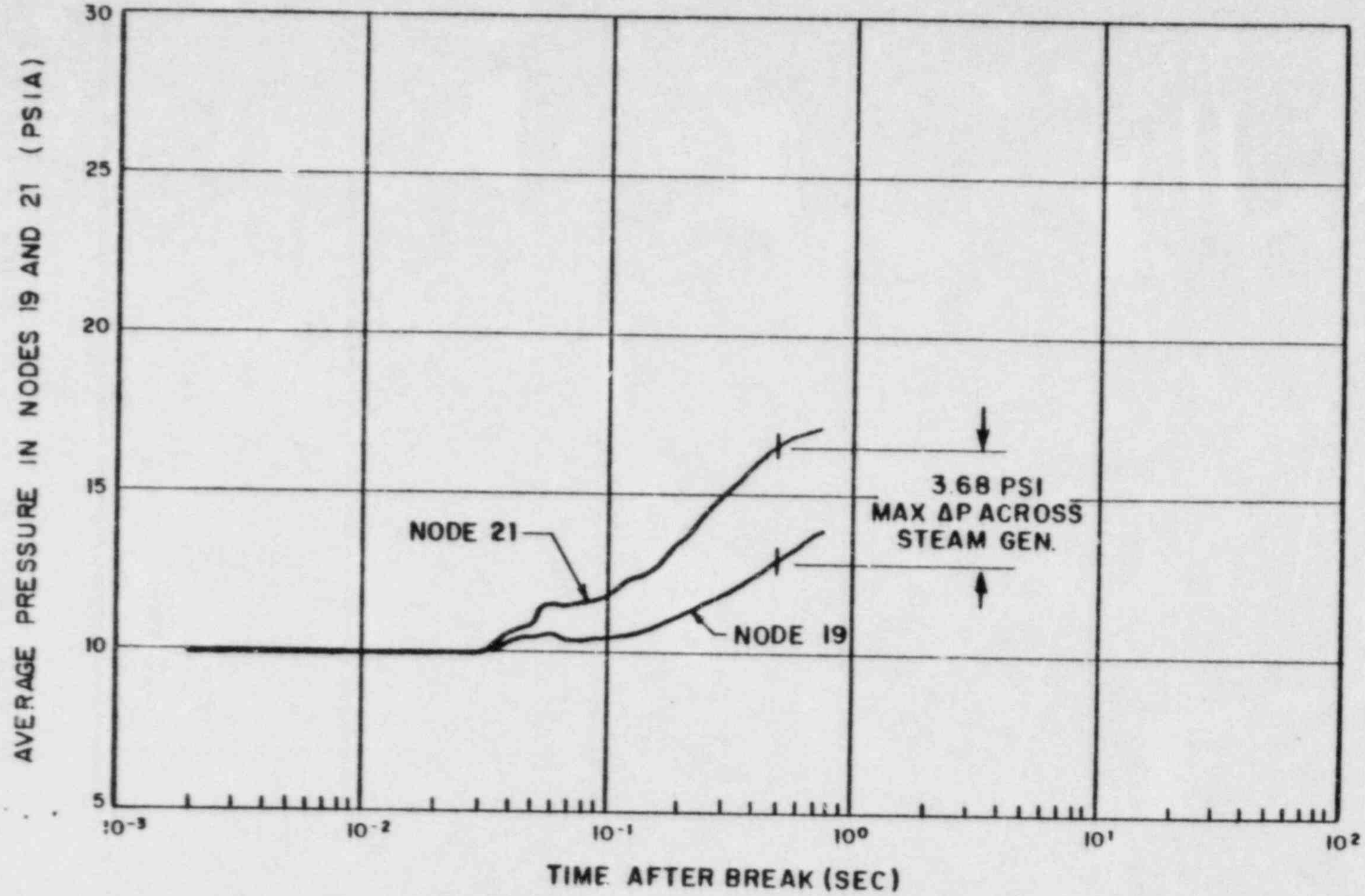

NOTE

STEAM GENERATOR PUMP SUCTION LOOP
CLOSURE WELD LDR IN NODES 2 AND 5.

FIGURE 6.2-34D
PRESSURE RESPONSE
STEAM GENERATOR CUBICLE
MILLSTONE NUCLEAR POWER STATION
UNIT 3
FINAL SAFETY ANALYSIS REPORT